Living inside Sea Ice

-

Distribution and Functional Characterisation of Antifreeze Proteins in Polar Diatoms

Dissertation

zur Erlangung des akademischen Grades eines

Doktors der Naturwissenschaften

- Dr. rer. Nat. -

am Fachbereich 2 (Biologie/Chemie)

der Universität Bremen

vorgelegt von

Christiane Uhlig

Bremen

Oktober, 2011

1. Prüfer: Prof. Kai Bischof

2. Prüfer: Prof. Ulrich Bathmann

Für meine Mutter Monika

Was Menschen in die Polargebiete trieb, war die Macht des Unbekannten über den menschlichen Geist. Sie treibt uns zu den verborgenen Kräften und Geheimnissen der Natur, hinab in die unermesslich kleine mikroskopische Welt und desgleichen hinaus in die unerforschten Weiten des Universums. Sie lässt uns keine Ruhe, bis wir den Planeten, auf dem wir leben, von der tiefsten Tiefen des Ozeans bis zu den höchsten Schichten der Atmosphäre kennen.

Fridtjof Nansen

Danksagung

Ich danke Prof. Ulrich Bathmann und Prof. Kai Bischof für die Begutachtung dieser Arbeit. Prof. Rudolf Amann danke ich, dass er sich kurzfristig bereit erklärt hat die Aufgabe des 3. Prüfer zu übernehmen. Bei Prof. Kai Bischof und Andreas Krell bedanke ich mich für die Hilfe zur Einwerbung des Stipendiums, welches diese Arbeit überhaupt erst ermöglicht hat. Der Studienstiftung des deutschen Volkes danke ich für die finanzielle Unterstützung.

Ich bedanke mich ganz besonders bei der Meereis-Gruppe, die mehr ist als nur eine Arbeitsgruppe. Besonders danke ich Gerhard Dieckmann, dass ich in Deiner Arbeitsgruppe meine Arbeit durchführen durfte und für Deine Unterstützung in allen möglichen organisatorischen und persönlichen Dingen. Klaus Valentin danke ich für die Unterstützung, kreativen Titelvorschläge und den Einsatz dafür, dass ich noch eine Weile am AWI bleiben kann. Erika, unsere gute Fee, ein großes Dankeschön für all Deine Unterstützung im Labor, die Expeditions-Logistik, Deine Aufmunterungen, Kuchen, Mittagessen und für die unzähligen anderen großen und kleinen Dinge. Jessi, danke für die Gespräche, sei es wissenschaftlich oder privat, und für die schönen Abende in Bremen! Danke an Niko, mein Küchenchef! Danke auch an Andreas, für Deine Tipps und Betreuung; Micha, für die Bürogesellschaft; Madda, als AFP-Mitstreiterin; Katrin, Ramona, Tim und Anika für die Unterstützung im Labor. Nicht nur das Arbeiten mit Euch, sondern auch alle anderen Aktivitäten haben mir unglaublich viel Spass gemacht!

Bei Ulrich Bathmann, Gerhard, Klaus und Erika möchte ich mich insbesondere bedanken, dass Ihr mir das schwierige und traurige letzte Jahr während der Doktorarbeit mit Eurer Unterstützung und Flexibilität so einfach wie eben möglich gemacht habt.

Ich bedanke mich bei Bánk Beszteri für die Unterstützung und Beratung in vielen Fragen, sei es Bioinformatik, Phylogenie, Taxonomie von Diatomeen oder auch Diplomatie. Ein Dank geht auch an Stephan Frickenhaus für die bioinformatische Unterstützung. Uwe John danke ich für seine Ratschläge in molekularbiologischen Fragen und dass er sich als Prüfer bereit erklärt hat. Ich möchte mich bei den Mitgliedern der AGs Cembella, Medlin und Pörtner dafür bedanken, dass sie mich freundlich in Ihren Laboren aufgenommen und

bei Engpässen mit dem ein oder anderen Enzym oder Sonstigem ausgeholfen haben. Ein Dank gilt auch denen, die diese Arbeit oder Teile davon Korrektur gelesen haben: Gerhard, Sven, Ivo, Rainer, Harald, Anne und Johanna.

Ich bedanke mich bei meinen Kooperationspartern in Greifswald für die freundliche Aufnahme während meiner Besuche. Prof. Thomas Schweder und Prof. Winfried Hinrichs danke ich, dass sie die Zusammenarbeit ermöglicht haben. Johannes Kabisch möchte ich dafür danken, dass er mich in die Geheimnisse des Rekombinierens, Klonierens und Exprimierens eingeweiht hat, und auch für die Fahrradleihgaben oder nächtliche Verpflegung nach langen Labortagen. Gottfried Palm danke ich für die Einweisung in das Aufreinigen von Proteinen.

I would like to thank Sebastian Gerland and Mats Granskog from the Norsk Polar Institut in Tromsø for the opportunity to join the fieldwork in NyÅlesund, which was a great experience. Ich danke Marcel Nicolaus, dass er den Kontakt für diese Möglichkeit hergestellt hat.

Furthermore, I would like to thank the people who crossed my way at AWI or somewhere else in the world, who had time for a chat in the kitchen or lab, or just a smile that made my days nicer.

Ein Dank geht an meine Mädels zu Hause, die das ein oder andere Mal wegen Feldarbeiten, Konferenzen oder Laborarbeit auf mich verzichten mussten. Danke an Anne für das Teilen des "Doktorarbeits-Leids". Danke Michael, für die Gesprächsthemen, die nicht die Arbeit betreffen. Thanks, Joakim, for always having a nice word and cheering me up!

Ich möchte mich bei meiner Familie bedanken, insbesondere bei meinen beiden Schwestern Babrara und Johanna, für Eure Unterstüzung, Besuche und Ermutigungen.

Zuletzt möchte ich mich bei Dir, Sven, für Alles bedanken, besonders für Deine Geduld, meine Launen auszuhalten und Deine Unterstützung in der letzten, stressigen Zeit. Für Stunde um Stunde des Korrekturlesen und der Diskussionen, ohne Dich wäre diese Arbeit nicht das geworden was sie jetzt ist. Danke für das Leben neben der Arbeit!

Danke! Thanks! Tack! Kiitos! Gracias!

Contents

Summary/Zusammenfassung **VII**

1 Introduction **1**

1.1 The sea ice habitat . . . 2

1.1.1 Sea ice formation and inclusion of organisms . . . 2

1.1.2 Sea ice microbial communities and abiotic conditions . . . 4

1.1.3 Adaptation mechanisms of sea ice diatoms . . . 5

1.2 Antifreeze proteins . . . 7

1.2.1 Functions and molecular principles . . . 7

1.2.2 Distribution and function of AFPs from sea ice diatoms . . . 10

1.2.3 Novel technologies to study AFPs . . . 12

1.3 Objectives and outline of this thesis . . . 14

2 Recrystallisation Inhibition in Arctic and Antarctic diatom isolates **17**

2.1 Introduction . . . 18

2.2 Material and Methods . . . 20

2.2.1 Recrystallisation inhibition and crystal deformation assays . . . 20

2.2.2 Diatom cultures . . . 21

2.2.3 Strain identification . . . 24

2.2.4 Experimental procedures . . . 25

2.3 Results . . . 27

2.3.1 Comparison of methods for determination of recrystallisation inhibition . . . 27

2.3.2 Strain identification . . . 28

2.3.3 Physiology and AFP activity under temperature and salinity stress 30

2.3.4 AFPeq content estimation . . . 33

2.3.5 Stability under temperature and protease 45
2.4 Discussion 48
2.4.1 Methods for RI and AFP measurement 48
2.4.2 Taxonomy and ecology 49
2.4.3 Physiology and AFP activity under salinity and temperature stress 50
2.4.4 Content and function of AFPs in diatoms 51
2.5 Supplementary material 55

3 Heterologous expression, refolding and functional characterisation of two antifreeze proteins from *Fragilariopsis cylindrus* (Bacillariophyceae) 65
3.1 Introduction 66
3.2 Material and methods 68
3.2.1 Vector construction 68
3.2.2 Selection of expression constructs and heterologous expression . . . 69
3.2.3 Inclusion body purification 71
3.2.4 Refolding and purification of recombinant AFPs 71
3.2.5 Determination of protein concentration and gel electrophoresis . . . 72
3.2.6 Antifreeze assays 72
3.2.7 Functional characterisation 73
3.2.8 Phylogeny 74
3.3 Results 74
3.3.1 Expression and cleanup 74
3.3.2 Functional characterisation 75
3.3.3 Phylogeny 81
3.4 Discussion 81
3.4.1 Quality and characteristics of recAFPs 81
3.4.2 TH potential 83
3.4.3 New crystal deformation shape 85
3.4.4 Phylogeny and function of *F. cylindrus* AFP sequences 86
3.5 General remarks to strain classification 87

3.6 Supplementary material 88

4 Differential abundance and phylogenetic diversity of AFP transcript fragments in environmental transcriptomes from polar sea ice 93

4.1 Introduction 94

4.2 Material and Methods 96

4.2.1 Sampling 96

4.2.2 RNA preparation 98

4.2.3 Construction of cDNA libraries and 454 sequencing 98

4.2.4 Sequence retrieval and phylogenetic placement 99

4.3 Results 101

4.3.1 AFP candidates 101

4.3.2 Phylogeny of environmental AFP sequences 101

4.4 Discussion 106

4.4.1 Abundance of AFP sequences 106

4.4.2 Identification of target genes - pplacer versus BLAST 107

4.4.3 Presence of AFP genes *in situ* versus molecular biodiversity 108

4.4.4 Importance of clade I_D 109

4.5 Supplementary material 111

5 General discussion 117

5.1 Distribution and phylogeny of diatom AFPs 117

5.1.1 Distribution of AFP activity and genes in diatoms 117

5.1.2 Phylogeny of AFP genes from diatom isolates and environmental samples 121

5.2 Functional characterisation of AFPs from sea ice diatoms and their ecological significance 123

5.2.1 Functional characterisation of recombinant AFP isoforms 123

5.2.2 Subcellular localisation and function 124

5.2.3 Further considerations on the ecological significance of diatom AFPs 127

5.3 Future research and perspectives 130

6 References **132**

A Tables species **149**

B Lists of figures and tables **153**

List of figures 153

List of tables 155

Summary

Antifreeze proteins (AFPs) are an important adaptation mechanism for organisms subjected to subzero temperatures. The motivation of this thesis was to elucidate the distribution of AFPs in sea ice diatoms and to study their function. The findings were used to deduce the mechanisms of action and relevance *in vivo*.

Diatom isolates were tested in culture experiments for the presence of recrystallisation inhibition activity, as a measure for AFP activity. Seven Arctic and four Antarctic diatom isolates were subjected to a temperature decrease and salinity shift resembling the inclusion of the diatoms into sea ice. All tested polar diatom species showed AFP activity, ten thereof even without being stressed. In three species, AFP activity was furthermore up-regulated by the temperature and salinity shift. Cell numbers and photosynthetic quantum yield indicated that cellular damage caused by the stress was more severe for water column isolates than for isolates from the ice column. The correlation of recrystallisation to the protein concentration for a *Fragilariopsis nana* Ant cell extract and a recombinant AFP allowed the calculation of AFP concentrations as AFP equivalents. Intracellular concentrations of 0.3 μM to 68.5 μM AFP equivalents confirmed the function of AFP as recrystallisation inhibitor and even come close to the concentrations required for thermal hysteresis. As AFP equivalents made up 0.1% to 5% of the total cell protein, diatoms invest a large amount of energy to produce AFPs. This indicates that AFPs are an important factor for diatom success in sea ice.

Further, two isoforms of AFPs from *Fragilariopsis nana* were heterologously expressed in *Escherichia coli*, to study their molecular function. Recombinant proteins were deposited in inclusion bodies, but successfully refolded to functionally active proteins with respect to crystal deformation, recrystallisation inhibition and thermal hysteresis. The two isoforms showed different characteristics. One isoform produced a thermal hysteresis of up to 1.53 °C ± 0.53 °C and modified ice crystal growth to formation of hexagonal bi-pyramidal shapes, whereas the other isoform produced a thermal hysteresis of up to

2.34 °C ± 0.25 °C and ice crystals in the form of hexagonal columns. Thermal hysteresis activity of both proteins was positively correlated with protein concentration. The AFP activity increased with increasing buffer salinity in a linear correlation. High AFP concentrations or buffer salinities caused radial dendritic burst patterns of ice crystals in AFP solution. Thermal hysteresis potentials, crystal deformation habits and burst patterns led to the classification of both AFPs as hyperactive AFPs. In addition, the two isoforms differed with respect to the signal for subcellular localisation. Preceding the antifreeze domain, the gene of the first isoform carries a signal peptide indicating the secretion into the extracellular space, whereas the second isoform has a long N-terminal sequence of unknown function. We thus propose that AFPs have different functions *in vivo*, with distinct localisations of the proteins inside or outside the cell.

To investigate AFP activity *in situ*, five cDNA libraries of eukaryotic communities from Arctic and Antarctic sea ice were analysed for abundance and phylogenetic relationship of AFP sequences. AFP transcripts were found in all sea ice cDNA libraries from the Arctic (Kongsfjord) and Antarctic (Weddell Sea and Dumont d´Urville Sea). Abundances of AFPs ranged from 115 to 1824 AFP transcripts per 100.000 reads. The different abundances did not correlate with taxonomic distribution or environmental parameters of the respective samples. Phylogenetic placement assigned 90% of the sequences to a clade of AFPs from the diatoms *Navicula glacei*, *Chaetoceros neogracile* and the crustacean *Stephos longipes*. The remaining 10% were placed into a separate clade of *Fragilariopsis* AFP sequences. In the Arctic sample all AFP sequences were assigned to the *Fragilariopsis* clade, whereas in only one Antarctic sample were some sequences found in this clade. These findings indicate that AFPs play an important role for eukaryotic sea ice organisms in their natural habitat and that the *Navicula/Chaetoceros* clade is more prominent than the *Fragilariopsis* clade under the conditions investigated.

Zusammenfassung

Antifreeze-Proteine (AFPs, Gefrierschutzproteine) sind ein wichtiger Anpassungsmechanismus für Organismen, die Temperaturen unter dem Gefrierpunkt ausgesetzt sind. Die Motivation dieser Arbeit war es, die Verbreitung von AFPs in Meereis-Diatomeen sowie die Funktionsweise dieser Proteine zu untersuchen. Die hier erzielten Ergebnisse liefern Erkenntnisse über die Funktionsmechanismen und Bedeutung der AFPs *in vivo*.

Verschiedene Diatomeen-Arten wurden in Kultivierungs-Experimenten auf die Inhibition von Rekristallisation, die als Maß für die Anwesenheit von AFPs angesehen wurde, untersucht. Sieben arktische und vier antarktische Diatomeen-Isolate wurden einer Temperatur-Erniedrigung und einer Salinitäts-Erhöhung ausgesetzt. Dies sind Bedingungen, die den Einschluss der Diatomeen ins Meereis simulieren. Alle Isolate aus den Polargebieten zeigten Rekristallisations-Inhibition, zehn der untersuchten Arten sogar ohne zuvor den genannten Stressbedingungen ausgesetzt worden zu sein. In drei Arten wurde die Aktivität außerdem durch die herabgesetzte Temperatur und die erhöhte Salinität verstärkt. Ein deutlicher Einbruch der Zellzahlen und des photosynthetischen Quanten-Yields bei Isolaten aus der Wassersäule zeigte, dass diese stärker durch den Stress geschädigt wurden, als die Isolate aus dem Meereis. Die Korrelation der Rekristallisations-Inhibition zu den Proteinkonzentrationen eines Zellextrakts von *Fragilariopsis nana* sowie eines rekombinanten AFP ermöglichte es, AFP-Konzentrationen in Form von AFP-Äquivalenten zu berechnen. Intrazelluläre Konzentrationen von 0.3 μM bis 68.5 μM bestätigten, dass die AFPs als Rekristallisations-Inhibitoren wirken, erreichen aber auch Konzentrationen, die für thermale Hysterese (Gefrierpunkts-Erniedrigung) nötig sind. Der hohe Anteil von 0.1% bis 5% AFP am Gesamtzell-Proteingehalt zeigt, dass Diatomeen viel Energie aufwenden um AFPs zu produzieren. Dies wiederum weist darauf hin, dass AFPs von großer Bedeutung für das Überleben der Diatomeen im Meereis sind.

Um die molekularen Wirkungsmechanismen von Diatomeen-AFPs zu untersuchen, wurden zwei AFP-Isoformen aus *F. nana* heterolog in *Escherichia coli* exprimiert. Die rekombinanten Proteine wurden in *E. coli* zwar in denaturierter Form (inclusion bodies) abgelegt, konnten aber zu funktionell aktiven AFPs zurückgefaltet werden, die z.B. die Rekristallisation von Eis inhibierten. Die beiden Isoformen zeigten unterschiedliche Eigenschaften. Eine der Isoformen erzeugte eine thermale Hysterese von 1.53 °C ± 0.53 °C und veränderte die Form von Eiskristallen hin zu einer Bildung von Bi-Pyramiden mit hexagonaler Grundfläche. Die zweite Isoform hingegen erzeugte eine thermale Hysterese von bis zu 2.34 °C ± 0.25 °C. Eiskristalle in einer Lösung dieses AFP wuchsen in Form einer Säule mit hexagonaler Grundfläche. Die Höhe der thermalen Hysterese korrelierte positiv mit der AFP-Konzentration und die Aktivität stieg linear mit zunehmendem Salzgehalt des Puffers an. Bei hohen AFP-Konzentrationen oder hohen Puffer-Salinitäten wurde ein explosionsartiges Wachstum der Eiskristalle in radial symmetrischen verästelten Formen beobachtet. Die Höhe der thermalen Hysterese sowie die Muster des explosionsartigen Wachstums klassifizieren beide AFP-Isoformen als hyperaktive AFPs. Die zwei Isoformen unterscheiden sich weiterhin im Hinblick auf die Signale zur zellulären Lokalisation. Während auf dem Gen der ersten Isoform vor der AFP-Domäne ein Signalpeptid zu finden ist, welches auf die Exkretion des AFP hinweist, hat das Gen der zweiten Isoform an gleicher Stelle eine Proteinsequenz unbekannter Funktion. Diese Signale und die verschiedenen Eigenschaften deuten darauf hin, dass verschiedene AFP-Isoformen *in vivo* an bestimmten Orten innerhalb und außerhalb der Zellen unterschiedliche Funktionen erfüllen.

Um die Aktivität von AFP-Genen *in situ* zu ermitteln, wurden fünf cDNA (komplementäre DNS) Bibliotheken eukaryotischer Meereis-Gemeinschaften aus der Arktis und Antarktis im Hinblick auf die Häufigkeit und Phylogenie von AFP-Sequenzen untersucht. AFP-Transkripte wurden in allen Proben aus der Arktis (Kongsfjord) und der Antarktis (Weddell-Meer und Dumont d´Urville Meer) gefunden. Die Häufigkeit der AFPs reichte von 115 bis hin zu 1824 AFP-Transkripten pro 100.000 Sequenzen. Die unterschiedlichen Häufigkeiten von AFP-Transkripten korrelierten weder mit der Artenzusammensetzung

noch mit den Umweltbedingungen, die für die entsprechenden Proben bestimmt wurden. Die phylogenetische Analyse ordnete 90% aller AFP-Transkripte einer Gruppe von AFP-Sequenzen aus den Diatomeen *Navicula glacei*, *Chaetoceros neogracile* und dem Copepoden *Stephos longipes* zu. Die restilichen 10% der AFP-Sequenzen wurden einer Gruppe von *Fragilariopsis*-AFPs zugeordnet, welche von der vorhergehenden Gruppe getrennt ist. Hierbei wurden in der arktischen Probe alle Sequenzen der Gruppe von *Fragilariopsis* AFPs zugeordnet, während nur eine der antarktischen Proben einige Sequenzen in dieser Gruppe aufwies. Die Ergebnisse deuten darauf hin, dass AFPs unter natürlichen Bedingungen eine wichtige Funktion für eukaryotischen Meereis-Gemeinschaften haben, und dass die Gruppe der *Navicula*/*Chaetoceros*-AFPs unter den untersuchten Bedingungen eine größere Bedeutung hat als die Gruppe der *Fragilariopsis*-AFPs.

1 Introduction

Proteins with cryoprotective functions, i.e. antifreeze proteins (AFPs), are found in a range of organisms from all kingdoms of life. Expression of such specific proteins aids the organisms to cope with the threats caused by subzero temperatures, for example the formation of ice crystals, which can cause disruption of cellular membranes. DeVries and Wohlschlag (DeVries1969) first reported the presence a glycoprotein, which lowered the freezing point of blood in the Antarctic fish *Trematomus borchgrevinki*. In the subsequent decades, proteins with similar functions were found in insects (Patterson1979), plants (Griffith1992), bacteria and fungi (Duman and Olsen 1993), microalgae (Raymond et al. 1994) and a crustacean (Kiko 2010) isolated from terrestrial habitats or sea ice. This thesis aims to elucidate the importance of AFPs for diatom success in sea ice and to study the molecular function of diatom AFPs.

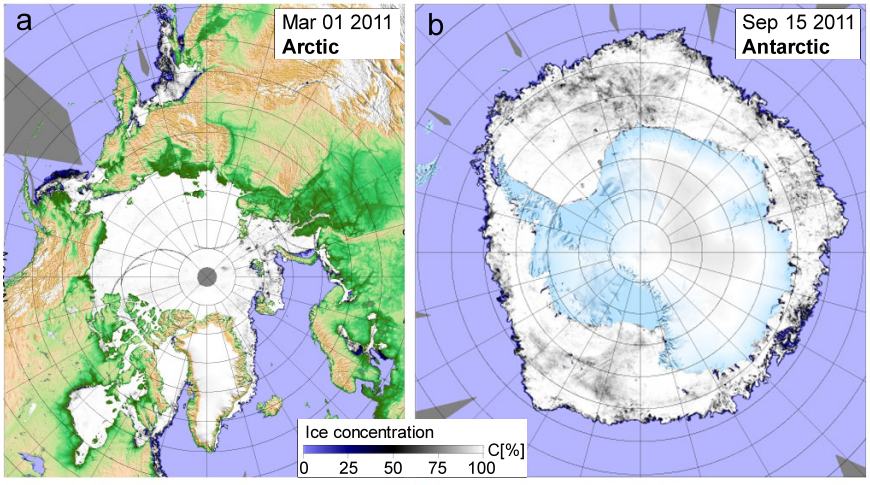

Figure 1.1: Maximal sea ice extents in (a) the Arctic and (b) the Antarctic in 2011 obtained by remote sensing (Spreen et al. 2008). Source of the satellite images http://www.iup.uni-bremen.de:8084/amsr/amsre.html (last accessed: 16 Sept 2011)

Polar sea ice can be considered one of the largest habitats on earth covering areas of 14 million square kilometres in the Arctic and 16 million square kilometres in the Antarctic during its maximum extent in winter and spring (Comiso and Nishio 2008) (Fig. 1.1). Sea ice algae in both Polar Regions can make up 25% of the total production in ice influenced regions (Legendre et al. 1992; Arrigo and Thomas 2004) and especially diatoms flourish in the ice (Thomas and Dieckmann 2002; Arrigo and Thomas 2004). This group of microalgae is well adapted to the habitat (Mock and Thomas 2005) and one of the mechanisms seems to be the production of antifreeze proteins. In contrast to AFPs from fish and insects, diatom AFPs have only been discovered quite recently (Raymond et al. 1994), and not yet studied comprehensively.

The first section of this introduction describes the habitat sea ice, explaining sea ice formation processes that cause the introduction of organisms into sea ice. Furthermore, the abiotic conditions inside the sea ice habitat and the respective adaptation mechanisms of the organisms are shown. The second section of the introduction comprehensively presents antifreeze proteins as one of these adaptation mechanisms. The general functions and molecular mechanisms derived from studying fish, insect and plant AFPs are presented. This is followed by a review on the research done on diatom AFPs as well as an introduction to molecular techniques, which can be applied to study antifreeze proteins. The introduction closes with presentation of the objectives and outline of the thesis.

1.1 The sea ice habitat

1.1.1 Sea ice formation and inclusion of organisms

In autumn, when sea water temperature drops below its freezing point (approx. -1.86 °C), small ice crystals of mm to cm size, called frazil ice, form and float at the sea surface (Lange et al. 1989). Frazil ice formation can also occur in water layers just below the surface, followed by a rise of the crystals up to the sea surface. After formation of a thick ice slurry, consolidation of the ice under turbulent conditions results in the formation of

Figure 1.2: Diatoms attached to the edges of ice platelets being grazed by amphipods

small ice floes of 30 cm to 3 m diameter, the so-called pancake ice. The loose ice cover dampens the wave action and thus the pancakes freeze together to form a continuous ice cover, later termed pack ice. Under calmer conditions, i.e. low wind and wave action, a thin layer of flat congelation ice forms (Lange et al. 1989; Eicken and Lange 1989) and the ice cover thickens by vertical growth of large ice crystals. In the process of sea ice formation, the salt ions from seawater are expelled from the ice structure (Weeks and Ackley 1982). This brine first surrounds the smaller ice crystals, but when the ice structure consolidates, the brine collects inside channels and pores of μm to cm size (Fig. 1.3 a) (Weissenberger et al. 1992). An additional ice type, particularly in Antarctic coastal areas, is platelet ice, which forms from supercooled water in the vicinity of ice shelves (Dieckmann et al. 1986). Platelet ice accumulates below an existing sea ice cover to extensive aggregations contributing to sea ice thickness but also constituting a rich and unique habitat for microalgae, other microorganisms (Dieckmann et al. 1986; Dieckmann et al. 1992) and higher trophic levels (Bluhm et al. 2010) (Fig. 1.2).

Marine microorganisms become incorporated into the ice through scavenging of particles by frazil ice crystals, when they pass through the water column (Garrison et al. 1989), or during the formation of platelet ice (Dieckmann et al. 1986). Organisms are, furthermore, retained in the ice structure, when waves pump sea water through a thin sea ice cover (Shen and Ackermann 1990). When the ice consolidates, the organisms end up

in the brine channels and pores (Fig. 1.3 a). The biomass in the ice can often exceed that in the underlying water column (Garrison et al. 1989). For example, chlorophyll values in the ice can be two to three orders of magnitude higher than those in the underlying water column (Eicken 1992; Lizotte 2001).

1.1.2 Sea ice microbial communities and abiotic conditions

The community of organisms incorporated and thriving in the ice comprises viruses, bacteria and microalgae and small metazoans (Thomas and Dieckmann 2002). A major part of the biomass within sea ice is found in the lower part of the ice column and constitutes the bottom ice community (Fig. 1.3 b and c). Further communities can be found throughout the ice column (internal community) or at the surface of the ice column below the snow cover (surface community) (Horner et al. 1992). In the Arctic, surface communities or communities in melt ponds, which are established by melting processes in decaying sea ice, are of importance as well (Horner et al. 1992; Kramer and Kiko 2011).

Throughout the ice column, environmental conditions like temperature, salinity and light differ significantly. An example of temperature and salinity profiles of an ice core from the Kongsfjord is shown in Fig. 1.3 d. Bottom ice communities encounter temperatures and salinities similar to those of the underlying seawater, typically a salinity of 34 and temperature of -1.86 °C. Internal communities have to cope with lower temperatures and higher salinities, when the air temperature is lower than the seawater temperature. Salinity increases from the bottom to the top with decreasing temperature ot the ice as salt ions are not included into the ice matrix (Cox and Weeks 1983). Accordingly, the brine volume and thus habitable space decreases. Temperatures at the ice surface depend on the air temperature and snow cover and can easily drop to -20 °C with corresponding brine salinities of over 200 (Cox and Weeks 1983). In contrast, light can be reduced by up to 1000-times at the bottom ice community as it decreases with passage through the snow cover and ice column due to backscatter and absorption (Eicken 1992). Similar to the spatial distribution inside the ice column, the conditions change for organisms that are being incorporated into the ice matrix during sea ice formation.

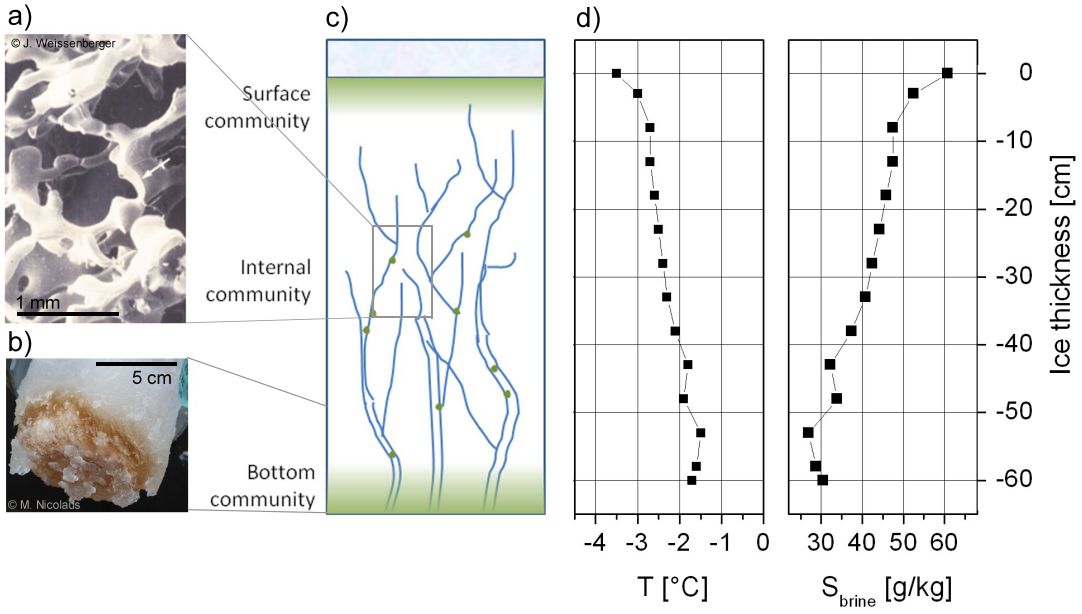

Figure 1.3: The sea ice habitat: (a) Resin cast of brine channels, picture from Weissenberger et al. (1992). (b) Ice core with dense bottom ice community. (c) Schematic drawing of a sea ice column, showing the different communities. The internal community can be found throughout the entire ice column inside the brine channels. (d) Temperature (T) and brine salinity (S_{brine}) profiles of an ice core drilled 8^{th} May 2009 in Kongsfjord, Svalbard (sampling site of study in chapter 2). Brine salinity was calculated according to Assur (1958).

1.1.3 Adaptation mechanisms of sea ice diatoms

Despite the adverse and variable conditions inside the sea ice brine pockets and channels, the organisms thrive and proliferate due to a whole suite of physiological and biochemical adaptations (Mock and Thomas 2005). Since lipid membrane fluidity decreases at lower temperatures, the composition is adjusted to a higher proportion of unsaturated, methyl-branched or *anteiso*-branched fatty acids (Russell 1997). Membrane fluidity is essential for the integrity of cell membranes in general and membrane bound cellular processes, like for example photosynthesis. Ice algae are generally low light adapted, showing photosynthetic saturation and inhibition already at low irradiance (Kirst and Wiencke 1995). In

comparison to the pigment composition of temperate diatom species, sea ice diatoms have a higher concentration of fucoxanthin (Lizotte et al. 1998). This pigment absorbs light at wave lengths, which penetrate sea ice and snow (Lizotte et al. 1998) and is responsible for the typical brownish colour of diatom rich sea ice assemblages (Fig. 1.3 b). In the brine, the availability of free water molecules is reduced by both freezing of pure water and high salinity of the brine. To avoid dehydration by osmotic water efflux from the cell, the microorganisms adjust the osmolyte concentration inside the cell e.g. by accumulation of salts or compatible solutes to the surrounding medium (Thomas and Dieckmann 2002; Kirst 1990). Sea ice organisms have the ability, not only to adapt to these extreme conditions, but also to acclimate in short time frames of minutes to hours (Mock and Thomas 2005), a necessity since sea ice is not a static habitat but highly dynamic in its melting and refreezing processes.

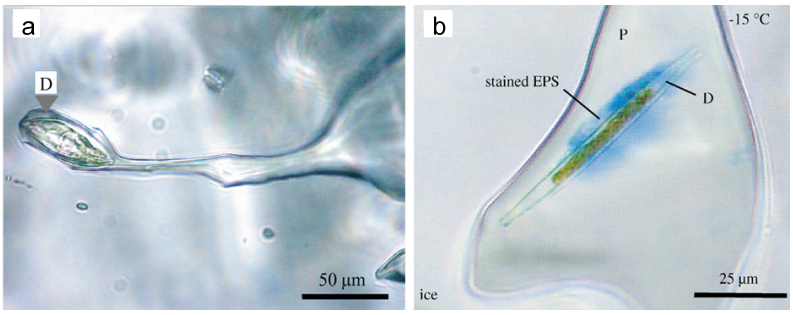

Figure 1.4: Diatoms in brine pockets. (a) and (b) Brine pockets (P) enclosing sea ice diatoms (D). The right picture shows EPS stained with alcian blue. Pictures from Krembs et al. (2002).

By secretion of organic substances, microorganisms in sea ice establish microhabitats that buffer the cells against above mentioned stressors and environmental changes (Thomas and Dieckmann 2002). Large amounts of exopolymeric substances (EPS), polysaccharide components accumulated as gels around cells (Fig. 1.4), were found in Arctic sea ice (Krembs et al. 2002). EPS produced by sea ice diatoms were proposed to have a buffering role and to protect cells from harmful ice crystals (Krembs et al. 2002). This complements earlier findings by Raymond and colleagues who report the presence of proteinaceous exhudates from sea ice diatom assemblages with cryoprotective functions (Raymond et al. 1994; Raymond 2000).

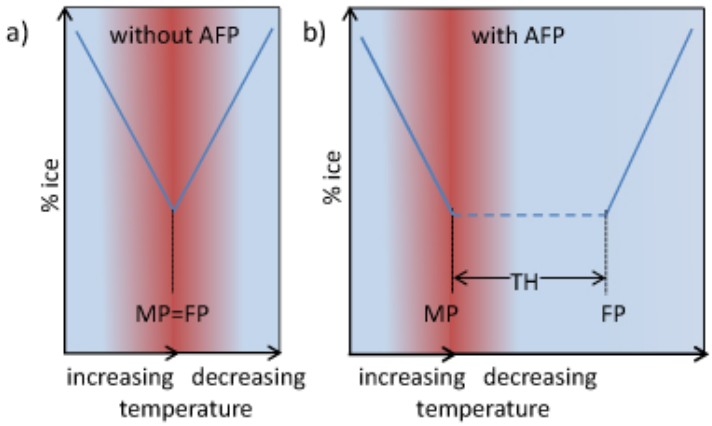

Figure 1.5: When the temperature is raised, an ice crystal decreases in size until it completely melts (MP - melting point). (a) Lowering the temperature results in immediate growth of a small remaining ice crystal (FP - freezing point). (b) In the presence of AFP an offset between the MP and FP is observed (TH - thermal hysteresis).

1.2 Antifreeze proteins

1.2.1 Functions and molecular principles

Antifreeze proteins and antifreeze-glycoproteins (AF(G)Ps) were found to lower the freezing point of a solution below the melting point, i.e. cause thermal hysteresis (TH) (Fig. 1.5), and are therefore also called thermal hysteresis proteins (DeVries and Wohlschlag 1969; Duman and DeVries 1976). This function is especially known from fish and insects, which by this means avoid deadly freezing of the blood or haemolymph (DeVries 1983; Duman 2001).

AFPs from plants were not found to cause significant thermal hysteresis but mainly inhibit recrystallisation, and are thus called recrystallisation inhibitors (Griffith and Yaish 2004). Recrystallisation (Fig 1.6 a, b) is the growth of larger ice crystals at the expense of smaller ones (Knight and Duman 1986), which can cause damage to cell membranes and tissues (Worrall et al. 1998). Other effects of AFPs are the pitting of ice surfaces (Raymond et al. 1989) (Fig. 1.6 i) and the distortion of crystal shapes (Raymond and DeVries 1977) (Fig. 1.6 c-h). A single protein can also exhibit several of these functions (Knight et al. 1988).

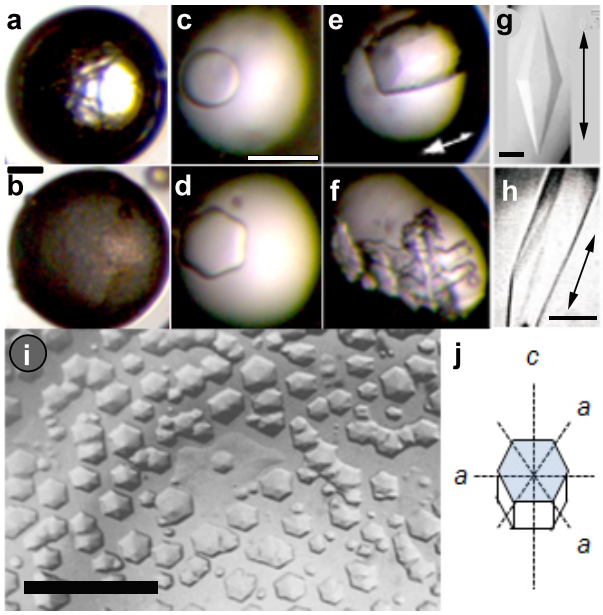

Figure 1.6: Effects of AFPs on ice: (a, b) Recrystallisation inhibition: (a) The negative control appears clear after the incubation period due to recrystallisation, (b) in the presence of an AFP the sample appears turbid due to recrystallisation inhibition. (c-h) Crystal deformation patterns in the presence of AFPs: (c) The negative control shows a round flat ice crystal. (d-f) Crystal patterns observed with hyperactive AFPs show hexagonal shapes (d, e) and a dendritic, radial burst pattern (f). Scale bars for (a-f) are 50 μm. (g, h) In the presence of the moderate type I fish AFP crystals develop to a hexagonal bi-pyramid (g) and show a spicular burst pattern (h). Scale bars 100 μm in (g) and 250 μm in (h), pictures (g, h) from Graether et al. (2000). Arrows indicate direction of the c-axis, if not perpendicular to the paper plane like in (c, d, f). (i) Pitted basal plane of an ice crystal in the presence of an ice active substance. Scale bar is 1 mm, picture from Raymond et al. (1994). (j) Schematic drawing of an ice crystal showing the crystal faces and axes. The upper basal plane is shaded in blue, white planes are the prism planes.

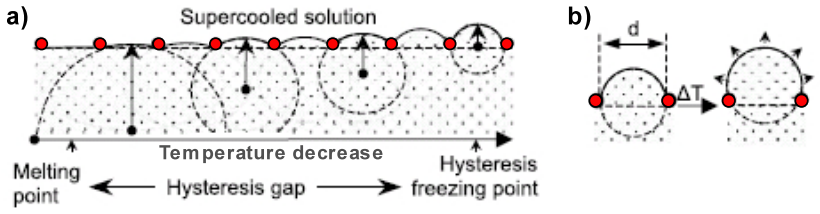

Figure 1.7: Two-dimensional illustrations of spherical ice-caps growing between adsorbed antifreeze proteins (red dots) on an ice surface below the melting point. (a) The convexity changes with temperature until the diameter of the cap equals the adsorbance spacing d, (b) and the crystal grows explosively. Modified after Kristiansen and Zachariassen (2005).

AFPs have been shown to attach to the ice surface via hydrophilic or hydrophobic interactions (e.g. see Graether et al. 2000; Sönnichsen et al. 1996). According to the adsorption inhibition model by Raymond and DeVries (1977) new water molecules can only be added to the ice surface in between the attached proteins (Fig. 1.7). Inside the thermal hysteresis gap, curved ice-caps develop and the crystal does not grow visibly (Fig. 1.7 a) (Raymond and DeVries 1977; Kristiansen and Zachariassen 2005). Once a critical temperature and curvature is reached, the crystal bursts explosively (Fig. 1.7 b) (Kristiansen and Zachariassen 2005).

Recrystallisation inhibition (RI) originates from the altered energy cost of grain boundary migration for water molecules when the ice surface is covered by AFPs (Knight et al. 1988). Distorted ice crystals and pits on ice surfaces (Fig. 1.6 c-i) develop due to the attachment of AFPs to defined faces of a single ice crystal (Raymond et al. 1994; Scotter et al. 2006) (see also Fig. 1.6 j). Ice growth is inhibited at these faces and can only occur at the remaining protein-free crystal faces (Raymond et al. 1994; Scotter et al. 2006). Depending on the nature of the AFP, typical ice crystal shapes develop (Fig. 1.6 c-h). So-called moderate AFPs, e.g. found in fish, with maximal TH between 0.7 °C and 1.5 °C (Duman 2001), bind to the prism planes and thus cause hexagonal bi-pyramidal crystals with bursts along the *c*-axes of the ice crystal (Scotter et al. 2006) (Fig. 1.6 g, h, j). So-called hyperactive AFPs, e.g. found in insects, cause TH of 3 °C to 6 °C (Duman 2001), usually bind to the prism and basal planes (Graether et al. 2000) and cause bursts of radial symmetry in directions of the *a*-axes (Scotter et al. 2006) (Fig. 1.6 d, e, f, j).

1.2.2 Distribution and function of AFPs from sea ice diatoms

In contrast to the broad knowledge on AFPs from fish, insects and plants, only a few studies were published with information on AFPs from sea ice diatoms. Especially on the molecular level, i.e. characteristics of single isoform AFPs and the interaction between AFPs and ice as well as information on the phylogeny and evolution of AFPs based on nucleotide or protein sequences, relative little information was available at the start of the work presented here. In 1994, Raymond and colleagues described ice pitting activity from interstitial water of a diatom rich platelet layer in McMurdo Sound in the Antarctic. The activity was determined to be caused by a proteinaceous macromolecular fraction (Raymond et al. 1994). In this and a later study similar activity was obtained from cell lysates of seven the Antarctic diatom species, whereas no activity was found in temperate diatom species (Raymond et al. 1994; Raymond 2000). Furthermore, it was determined that the active substances were probably gylcoproteins of heterogeneous size distribution, which occurred extracellularly and were solute dependent in their activity (Raymond 2000). Janech et al. (2006) report the production of ice binding proteins from four more sea ice diatom cultures from the Antarctic and for the first time also from Arctic species (see Appendix A for details on the investigated species Tables A.1, A.2). The authors used the terms ice active substances (IAS) and ice binding proteins (IBPs) as the proteins were especially effective in pitting of ice surfaces and causing other deformities, but did not cause considerable freezing point depression (Raymond et al. 1994; Raymond 2000; Janech et al. 2006). However, as outlined by Kiko (2010) the concentrations tested were probably too low to detect TH, and the proteins cause effects on ice similar to those observed for fish and insect AFPs (e.g. compare Raymond et al. 1989 and Raymond et al. 1994). To avoid confusion, in this thesis the term AFP will be used for all groups, as proposed by (Kiko 2010).

The *in situ* function of the sea ice diatom AFPs is not yet clear and will strongly depend on the protein concentration. For RI, e.g. only 100-500 times less AFP is needed than for TH (Ewart et al. 1999). Raymond et al. (1994) proposed that ice pitting activity might cause a roughening of ice platelet surfaces (Fig. 1.2). This could aid attachment

of cells to the ice or increase light scattering, resulting in higher light availability for photosynthesis (Raymond et al. 1994). Extracellular AFPs could also help to maintain the brine channel structure similar as described for EPS (Raymond 2000; Krembs et al. 2000). It was proposed that RI might reduce freeze-thaw damage of cells or organelles and thus act as cryoprotectants in diatoms (Raymond 2000; Raymond and Knight 2003).

Studies using molecular techniques on sea ice diatoms in have revealed further information on their AFPs. First evidence of diatom AFP genes was obtained from a salt stress expressed sequence tag (EST) library from *Fragilariopsis nana*[1] (Krell et al. 2008) and about the same time by protein sequencing and subsequent PCRs from *Navicula glacei* (Janech et al. 2006). These sequences were related to AFPs from the snow mold *T. ishikariensis* and to hypothetical proteins from the bacteria *Cytophaga hutchinsonii* and *Shewanella denitrificans* (Janech et al. 2006; Krell et al. 2008). It was proposed that the diatoms might have acquired AFP genes via horizontal gene transfer (HGT) from either the fungi or bacteria (Janech et al. 2006). Diatom AFPs, however, might also have evolved by convergent evolution from ancestral genes with different functions as reported for plant and fish AFPs (Griffith and Yaish 2004; Cheng 1998; Sandve et al. 2008). As AFPs were neither found in any temperate diatom species (Raymond 2000; Janech et al. 2006), nor were related genes observed in the genomes of the temperate diatoms *Phaeodactylum tricornutum* and *Thalassiosira pseudonana* (Armbrust et al. 2004; Bowler et al. 2008), they seem to be an adaptation mechanism to cold and icy environments (Janech et al. 2006). AFP genes from both, *F. nana* and *N. glacei* carried signal peptides indicating the secretion of the proteins (Krell 2006; Janech et al. 2006) previously hypothesised by Raymond (2000). One sequence of the *F. nana* AFPs did not carry a signal for subcellular localisation (Krell et al. 2008).

[1] The *Fragilariopsis* strain used in our lab, which was isolated by Thomas Mock from the Weddell Sea in 1999, was called *F. cylindrus* in previous studies by Janech et al. (2006), Krell et al. (2008), Bayer-Giraldi et al. (2010), Bayer-Giraldi et al. (2011) and chapters 3 and 4 of this study. According to Lundholm and Hasle (2008) this strain is *F. nana*. In this thesis (except for chapters 3 and 4) the strain and sequences derived thereof are corrected to *Fragilariopsis nana*.

The nucleotide and protein sequences of the diatom and closely related AFPs differ considerably from the well-studied fish, insect and plant AFPs (Janech et al. 2006; Krell et al. 2008). Characterisations of this new group of AFPs include ice pitting, TH activity, crystal morphology, recrystallisation inhibition (RI) and biochemistry from one bacterial (Raymond et al. 2007), one fungal (Hoshino et al. 2003) and one diatom AFP (Janech et al. 2006). The bacterial *Colwellia sp.* AFP was approximately 25 kD in size and showed both, ice binding and RI activity, but only low TH (<0.1 °C, concentration not specified) (Raymond et al. 2007). Purified *Thyphula ishiraiensis* AFP, 23 kDa in size, caused crystal deformation and a TH of approx. 0.95 °C at a concentration of 20 mg protein mL^{-1} (Hoshino et al. 2003). The diatom AFP was an approx. 25 kDa protein, which caused ice pitting on the basal plane of ice crystals, whereas TH was not determined (Janech et al. 2006).

1.2.3 Novel technologies to study AFPs

In addition to the classical approach of measuring antifreeze activity in cell lysates or culture media (Raymond et al. 1994; Raymond 2000; Janech et al. 2006), molecular tools can be applied to study the function and characteristics of AFPs. As already shown in initial molecular studies on diatom AFPs by Janech et al. (2006) and Krell et al. (2008) information can be gained that is not accessible with the classical methods. Sequencing of whole genomes, like that of the Antarctic ice diatom *F. nana* (T. Mock, personal communication), will reveal all AFP isoforms present in one species. The recombinant expression of proteins offers a tool to produce high amounts of pure protein, which can then be used for functional characterisation *in vitro* or structural studies via X-ray or nuclear magnetic resonance (NMR) (Sönnichsen et al. 1996; Ewart et al. 1999; Jia and Davies 2002; Liu et al. 2007; Nishimiya et al. 2008).

All molecular studies on diatom AFPs have so far been pursued on unialgal cultures in laboratory. Metagenomics and metatranscriptomics now offer tools to analyse the presence and activity of genes in the environment as well as provide insights on gene evolution, e.g. horizontal gene transfer (reviews by Heidelberg et al. 2010; Mock and

Kirkham 2011). Metagenome and metatranscriptome data contribute significantly to the knowledge on community composition and function, especially for prokaryotes in marine environments (e.g. Venter et al. 2004; Rusch et al. 2007; Yooseph et al. 2007; Frias-Lopez et al. 2008). Metagenome sequencing is, however, difficult to apply for eukaryotic communities, e.g. due to the large genome size of eukaryotes compared to prokaryotes, the presence of introns and the high repetitiveness (Heidelberg et al. 2010; Grant et al. 2006). Transcriptomic studies are more applicable for eukaryotes and give information on the actual gene activity of communities *in situ* (John et al. 2009). Metgenomic and metatranscriptomic data can also be employed to analyse the presence, activity and phylogeny of single gene classes in the environment in comparison to cultured organisms (Sebastian and Ammerman 2009). Metatranscriptomics are thus a suitable tool to study the activity of AFPs in sea ice communities under given environmental conditions.

1.3 Objectives and outline of this thesis

Antifreeze proteins have been studied only in a few diatom isolates and environmental communities, mainly from the Antarctic. However, the molecular mode of action and precise function of diatom AFPs is still not clear. This thesis aims to further our knowledge on diatom AFPs by investigating AFP activity in diatom isolates with the focus on Arctic species. The function of intracellular diatom AFPs is elucidated by studying the molecular properties of two heterologously expressed AFPs and merging this information with estimates on intracellular AFP concentrations. Information on *in situ* activity of AFP genes is gained by analysing AFP genes from environmental eukaryotic sea ice communities. The thesis is based on three studies, applying cultivation-based methods and molecular tools. Each study is presented in a separate chapter, a summary of which appears below.

Chapter 2 examines the distribution and activity of AFPs in several Arctic and Antarctic diatom isolates. Unialgal diatom cultures were subjected to conditions resembling the formation of sea ice and organism inclusion in the brine pockets in the central ice column, i.e. a temperature shift of 4 °C to -4 °C and accompanying salinity change from 34 to 70. Assessing the recrystallisation inhibition activity of cell lysates provided insights into the presence and regulation of antifreeze components. A comparison with RI activity of a recombinant AFP was used to estimate the concentration and function of AFPs in diatoms. This chapter addresses the hypotheses that AFP activity must be widespread throughout the diatom phylogeny and also be present in Arctic species, and that AFPs are an essential adaptation for diatom survival in sea ice. Furthermore, intracellular concentrations have to be high enough to be adequate for effective functioning.

Chapter 3 describes the heterologous expression and characterisation of two antifreeze proteins from *Fragilariopsis nana*. Molecular methods were applied to produce single isoform AFP in *Escherichia coli*. Thermal hysteresis, recrystallisation inhibition and crystal deformation patterns are used as the basis to discuss the functions of two different AFP isoforms. Information on the molecular action of the recombinant AFP with ice crystals and on the dependence of the activity from protein and solute concentration was derived. This chapter aims to answer the question, if AFPs have similar molecular properties as fish or insect AFPs, although the protein sequences are basically different.

Chapter 4 reports the presence of AFP sequences in environmental samples from sea ice, which resemble those found in diatoms. Large scale sequencing of cDNA from eukaryotic sea ice communities was applied to study the functional expression and phylogenetic relationship of AFP genes *in situ*. Relative abundance and phylogeny of the environmentally active AFP genes are compared to the taxonomical composition of the respective community and to the environmental conditions in the sample. This chapter addresses the hypothesis that AFP genes have to be present and active in eukaryotic sea ice communities and are of relevance for diatoms *in situ*.

In the concluding discussion the main findings are summarised and the distribution and phylogeny of diatom AFPs is evaluated with respect to the habitats and diatom taxonomy. The subcellular localisation and function of AFPs in diatoms is discussed. Possible ecological roles of diatom AFPs in the sea ice habitat are considered and an outlook on future research is given.

List of publications

This doctoral thesis is based on the following manuscripts (Chapters 2 and 4) and publication (Chapter 3):

Chapter 2: Christiane Uhlig, Tim Eberlein, Anika Seidler, Maddalena Bayer-Giraldi, Bánk Beszteri, Andreas Krell, Gerhard S. Dieckmann. Recrystallisation Inhibition in Arctic and Antarctic diatom isolates, Manuscript draft

The experiments were planned by myself and Andreas Krell. I established the monoclonal diatom cultures. Experiments and data acquisition were realised by me with support of Tim Eberlein and Anika Seidler. I interpreted the data and wrote the manuscript with contributions of the co-authors.

Chapter 3: Christiane Uhlig, Johannes Kabisch, Gottfried J. Palm, Klaus Valentin, Thomas Schweder, Andreas Krell. Heterologous expression, refolding and functional characterisation of two antifreeze proteins from *Fragilariopsis cylindrus* (Bacillariophyceae), Cryobiology (2011), doi:10.1016/j.cryobiol.2011.08.005

The idea for this manuscript was developed by myself and Andreas Krell. Heterologous expression and cleanup of the AFPs were done by myself with support of the co-authors in Greifswald. Functional characterisation and data interpretation were done by me. I wrote the manuscript in collaboration with all co-authors.

Chapter 4: Christiane Uhlig, Fabian Kilpert, Klaus Valentin, Jessica Kegel, Andreas Krell, Thomas Mock, Bánk Beszteri. Differential abundance and phylogenetic diversity of AFP transcript fragments in environmental transcriptomes from polar sea ice, to be submitted to FEMS Microbiology Ecology, Thematic Issue Polar and Alpine Microbiology

The idea for this manuscript was developed by myself and Bánk Beszteri. Data analysis was conducted by myself, with support of Fabian Kilpert for the phylogenetic placement of the environmental AFP sequences. The manuscript was written by myself with contributions of the coauthors.

2 Recrystallisation Inhibition in Arctic and Antarctic diatom isolates

Christiane Uhlig, Tim Eberlein, Anika Seidler, Bánk Beszteri, Maddalena Bayer-Giraldi, Andreas Krell, Gerhard S. Dieckmann

Abstract

Diatoms constitute one of the major fractions of biological assemblages in sea ice. They contribute significantly to polar primary production and serve as important food source for higher trophic levels. Diatoms are able to thrive in sea ice due to a suit of adaptation mechanisms including the production of antifreeze proteins (AFPs). By subjecting cultures of Arctic and Antarctic diatom species to high salinity and subzero temperatures, we studied the abundance and activity of AFPs in polar diatom species spread over the entire diatom phylogeny. AFP activity, measured as recrystallisation inhibition, was observed in all 11 isolates, irrespective whether they were isolated from the water column or from sea ice. AFP activity was regulated by temperature and salinity stress in *Entomoneis sp.*, *Navicula sp.* sensu lato III and *Porisira glacialis*, whereas the 8 other species did not show a clear regulation. Recrystallisation, measured with an optical recrystallometer, showed an exponential decay function relative to the protein concentration for a *Fragilariopsis nana* cell extract and a recombinant AFP. This correlation allowed us to estimate AFP concentration as AFP equivalents per cell. Concentrations of 0.3 to 68.5 μM AFP equivalent confirm the intracellular function of diatom AFPs as recrystallisation inhibitors, but also lie in the range of concentrations required for thermal hysteresis.

2.1 Introduction

Subjected to a seasonally changing extent, sea ice expands up to $16{\cdot}10^6$ km^2 in Antarctica and $14{\cdot}10^6$ km^2 in the Arctic, thus constituting one of the largest ecosystems in the world (Comiso and Nishio 2008). When sea ice forms pelagic organisms become incorporated into microscopic channels and pockets (Gleitz and Thomas 1992; Eicken 1992) inside the ice matrix. In the ice the organisms encounter subzero temperatures as low as -20°C and corresponding brine salinities of over 200 (Cox and Weeks 1983). Although the organisms are exposed to rapid changes and extremes in abiotic conditions compared to the relatively stable sea water system, biomass within the sea ice can exceed that in the water column below by as much as a factor of 10^3 (Eicken 1992; Thomas and Dieckmann 2002). In Antarctic waters, photosynthetic sea ice organisms contribute to up to 5% of the annual primary production (Lizotte 2001). Diatoms frequently dominate sea ice assemblages, contributing significantly to primary production (Lizotte 2001) and serving as food source for higher trophic levels (e. g. krill, metazoans) (Krembs et al. 2000; Thomas and Dieckmann 2002; Loeb et al. 1997).

Organisms inhabiting brine channels and pores in sea ice are successful due to a whole suite of physiological and biochemical adaptations (Mock and Thomas 2005). By accumulation of salts as well as compatible solutes such as glycerol, sorbitol or proline (Kirst 1990) cells regulate osmolality and thus turgor pressure, when subjected to elevated salinity. Through formation of poly-unsaturated fatty acids, membrane fluidity is maintained under low temperatures (Nichols et al. 1995). Exopolymeric substances produced by bacteria and diatoms (e.g. *Melosira arctica*) can alter brine pore morphologies (Krembs et al. 2011) and create a microenvironment that protects the cells from dehydration and potentially harmful ice crystals (Krembs et al. 2002). Raymond et al. (1994; 2003) previously reported the release of ice active proteins by sea ice diatoms. These proteins can inhibit recrystallisation, which is the growth of larger ice crystals at the expense of smaller ones, and thus circumvent or reduce mechanical damage caused by ice crystals (Raymond and Knight 2003; Janech et al. 2006). The proteins were reported to bind to the ice, thus

causing pitting on ice surfaces (Raymond et al. 1989). Recently, AFPs from the diatoms *Chaetoceros neogracile* and *Fragilariopsis nana* were also found to produce thermal hysteresis, i.e. to non-colligatively depress the freezing point (Gwak et al. 2010; Uhlig et al. 2011; Bayer-Giraldi et al. 2011). The *in situ* function of ice active proteins produced by diatom is still under discussion but strongly depends on the *in situ* concentrations. Recrystallisation inhibition (RI) requires only 100 to 500 times less protein than thermal hysteresis (TH) (Ewart et al. 1999). Due to the different characteristics and effects, the nomenclature of these proteins varies and a multitude of methods has been developed to study AFPs. Compliant with Kiko (2010 and Bayer-Giraldi et al. (2010) we will use the term antifreeze proteins (AFPs). In this study we assess the recrystallisation inhibition activity of AFPs using two different methods. A Clifton Nanolitre Osmometer was used to measure AFP activity in terms of RI and crystal deformation and compared to RI measured by an optical recrystallometer (Wharton et al. 2007).

Up to now information on AFP activity in diatoms is rather sparse. Several studies report AFPs from single Antarctic diatom species like *Navicula glacei* (Janech et al. 2006), *Fragilariopsis nana* and *F. curta* (Krell et al. 2008; Bayer-Giraldi et al. 2010), *Chaetoceros neogracile* (Gwak et al. 2010), and ice associated diatom assemblages (Raymond et al. 1994; Raymond 2000; Raymond and Knight 2003). Raymond (2000) report ice pitting activity in a sample dominated by pennate diatom from Resolute, Canada, Arctic. The presence of diatom AFPs thus seems to be a bipolar phenomenon. As yet, there is no information available on the broad phylogenetic distribution of AFPs in Bacillariophyta.

By demonstrating the presence of AFPs in several new diatom genera and families, especially from the Arctic, this study contributes to the knowledge on the phylogenetic and local distribution of AFPs in diatoms. The optical recrystallometer and a calibration with a recombinant AFP, allowed us to estimate AFP equivalent concentrations within the cell. Intracellular concentrations calculated are well within the range necessary for recrystallisation inhibition and close to concentrations required for thermal hysteresis.

2.2 Material and Methods

2.2.1 Recrystallisation inhibition and crystal deformation assays

The presence of AFPs in cell extracts was measured using an optical recrystallometer (Otago Instruments) (Wharton et al. 2007) and a nanolitre osmometer (according to Kiko 2010) (Clifton Technical Physics). Both instruments can be used to measure recrystallisation. A freshly frozen sample appears opaque due to the formation of a multitude of small crystals, since little light will pass through the sample. Recrystallisation causes the growth of lager crystals, the scatter inside the sample decreases, more light passes through and the sample appears brighter or transparent. In the presence of a recrystallisation inhibitor (e.g. AFP) the opacity does not or hardly decrease.

For measurements with the optical recrystallometer 150 μL sample was transferred to the bottom of a glass tube that serves as sample holder and frozen in a freezer for 1 h at -20 °C. The tube was transferred on ice to the instrument, quickly wiped with a paper towel to remove condensation and inserted into the measuring block. The sample was kept at -4.0 °C ± 0.2 °C for one hour and the transmission of light was logged. An index of recrystallisation (R_{OR}) was calculated as follows:

(2.1) R_{OR}=T_{60}-T_{10}, with T_t: transmission (in mV) at time t (in min).

Dilution series of *F. nana* Ant cell extract (5 - 200 μg mL^{-1}) and of a recombinant AFP (fcAFP) (Bayer-Giraldi et al. 2011) (0.02 - 20 μg mL^{-1}) were assayed in the optical recrystallometer. The calibration curve resulting from fcAFP was used to calculate the concentration of AFP equivalents (c_{AFPeq}) in cell extracts. The AFP fraction of total protein (AFPeq) was calculated by dividing the c_{AFPeq} by the total protein concentration used for the measurement (approx. 150 μg μL^{-1}).

(2.2) c_{AFPeq}(μg μL^{-1})=$10^{((R-4,6)/(-3,2))}$

(2.3) AFPeq (of total protein) = c_{AFPeq} / c_{total} · 100

In the nanolitre osmometer the sample was loaded in duplicates to the sample holder and deep frozen to approx. -40 °C. After reaching the annealing temperature of -4.0 °C the turbidity of samples was documented at 0 and 20 min incubations. In addition, the deformation of crystals caused by the presence of AFPs was determined. For this purpose, the crystals were melted until only one small crystal remained. Subsequently, the temperature was lowered slowly to initiate crystal growth. Without AFP activity, crystals grow as circular disks, whereas they show deformations to hexagons, stars, or other sharper edges in presence of AFP (Bravo and Griffith 2005). In order to compare nanolitre osmometer results from different samples, we developed a scheme to classify results for recyrstallisation and crystal deformation. Numbers denote respective observations: (1) presence of RI and deformed crystals in both samples, (2) RI in one of both samples and deformed crystals, (3) no RI but deformed crystals and (4) neither RI nor deformed crystals.

2.2.2 Diatom cultures

All Arctic diatom cultures, except for *Thalassiosira nordenskioeldii* CCMP 997, were isolated from sea ice collected in Kongsfjord from 2^{nd} till 8^{th} May 2009 (for details see Table 2.1 and 2.2). Antarctic cultures were kindly supplied by the UTS Sydney, University of East Anglia or were available at the Alfred Wegener Institute for Polar and Marine Research (Table 2.2). Previous studies by Mock and Valentin (2004) and Krell et al. (2007; 2008) were done with *F. nana* Ant (isolated by Mock, 1999), however, in those studies called *F. cylindrus*. Lundholm and Hasle (2008) identified this culture as *F. nana* and hence it will be referred to accordingly in our study.

Stock cultures were grown in ANT F/2 medium (Guillard and Ryther 1962) at 5 °C under continuous illumination of approximately 25 μmol photons m^{-2} s^{-1}. Cultures were clonal but non-axenic. Stock cultures were handeled by aseptic procedures, whereas experimental cultures were treated as clean as possible but non-sterile. A culture of the temperate diatom *Phaeodactylum tricornutum* was kept in ANT F/2 medium under continuous illumination of 25 μmol photons m^{-2} s^{-1} and 20 °C and used as negative control for AFP activity measurements.

Table 2.1: Arctic diatom species under investigation in this study. Listed are the isolate name and species, an abbreviation for each species that will be used throughout the manuscript, isolation site and position, a closer description, whether the isolates were isolated from the water or sea ice, as well as the source i.e. person, who isolated the clone (with isolation date) or who supplied the culture.

Name / species	Abbreviation	Isolation site position	Ice / water column	Source (**isolated by** / supplied by)
Navicula sp. sensu lato I KFI B2	Na.sp I	Arctic, Kongsfjord 78.8910N 12.3627E	ice	**C. Uhlig**, 2009
Fragilariopsis nana KFII A4	F.nana Arc	Arctic, Kongsfjord 78.9653N 12.3339E	ice	**C. Uhlig**, 2009
Navicula sp. sensu lato II KFIII A2	Na.sp II	Arctic, Kongsfjord 78.9653N 12.3339E	ice	**C. Uhlig**, 2009
Entomoneis sp. KFV B4	En.sp	Arctic, Kongsfjord 78.8539N 12.4661E	ice	**C. Uhlig**, 2009
Navicula sp. sensu lato III KFV C1	Na.sp III	Arctic, Kongsfjord 78.8539N 12.4661E	ice	**C. Uhlig**, 2009
Nitzschia sp. KFV C2	Ni.sp	Arctic, Kongsfjord 78.8539N 12.4661E	ice	**C. Uhlig**, 2009
Thalassiosira nordenskioeldii CCMP 997	T.nor	Arctic, North Atlantic,Tromsø 69.6667N 18.9667E	n.a.	**E. Syvertsen**, 1978

Table 2.2: Antarctic diatom species under investigation in this study. Listed are the isolate name and species, an abbreviation for each species that will be used throughout the manuscript, isolation site and position, a closer description, whether the isolates were isolated from the water or sea ice, as well as the source i.e. person, who isolated the clone (with isolation date) or who supplied the culture.

Name / species	Abbreviation	Isolation site position	Ice / water column	Source (**isolated by** / supplied by)
Fragilariopsis nana TM99	F.nana Ant	Antarctic, Weddell Sea n.A.	ice	**T. Mock**, 1999
Eucampia antarctica CCMP 1452	E.ant	Antarctic, McMurdo Sound 77.8333S 163.0000E (approx.)	n.a. ice edge 25m	**G. Fryxell**, 1991
Porosira glacialis UEA09	P.gla	Antarctic n.A.	n.A.	S. Chollet University of East Anglia, UK
Proboscia inermis UTS08	P.ine	Antarctic n.A.	n.A.	K. Petrou UTS Sydney, Australia

2.2.3 Strain identification

Cells were harvested on polycarbonate filters (pore size 1.2 μm, Millipore), immediately frozen in liquid nitrogen and stored at -80 °C. Genomic DNA was isolated using the DNeasy Kit Plant Mini Kit (Qiagen) according to the manufacturers protocol except for the following modification. For lysis, cells were washed off the filter with 400 μL AP1 buffer and incubated for 1 h at 65 °C after adding RNAse and Proteinase K to final concentrations of 1 μg μL^{-1} and 0.01 μg μL^{-1}, respectively. 18S rDNA was amplified using the Phusion Polymerase (Finzymes) and primers EukA (1F) and EukB (1528R) (Medlin et al. 1988) with the following cycling conditions: initial denaturation at 98 °C for 2 min, followed by 34 cycles each comprising 98 °C for 5 sec, 62 °C for 30 sec and 72 °C for 90 sec; and finally 72 °C for 5 min. PCR products were purified with the MinElute PCR Purification Kit (Qiagen) and amplified with each of the primers EukA (1F), E528F (528F) (Edgcomb et al. 2002) or 1055R (Elwood et al. 1985) and 1528R (EukB) (Medlin et al. 1988) using the ABI Prism BigDye Terminator v3.1 Cycle Sequencing Kit (Applied Biosystems) in a temperature program of one initial step of 96 °C for 1 min followed by 30 cycles of 96 °C for 10 sec, 60 °C for 5 sec and finally 60 °C for 3 min. Products were prepared with the DyeEx Kit (Qiagen) and analysed on an ABI Prism 3130xl Genetic Analyzer (Applied Biosystems).

Vector clipping and assembly of partial sequences was accomplished in Gap v4.10 from the Staden Package (Staden 1996). Assembled sequences were aligned in the SILVA Web Aligner (Pruesse et al. 2007) SSU database release version 103 including the ten nearest neighbour sequences of each sequence into the result. This database was merged in ARB (Ludwig et al. 2004) with the SILVA SSUref database release version 102, which was previously reduced to all diatom sequences and three bolidophytes as outgroup.

Additionally, cultures were characterised by light and scanning electron microscopy (SEM). Living samples were studied in Uthermöhl chambers using an Axiovert inverted microscope (Carl Zeiss). Raw material and frustules, cleaned according to Simonsen (Simonsen 1974), were dried onto circular glass coverslips. After coating samples with gold/palladium, SEM pictures were taken in a Quanta FEG 200 (FEI).

2.2.4 Experimental procedures

Six replicate cultures of each species were grown in 2 L Erlenmeyer flasks filled with 1.3 L ANT F/2 medium (Guillard and Ryther 1962) aerated with sterile filtered air. Temperature and light regime was kept at 5 °C and continuous illumination of 25 μmol photons m^{-2} s^{-1} in Rumed light thermostats (Rubarth Apparate GmbH). During the exponential growth phase the replicates were split into three replicates of control cultures that were kept at 5 °C and a salinity of 34, and three replicates of cultures treated at a lowered temperature of -4 °C and elevated salinity of 70. Salinity was elevated by addition of approx. 200 mL brine (25 g Sea Salts (Sigma) in 100 mL ANT F/2) into the culture flask at a rate of 1 mL min^{-1} (Ismatec REGLO Digital, Ismatec). To account for dilution effects the same amount of ANT F/2 medium was added to the non-treated cultures. The temperature of the thermostats was lowered to -4 °C simultaneously to the start of the brine addition. Cultures were monitored at respective conditions for 5 to 8 days after this treatment.

Samples for determination of cell densities were taken every other day, preserved in a final concentration of approx. 5% Lugol´s solution (Throndsen 1978) and stored at 5 °C in the dark for later enumeration. Additional samples were preserved in a final concentration of 5% buffered Formalin (Merck) and stored at 5 °C for later determination of potential bacterial contamination. Samples were stained with DAPI (4',6-diamidino-2-phenylindole-dichloride (Merck)) at 5 μg μL^{-1} final concentration, filtered on respective filters used for sampling, and studied with fluorescent light (365nm) under an Axioskop 2 (Carl Zeiss) microscope.

To determine the presence of AFPs, samples were taken immediately before the treatment, two days after the treatment and at the end of the experiment. Approximately 250 mL culture volume was filtered on polycarbonate filters (Millipore) of a pore size between 1.2 and 5.0 μm, depending on the cell size of the species. Filters were flushed with approx. 100 mL sterile filtered seawater to reduce bacterial contamination, before they were transferred into cryo vials and flash frozen in liquid nitrogen. Samples were stored at -80 °C until processing.

Physiology

Maximum photosynthetic quantum yield of photosystem II (F_v/F_m) was monitored daily or every other day as a proxy for general cell fitness (Maxwell and Johnson 2000). Cells were dark adapted at the experimental temperature for 15 min and subsequently analysed using a Xenon-PAM-Fluorometer (Walz, Germany). Cell densities were determined from Lugol preserved samples using Sedgwick-Rafter Cells (S50, Graticules) and a stereomicroscope (Carl Zeiss).

Preparation of cell extracts

Cells were washed off the filter with 1 mL homogenisation buffer (10 mM Tris, 100 mM NaCl, pH 8.0 at 4 °C) and transferred to a microcentrifuge tube. Disruption of cells was achieved by 5 cycles of 1 min continuous sonication at a power setting of 15 to 20% (Sonopuls HD 2070 sonicator, Bandelin). The samples were kept on ice during the entire treatment. The homogenate was centrifuged at 20,000 g at 4 °C for 15 min and the supernatant collected for further analysis. In cases of low protein concentration in the supernatant, sonication was repeated after adding 1 mL homogenisation buffer to the pellet produced during centrifugation. Protein concentrations of supernatants were determined with the modified Bradford assay described by Zor and Selinger (1996) measuring at wavelengths of 450 and 600 nm (instead of 590 nm) in a Synergy HT plate reader photometer (BioTek). A standard curve was prepared with BSA for each plate. Total protein concentration of the lysates was adjusted to a concentration of 150 μg mL^{-1} by concentration over Amicon Ultra-0.5 Centrifugal filter devices (10K) (Millipore) or dilution with the homogenisation buffer. For sample concentration the columns were used according to the manufacturers recommendations with centrifugation steps of 14,000 g at 4 °C for 8 min and a prior wash step with 400 μL of the cell extraction buffer. The presence of AFPs in cell extracts was measured using an optical recrystallometer (Wharton et al. 2007) and a nanolitre osmometer (Clifton Technical Physics) as described above.

Stability under temperature and protease

The effect of temperature and protease on antifreeze activity was tested for one sample of each species. Protein concentration in the cell extracts was 150 μg mL^{-1}. Pronase E (Sigma) was added to a final concentration of 1 mg mL^{-1}. Negative controls were run with BSA at 1 mg mL^{-1} instead of Pronase E. Samples were incubated for 1 h at 20 °C and tested for activity with the nanolitre osmometer. Subsequently, samples were incubated for an additional 20 min at 95 °C and the activity assayed. Selected samples were digested at higher protein concentration and analysed on SDS-PAGE (Laemmli 1970) with Coomassie staining to verify successful digestion.

2.3 Results

2.3.1 Comparison of methods for determination of recrystallisation inhibition

In the Clifton Nanolitre Osmometer the buffer control and the BSA negative controls did not show recrystallisation inhibition (RI) activity (Fig. 2.1 a). The presence of a non-AFP protein (BSA or *P. tricornutum* cell extract) resulted in some RI measured in the optical recrystallometer compared to the buffer control without protein (Fig. 2.1 a). Low protein content or low activity (i.e. buffer without BSA, all BSA concentrations, all *P. tricornutum* cell extracts and 5 and 10 μg μL^{-1} *F. nana* cell extract) resulted in high variability in the optical recrystallometer (Fig 2.1 a).

For the *F. nana* cell extracts we defined two different categories in the Clifton Nanolitre Osmometer; lower activity (category 2) for 5-50 μg protein mL^{-1} and higher activity (category 1) at 100-200 μg protein mL^{-1} (Fig. 2.1 a). Recrystallisation (R_{OR}) measured with the optical recrystallometer showed an inverse linear correlation to the protein concentration (μg mL^{-1}) on $\log_{10}$ scale for a *F. nana* cell extract and the recombinant AFP (fcAFP) (Fig. 2.1 b). For the *F. nana* cell extract the correlation was linear in a concentration range of 5-50 μg mL^{-1}. At 5 μg protein mL^{-1} *F. nana* cell extract showed RI

comparable to the negative control *P. tricornutum* (R=7.48 (±1.00) at 150 μg mL^{-1}). Above 50 μg protein mL^{-1} in *F. nana* cell extract, with R=2.44 (±0.50), no further decrease of recrystallisation was observed. For the recombinant fcAFP the correlation was linear from 0.02 to 20 μg mL^{-1}, with values between R=10.23 (±1.32) and R=0.45 (±0.27), respectively. The slopes of both regressions did not differ significantly with -3.95 (±0.89) for *F. nana* cell extract and -3.24 (±0.36) for fcAFP. By comparing both calibrations we set a valid calibration range of 2.44 <R >7.48 to calculate AFP equivalents of total protein (AFPeq) in the cell extracts.

2.3.2 Strain identification

Taxonomic identification of the Arctic isolates was based on 18S rDNA sequences, light microscopy and SEM, although species level identification was challenging, due to the scarcity of reference literature from these habitats. Results of all methods matched well except for isolate KFV C1, which grouped into the *Nitzschia* clade based on 18S analysis, whereas microscopic observations clearly indicated its classification into Naviculaceae. The three strains identified as *Navicula sp.* sensu lato will be referred to as *Navicula sp.* in the following. Species investigated in this study are listed in Tables 2.1 and 2.2, and light and electron micrographs, as well as phylogenies showing their classification based on 18S rDNA sequences, can be found in supplementary materials (Supplementary Fig. 2.15, 2.16, 2.17, 2.18, 2.19, 2.20, 2.20, 2.21, 2.22).

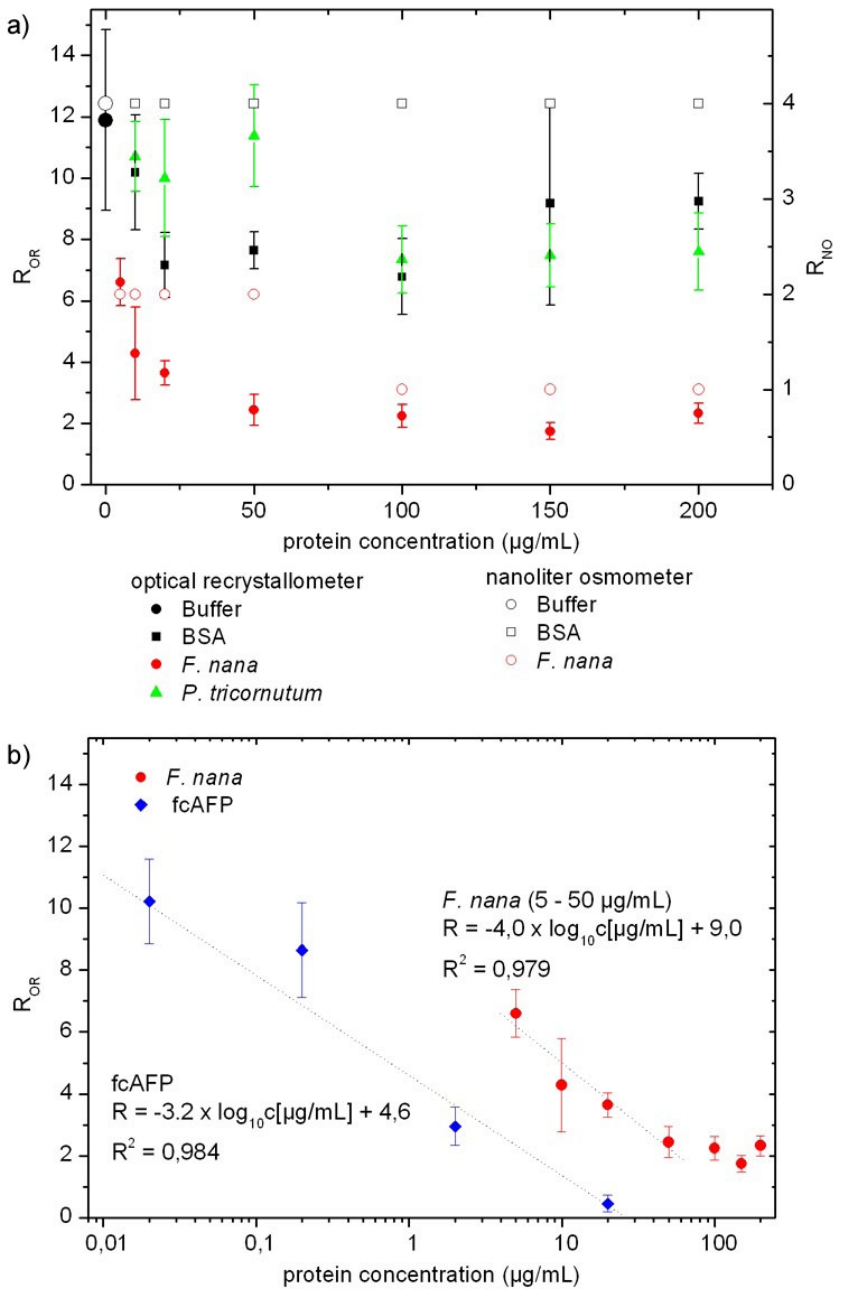

Figure 2.1: Recrystallisation (R) vs. protein concentration of BSA (black squares) and cell extracts of *F. nana* Ant (red circles), *P. tricornutum* (green triangles), recombinant *F. nana* AFP (fcAFP) (Bayer-Giraldi et al. 2011) (blue squares) and buffer without protein (black circles). (a) Comparison of R against protein concentrations measured with the optical recrystallometer (closed symbols) and the Clifton Nanolitre Osmometer (open symbols). (b) Linear inverse correlation of R to $\log_{10}$ of the protein concentration. A low R value indicates high recrystallisation inhibition, OR: optical recrystallometer, NO: nanolitre osmometer

2.3.3 Physiology and AFP activity under temperature and salinity stress

Navicula sp. I grew exponentially at rates of 0.49 (±0.06) (control) and 0.44 (±0.08) (treated) divisions day^{-1} (Supplementary Table 2.3). Regardless of the change in temperature and salinity, treated cultures maintained a similar growth as the controls. Photosynthetic quantum yield of the treated cultures decreased from 0.65 (±0.05) to 0.46 (±0.08) during treatment, whereas control cultures were stable at 0.66 (±0.01) up to day 4 (Fig. 2.2), subsequently declining until the end of the experiment. RI activity was present in all measured *Navicula sp.* I cultures. Activity increased for the treated cultures after the stress induction, whereas the activity of the non-treated culture stayed constant (Fig. 2.2 and 2.13).

Fragilariopsis nana Arc grew exponentially at rates of 0.49 (±0.04) (control) and 0.55 (±0.04) (treated) divisions day^{-1} (Supplementary Table 2.3). Upon stress induction, treated cultures show a decrease in cell number stabilising by the end of the experiment. The control cultures first continued growing until they reached the stationary phase, which was followed by a decrease in the last two days of the experiment. Photosynthetic quantum yield of the treated cultures declined upon treatment from 0.60 (±0.03) to 0.27 (±0.04), whereas control cultures were stable at 0.59 (±0.02) up to day 2 (Fig. 2.3), subsequently slightly decreasing until the end of the experiment. Prior to treatment (T0) control cultures did not show RI activity. All other treatments of *F. nana* Arc showed RI, with the maximal value for the treated cultures 7 days after the treatment (T2) (Fig. 2.3 and 2.13).

Navicula sp. II grew exponentially at rates of 0.44 (±0.02) (control) and 0.41 (±0.02) (treated) divisions day^{-1} (Supplementary Table 2.3). Regardless of the change in temperature and salinity, treated cultures maintained a slow growth until day 3 after the beginning of the treatment. The control cultures also reached their maximum cell number 3 days after T0, followed by a rapid decrease. Photosynthetic quantum yield of the treated cultures decreased upon treatment from 0.56 (±0.05) to 0.21 (±0.04), whereas

control cultures increased from 0.54 (±0.06) to 0.70 (±0.01) (Fig. 2.4). High RI activity was present in all *Navicula sp.* II cultures, yet activity in the treated cultures increased after the stress induction. Maximal RI values were obtained for the non-treated cultures at T2 (Fig. 2.4 and 2.13).

Entomoneis sp. grew exponentially at rates of 0.49 (±0.02) (control) and 0.48 (±0.01) (treated) divisions day^{-1} (Supplementary Table 2.3). The change in temperature and salinity arrested growth in the treated cultures. Control cultures reached the maximum 3 days after T0 and stayed in stationary phase. Photosynthetic quantum yield of the treated cultures decreased upon stress induction from 0.74 (±0.01) to 0.44 (±0.04), subsequently recovering to 0.57 (±0.05) towards the end of the experiment (Fig. 2.5). Control cultures showed a stable photosynthetic quantum yield of 0.73 (±0.02). Reasonable RI activity was only found in *Entomoneis sp.* cultures after the change of temperature and salinity, whereas only a slight activity was also found in the control samples at T2 (Fig. 2.5 and 2.13).

Navicula sp. III grew exponentially at rates of 0.44 (±0.03) (control) and 0.43 (±0.02) (treated) divisions day^{-1} (Supplementary Table 2.3). The change in temperature and salinity caused a slight decrease in cell numbers and arrested growth in the treated cultures, whereas control cultures continued growing. Photosynthetic quantum yield of the treated cultures decreased upon stress induction from 0.68 (±0.01) to 0.48 (±0.05) and thereafter recovered to 0.54 (±0.01) (Fig. 2.6). In control cultures photosynthetic quantum yield decreased slightly from day 3 until the end of the experiment. RI activity was elevated in *Navicula sp.* III cultures after the change in temperature and salinity, yet some activity was also found for the control samples except for T0 (Fig. 2.6 and 2.13).

Nitzschia sp. grew exponentially at rates of 0.47 (±0.03) (control) and 0.46 (±0.04) (treated) divisions day^{-1} (Supplementary Table 2.3). The change in temperature and salinity caused a decrease in cell numbers in treated cultures, with a subsequent slight recovery. Control cultures reached their maximum 1 day after T0, subsequently merging into stationary phase. Photosynthetic quantum yield of the treated cultures decreased upon treatment from 0.66 (±0.01) to 0.46 (±0.03) and thereafter recovered to 0.54 (±0.01).

Control cultures had a stable photosynthetic quantum yield of 0.67 (±0.01) upon day 3 after stress induction, followed by a slight decrease until the end of the experiment (Fig. 2.7). High RI activity was present in all measured *Nitzschia sp.* cultures. In the control cultures, activity increased over the course of the experiment, whereas it was not triggered by the change in temperature and salinity (Fig. 2.7 and 2.13).

Thalassiosira nordenskioeldii grew exponentially at rates of 0.55 (±0.05) (control) and 0.49 (±0.05) (treated) divisions day^{-1} (Supplementary Table 2.3). The change in temperature and salinity arrested growth in the treated cultures. Control cultures reached a maximum cell density 3 days after T0 and stayed in a stationary phase till the end of the experiment. Photosynthetic quantum yield of the treated cultures decreased upon stress induction from 0.72 (±0.01) to 0.49 (±0.05) Fig. 2.8) whereas control cultures showed a stable photosynthetic quantum yield of 0.72 (±0.01). RI activity was absent (control) or low (treated) at T0 in *T. nordenskioeldii* cultures, whereas it increased for treated and non-treated cultures at the later sampling points (Fig. 2.8 and 2.13).

Fragilariopsis nana Ant grew exponentially at rates of 0.68 (±0.09) (control) and 0.61 (±0.08) (treated) divisions day^{-1} (Supplementary Table 2.3). Upon stress induction, cell numbers in treated and non-treated cultures dropped until day 3 after the treatment. In both treatments growth resumed and the stationary phase was reached on day 6. The salinity and temperature stressed cultures attained maximum cell numbers of approx. 60% of those in the controls. Photosynthetic quantum yield of the treated cultures declined from 0.60 (±0.02) to 0.33 (±0.08), upon stress induction, whereas control cultures were stable at 0.59 (±0.01) until day 2 (Fig. 2.9) and subsequently decreased slightly until the end of the experiment. RI activity was present in all *F. nana* Ant cultures, but in the treated cultures increased continuously after subjection to the temperature and salinity stress (Fig. 2.9 and 2.13).

Eucampia antarctica grew exponentially at rates of 0.33 (±0.04) (control) and 0.36 (±0.06) (treated) divisions day^{-1} (Supplementary Table 2.3). Due to change in temperature and salinity, cell numbers of treated cultures dropped slightly and remained constant, whereas the control continued growing exponentially after one day. Photosynthetic quan-

tum yield of the treated cultures declined upon stress induction from 0.61 (±0.01) to 0.10 (±0.03), whereas control cultures were stable at 0.63 (±0.03) until the end of the experiment (Fig. 2.10). RI activity was found in *E. antarctica* cultures, yet protein concentration in the stressed cultures was too low to exhibit activity (Fig. 2.10 and 2.13).

Proboscia inermis grew exponentially at rates of 0.45 (±0.06) (control) and 0.50 (±0.02) (treated) divisions day^{-1} (Supplementary Table 2.3) after a short lag phase (Fig. 2.11). Upon stress induction, growth of treated cultures stopped. At the same time the cell numbers in control cultures decreased and resumed growing after day 1. Photosynthetic quantum yield of the treated cultures declined from 0.59 (±0.08) to 0.10 (±0.02) upon stress induction, whereas control cultures were stable at 0.56 (±0.03) until the end of the experiment (Fig. 2.11). RI activity was found in *P. inermis* cultures and increased in control cultures during the course of the experiment (Fig. 2.11 and 2.13).

Porisira glacialis grew exponentially at rates of 0.29 (±0.01) (control and treated) divisions day^{-1} (Supplementary Table 2.3). After the change in temperature and salinity, growth of treated cultures ceased, whereas the control cultures continued growing exponentially. Photosynthetic quantum yield of the treated cultures declined upon stress induction from 0.55 (±0.01) to 0.37 (±0.06). Control cultures showed maximum quantum yield values of 0.66 (±0.03) (Fig. 2.12). RI activity was not observed in control cultures of *P. glacialis* and increased in the treated cultures due to the temperature and salinity treatment (Fig. 2.12 and 2.13).

2.3.4 AFPeq content estimation

Applying the correlation of the recrystallisation measured with the optical recrystallometer (R_{OR}) to the protein concentration of fcAFP, we were able to calculate AFP equivalents (AFPeq) per cell. The slight recrystallisation inhibition in the negative control (*P. tricornutum*) at a protein concentration of 150 μg mL^{-1} (Fig. 2.1 a) resulted in a calculated value of 0.11% (±0.07%) AFPeq of total protein (cf. Eq. 2.2, 2.3; Fig. 2.13). This value was considered as a baseline and no predication on AFP activity or presence can be drawn from data below this baseline. In some cases, however, even when RI observed with the

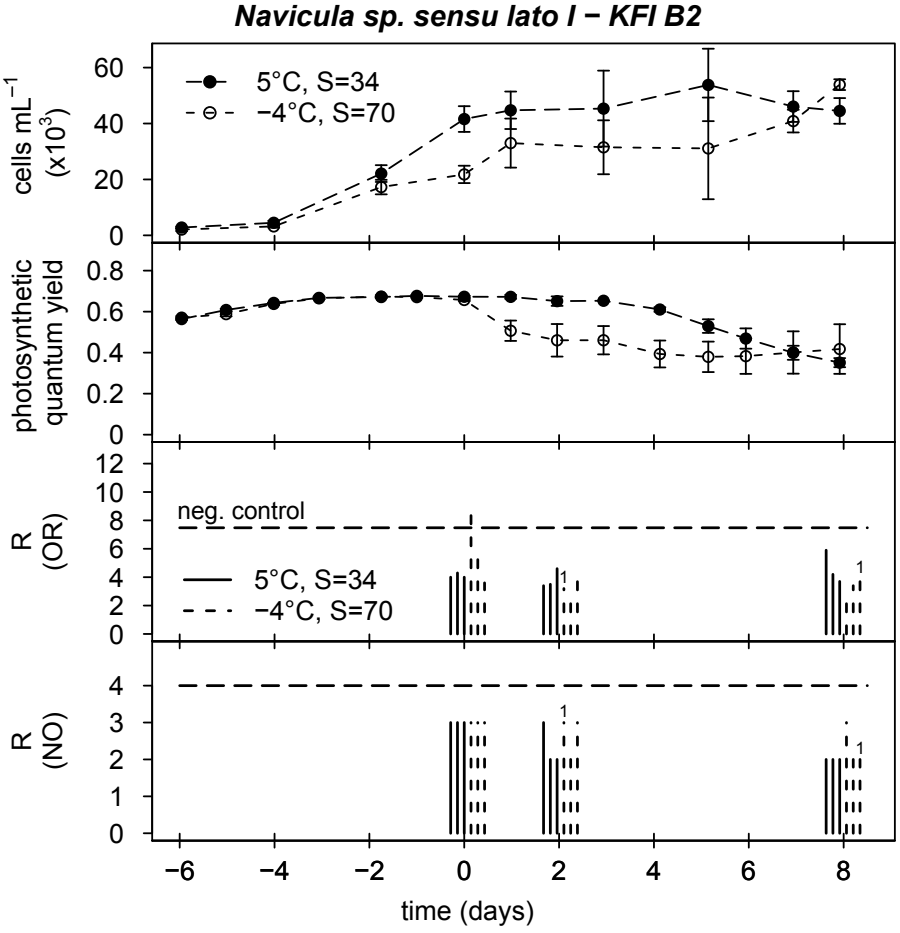

Figure 2.2: *Navicula sp.* sensu lato I - KFI B2: The cultures were treated alike until day 0, when they were split into triplicates of control and treated cultures. T0 sampling was performed just before the treatment. Dashed horizontal lines indicate values obtained for the negative control *P. tricornutum*. Total protein concentration of the cell extracts used for the R measurement was 150 μg mL^{-1} if not indicated differently by small numbers (1: 100-150 μg mL^{-1}, 2: 50-100 μg mL^{-1}, 3: 0-50 μg mL^{-1}). A low R value indicates high recrystallisation inhibition, NO: nanolitre osmometer, OR: optical recrystallometer.

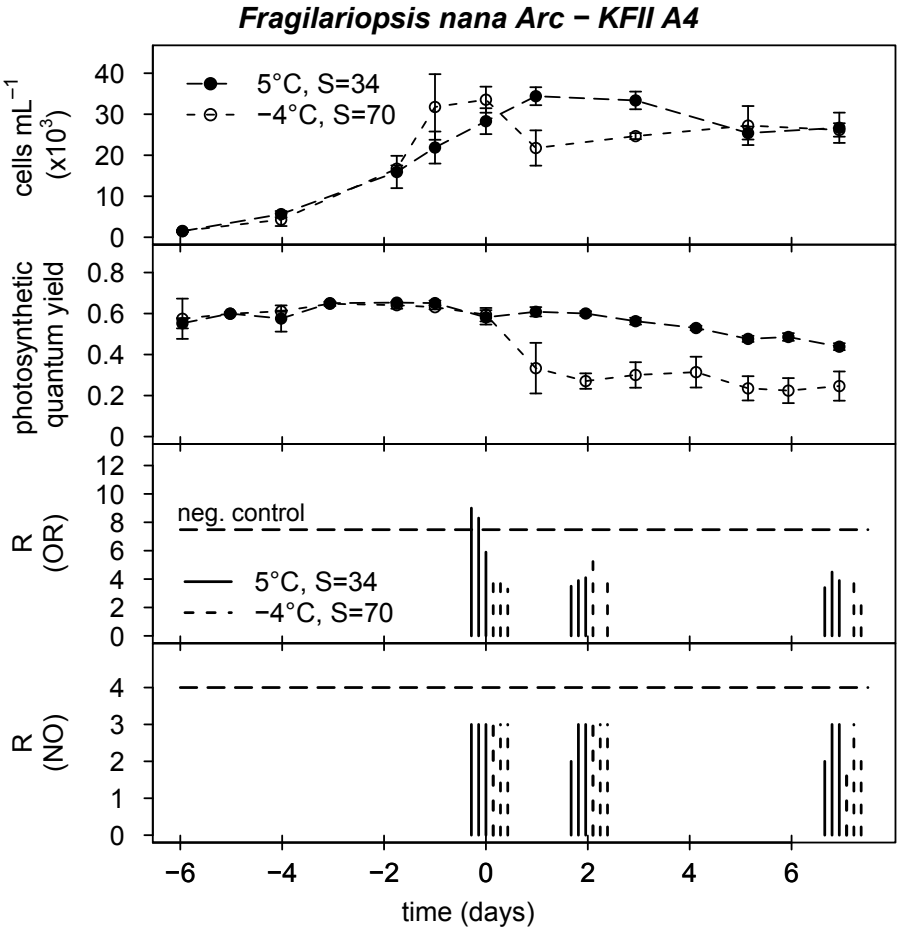

Figure 2.3: *Fragilariopsis nana* Arc - KFI B2: The cultures were treated alike until day 0, when they were split into triplicates of control and treated cultures. T0 sampling was performed just before the treatment. Dashed horizontal lines indicate values obtained for the negative control *P. tricornutum*. Total protein concentration of the cell extracts used for the R measurement was 150 μg mL^{-1}. A low R value indicates high recrystallisation inhibition, NO: nanolitre osmometer, OR: optical recrystallometer.

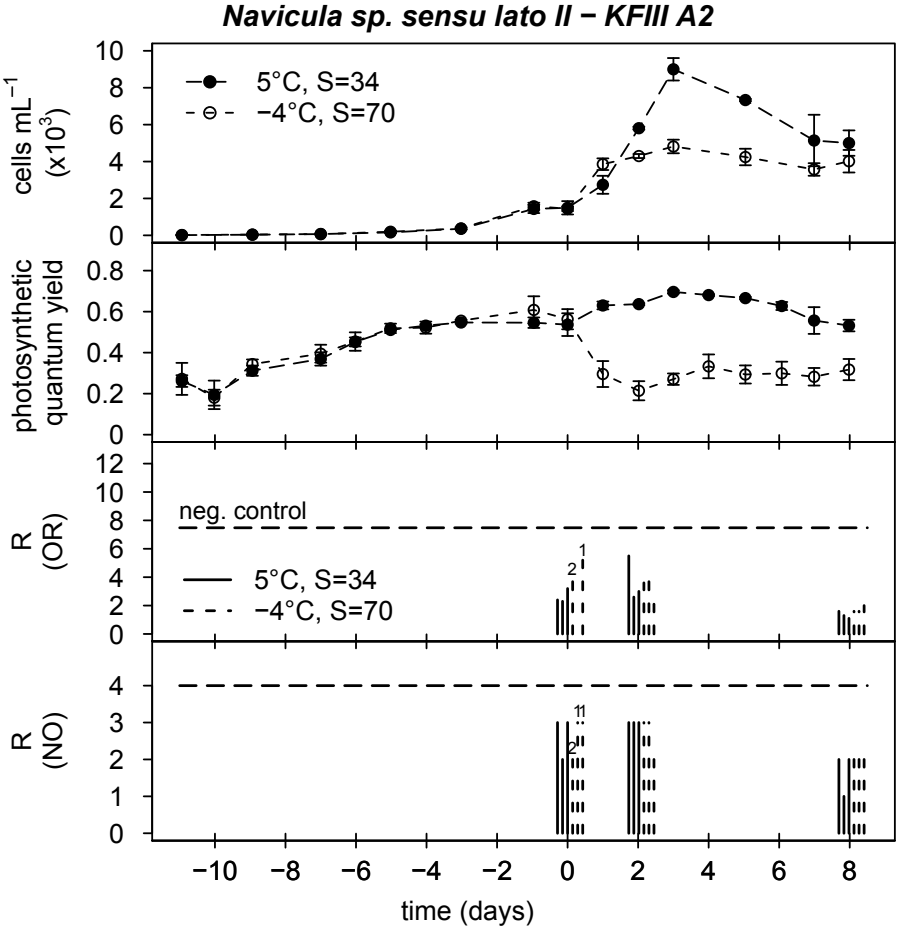

Figure 2.4: *Navicula sp.* sensu lato II - KFIII A2: The cultures were treated alike until day 0, when they were split into triplicates of control and treated cultures. T0 sampling was performed just before the treatment. Dashed horizontal lines indicate values obtained for the negative control *P. tricornutum*. Total protein concentration of the cell extracts used for the R measurement was 150 μg mL^{-1} if not indicated differently by small numbers (1: 100-150 μg mL^{-1}, 2: 50-100 μg mL^{-1}, 3: 0-50 μg mL^{-1}). A low R value indicates high recrystallisation inhibition, NO: nanolitre osmometer, OR: optical recrystallometer.

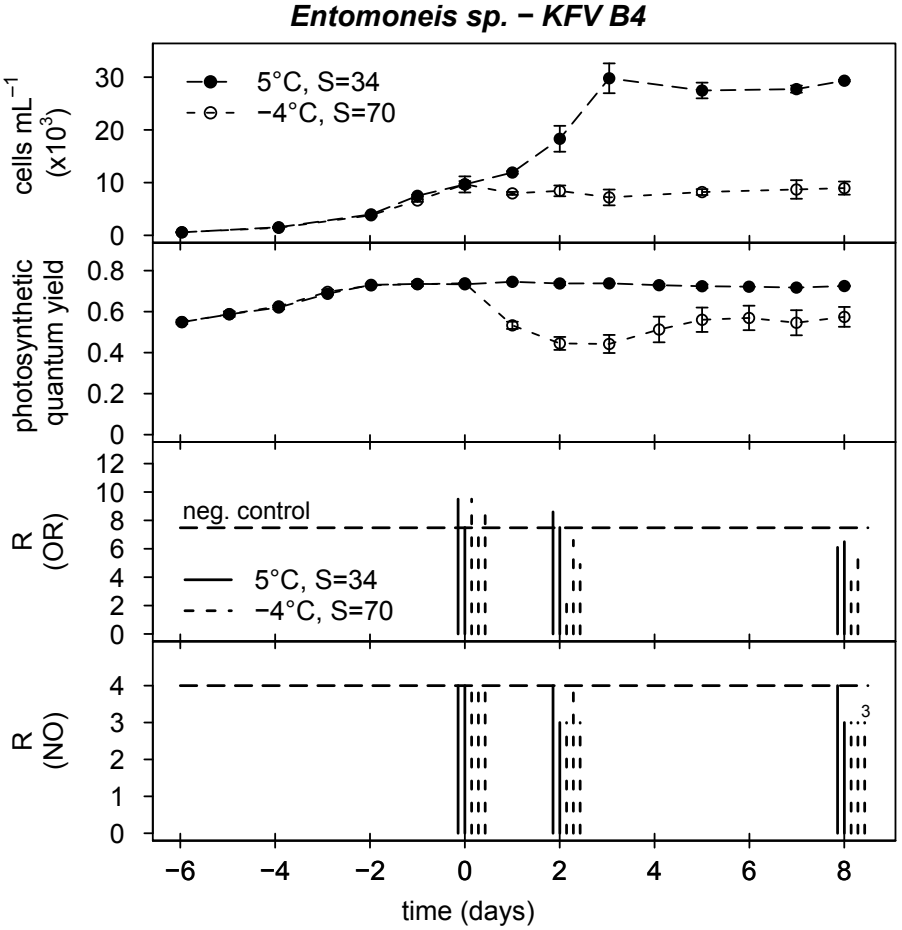

Figure 2.5: *Entomoneis sp.* - KFV B4: The cultures were treated alike until day 0, when they were split into triplicates of control and treated cultures. T0 sampling was performed just before the treatment. Dashed horizontal lines indicate values obtained for the negative control *P. tricornutum*. Total protein concentration of the cell extracts used for the R measurement was 150 μg mL^{-1} if not indicated differently by small numbers (1: 100-150 μg mL^{-1}, 2: 50-100 μg mL^{-1}, 3: 0-50 μg mL^{-1}). A low R value indicates high recrystallisation inhibition, NO: nanolitre osmometer, OR: optical recrystallometer.

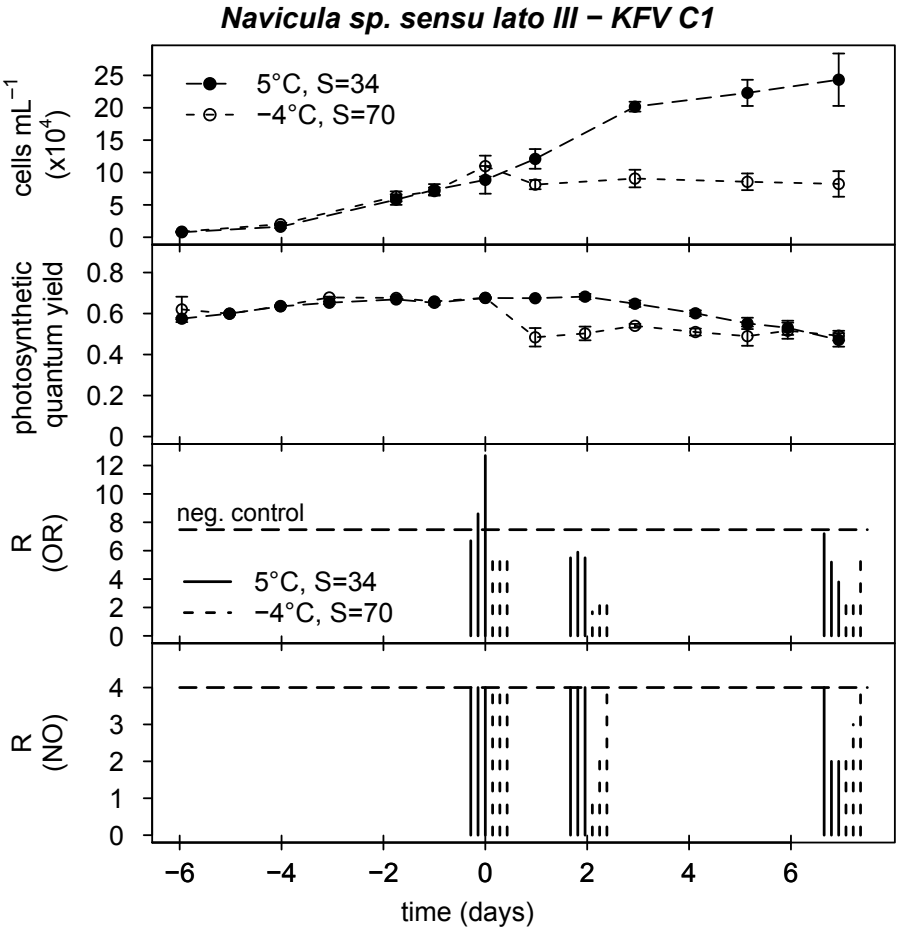

Figure 2.6: *Navicula sp.* sensu lato III - KFV C1: The cultures were treated alike until day 0, when they were split into triplicates of control and treated cultures. T0 sampling was performed just before the treatment. Dashed horizontal lines indicate values obtained for the negative control *P. tricornutum*. Total protein concentration of the cell extracts used for the R measurement was 150 μg mL^{-1}. A low R value indicates high recrystallisation inhibition, NO: nanolitre osmometer, OR: optical recrystallometer.

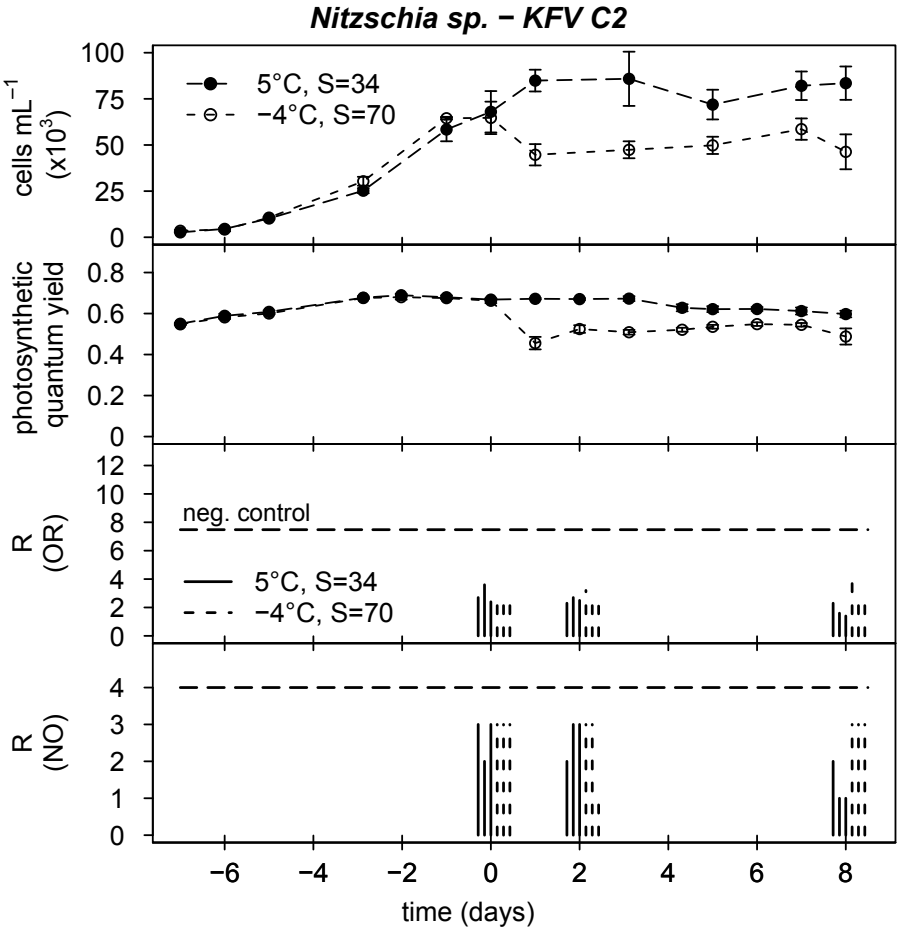

Figure 2.7: *Nitzschia sp.* - KFV C2: The cultures were treated alike until day 0, when they were split into triplicates of control and treated cultures. T0 sampling was performed just before the treatment. Dashed horizontal lines indicate values obtained for the negative control *P. tricornutum*. Total protein concentration of the cell extracts used for the R measurement was 150 μg mL^{-1}. A low R value indicates high recrystallisation inhibition, NO: nanolitre osmometer, OR: optical recrystallometer.

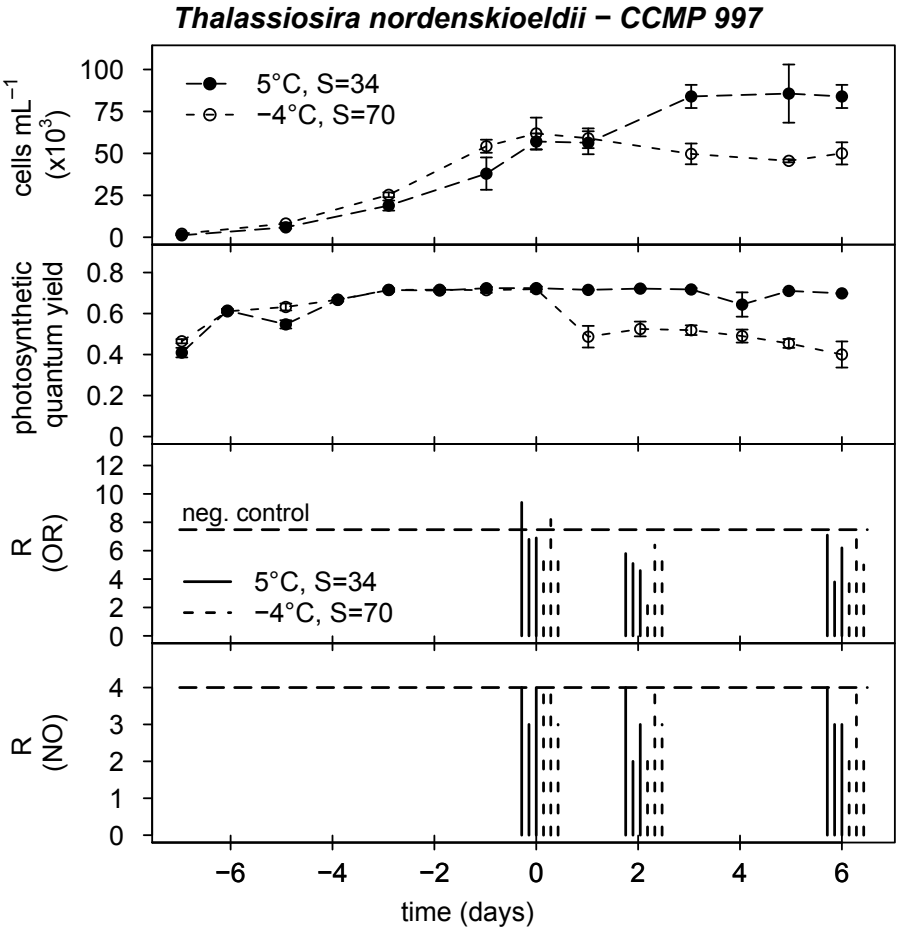

Figure 2.8: *Thalassiosira nordenskioeldii* - CCMP 997: The cultures were treated alike until day 0, when they were split into triplicates of control and treated cultures. T0 sampling was performed just before the treatment. Dashed horizontal lines indicate values obtained for the negative control *P. tricornutum*. Total protein concentration of the cell extracts used for the R measurement was 150 μg mL^{-1}. A low R value indicates high recrystallisation inhibition, NO: nanolitre osmometer, OR: optical recrystallometer.

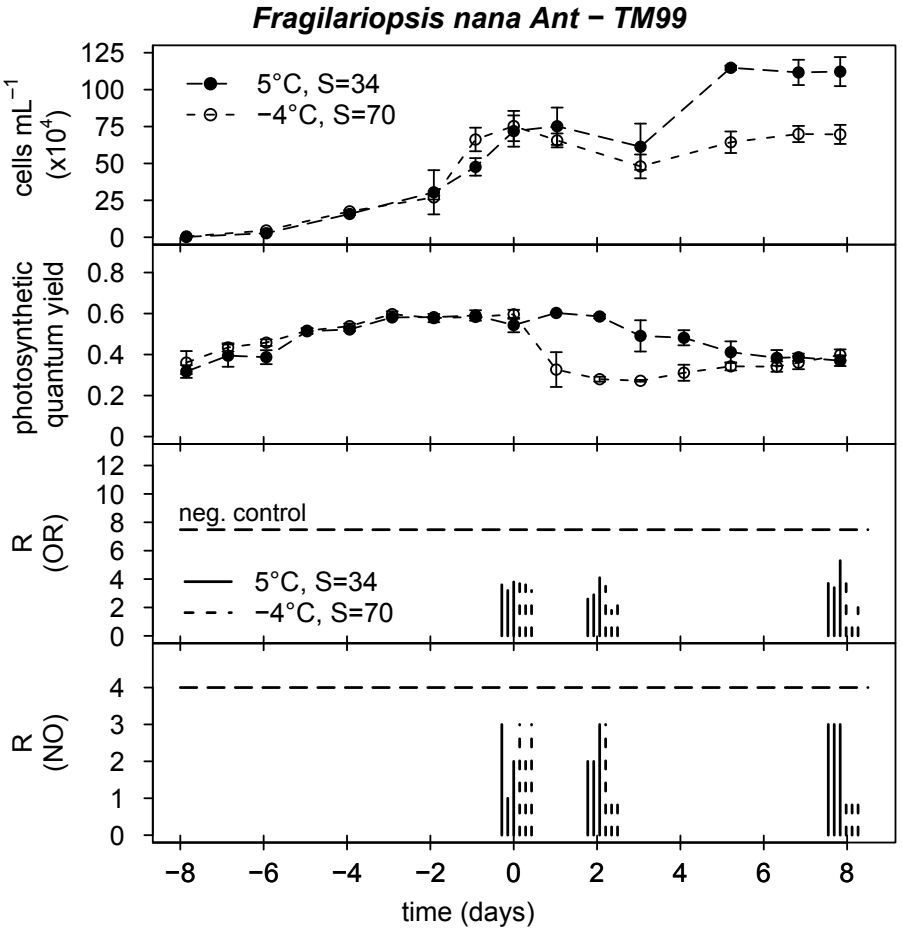

Figure 2.9: *Fragilariopsis nana* - TM99: The cultures were treated alike until day 0, when they were split into triplicates of control and treated cultures. T0 sampling was performed just before the treatment. Dashed horizontal lines indicate values obtained for the negative control *P. tricornutum*. Total protein concentration of the cell extracts used for the R measurement was 150 μg mL^{-1}. A low R value indicates high recrystallisation inhibition, NO: nanolitre osmometer, OR: optical recrystallometer.

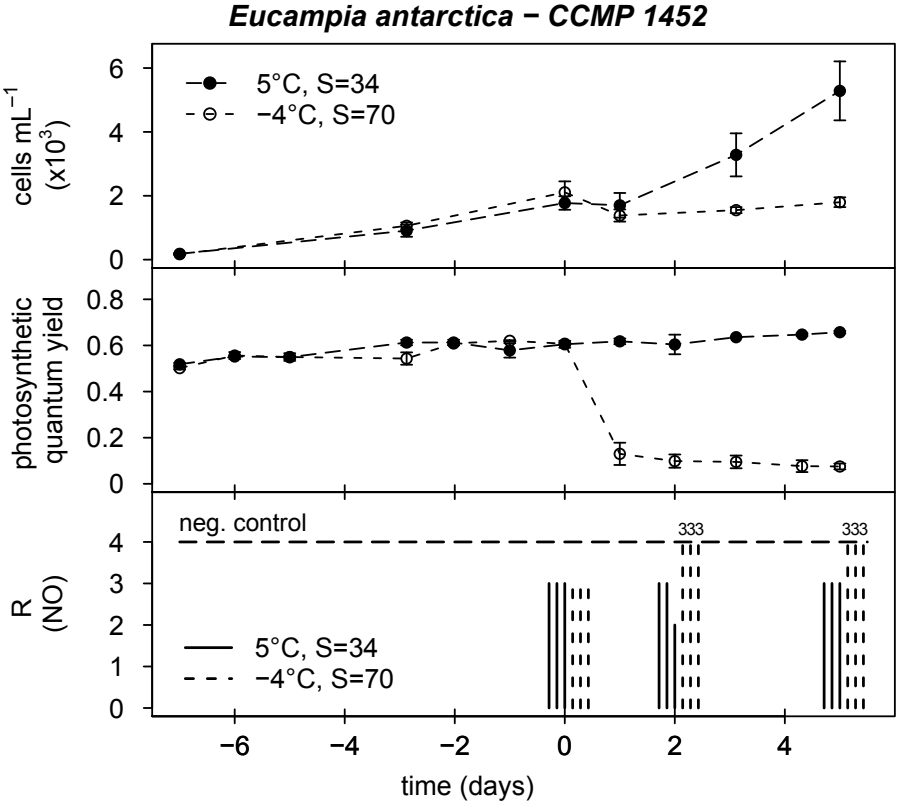

Figure 2.10: *Eucampia antarctica* - CCMP 1452: The cultures were treated alike until day 0, when they were split into triplicates of control and treated cultures. T0 sampling was performed just before the treatment. Dashed horizontal lines indicate values obtained for the negative control *P. tricornutum*. Total protein concentration of the cell extracts used for the R measurement was 150 μg mL^{-1} if not indicated differently by small numbers (1: 100-150 μg mL^{-1}, 2: 50-100 μg mL^{-1}, 3: 0-50 μg mL^{-1}). A low R value indicates high recrystallisation inhibition, NO: nanolitre osmometer, OR: optical recrystallometer.

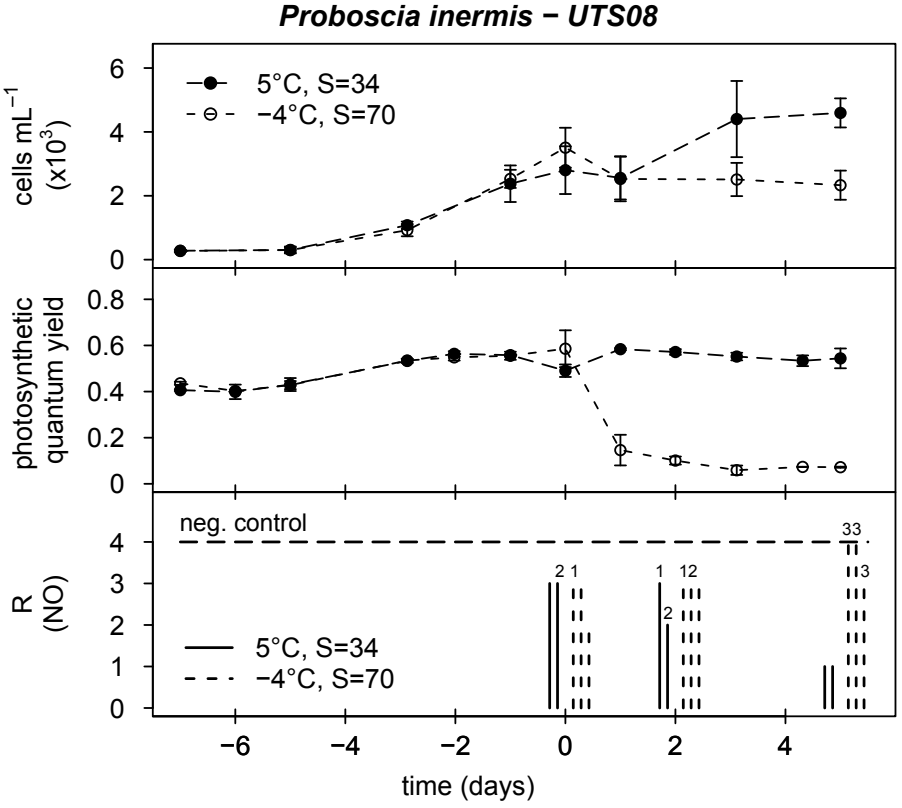

Figure 2.11: *Proboscia inermis* - UTS08: The cultures were treated alike until day 0, when they were split into triplicates of control and treated cultures. T0 sampling was performed just before the treatment. Dashed horizontal lines indicate values obtained for the negative control *P. tricornutum*. Total protein concentration of the cell extracts used for the R measurement was 150 μg mL^{-1} if not indicated differently by small numbers (1: 100-150 μg mL^{-1}, 2: 50-100 μg mL^{-1}, 3: 0-50 μg mL^{-1}). A low R value indicates high recrystallisation inhibition, NO: nanolitre osmometer, OR: optical recrystallometer.

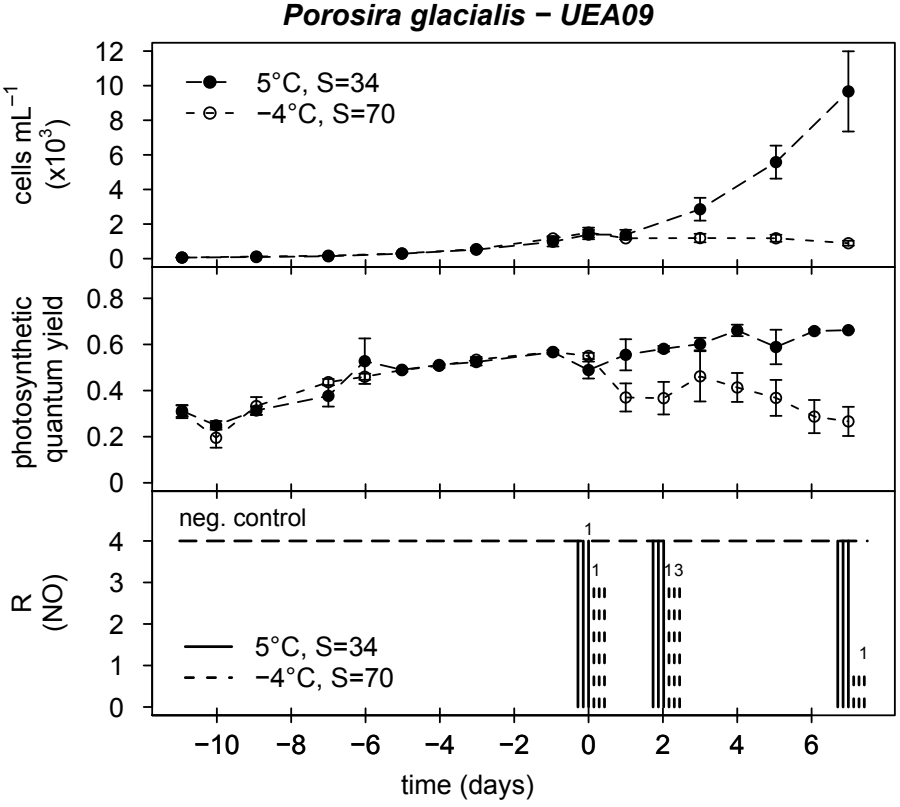

Figure 2.12: *Porosira glacialis* - UEA09: The cultures were treated alike until day 0, when they were split into triplicates of control and treated cultures. T0 sampling was performed just before the treatment. Dashed horizontal lines indicate values obtained for the negative control *P. tricornutum*. Total protein concentration of the cell extracts used for the R measurement was 150 μg mL^{-1} if not indicated differently by small numbers (1: 100-150 μg mL^{-1}, 2: 50-100 μg mL^{-1}, 3: 0-50 μg mL^{-1}). A low R value indicates high recrystallisation inhibition, NO: nanolitre osmometer, OR: optical recrystallometer.

optical recrystallometer resulted in AFPeq below this baseline, additional observations with the Clifton Nanolitre Osmometer did provide evidence on AFP activity (Fig. 2.2, 2.3, 2.5). AFPeq in all control cultures (T0, T1, T2) and cultures prior to treatment (T0) range from 0.05% (±0.03%) to 7% (±1%), whereas subsequent to treatment, cultures (T1 and T2) had 0.6% (±0.2%) to 5.6% (±4.7%) AFPeq (Fig. 2.13). Minimal values of AFPeq are thus about ten times higher after treatment (0.6%) than prior to treatment (0.05%), whereas maximal values cannot be separated (7% before vs. 5.6% after).

Total AFPeq per cell (i.e. g(AFPeq) cell^{-1}) increased with increasing cell size. For the small species *F. nana* Ant (45 μm^3) total AFPeq cell^{-1} was lowest with values of 0.02 to 0.08 pg total AFPeq cell^{-1}. In comparison, the large *Nitzschia sp.* II (18,000 μm^3) contained 10 to 58 pg total AFPeq cell^{-1}. Taking into account the total protein concentrations in the cells AFPeq in both species is about 0.3 to 7%. *Entomoneis sp.* did not follow this trend and had rather low total AFPeq content of 0.08 to 2.83 pg total AFPeq cell^{-1} compared to the cell size (5300 μm^3).

2.3.5 Stability under temperature and protease

Eight out of eleven protein extracts were susceptible to incubation for 1 h at moderate temperature of 20 °C with or without additional protease treatment (Fig. 2.14). The protein extract of *P. glacialis* completely lost AFP activity, whereas the other 7 affected samples showed only a reduced activity. Additional incubation at 95 °C resulted in a loss of activity for five more species (Fig. 2.14). For two species the activity was only lost after incubation at 95 °C and protease (*Navicula sp.* II, *T. nordenskioeldii*). For cell extracts of *F. nana* Arc, *Entomoneis sp.* and *P. inermis* no loss in activity was observed upon treatments at 20 °C, but activity was completely eliminated when incubated at 95 °C with either BSA or protease. A protease treatment and subsequent SDS-PAGE analysis with Coomassie staining showed that digestions were successful. A sample of Ovalbumin as well as cell extracts from *F. nana* Ant and *P. tricornutum* were degraded after incubation with Pronase E for 1 h at 20 °C (data not shown).

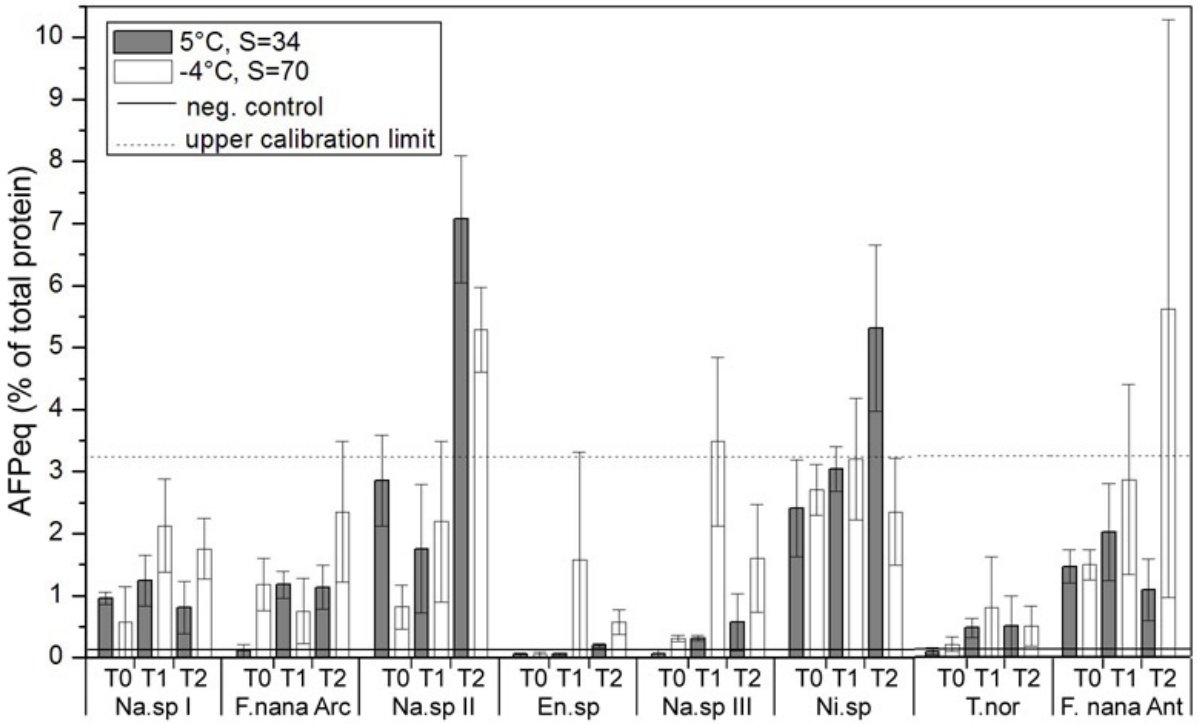

Figure 2.13: AFP equivalents (AFPeq) in % of total protein before treatment (T0), 2 days after treatment (T1), and 6 to 8 days after treatment (T2). Species abbreviations as follows: Na.sp I: *Navicula sp.* sensu lato I, F.nana Arc: *Fragilariopsis nana* Arctic isolate, Na.sp II: *Navicula sp.* sensu lato II, En.sp: *Entomoneis sp.*, Na.sp III: *Navicula sp.* sensu lato III, Ni.sp: *Nitzschia sp.*, T.nor: *Thalassiosira nordenskioeldii*, F.nana Ant: *Fragilariopsis nana* Antarctic isolate. The horizontal solid line at 0.1% indicates the value calculated for the negative control *P. tricornutum*. The horizontal dashed line at 3.3% indicates the upper calibration limit.

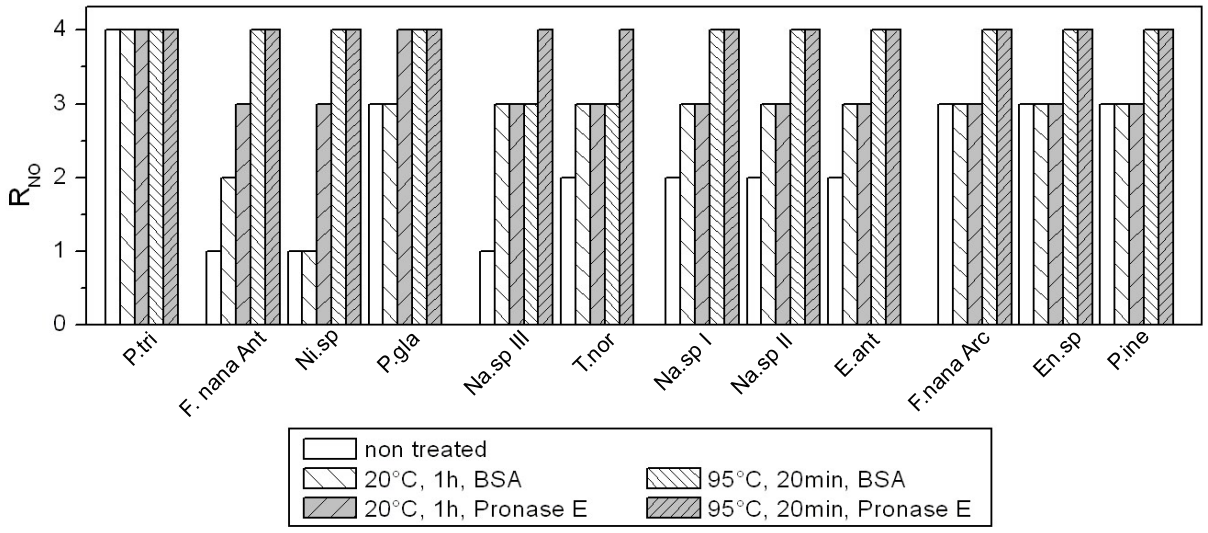

Figure 2.14: Stability of AFP activity with respect to protease and temperature treatment. Extracts were first incubated with Pronase E or BSA for 1 h at 20°C and subsequently with respective additives for 20 min at 95°C. Low R (recrystallisation) value indicates high recrystallisation inhibition.

2.4 Discussion

2.4.1 Methods for RI and AFP measurement

In comparison to the Clifton Nanolitre Osmometer, where microscopic observations are biased by the experimentator, data acquired with the optical recrystallometer is objective as readouts are done by the device (Wharton et al. 2007). The optical recrystallometer produces quantitative results indicated by the logarithmic function of standard curves (Fig. 2.1 b), whereas the nanolitre osmometer is half quantitative allowing the classification of results only into categories like no, low or high recrystallisation inhibition. The higher sensitivity of the nanolitre osmometer was advantageous for our study, e.g. the low protein content sample (5 μg mL^{-1}) of *F. nana* ANT cell extract clearly showed activity in the nanolitre osmometer (category 2), but was not distinguishable from the negative control in the optical recrystallometer (Fig. 2.1 a). AFP concentrations in some cell extracts were low, thus failing to produce RI. Nevertheless in those samples we were often able to determine crystal deformation with the nanolitre osmometer. A combination of both methods allowed us to draw conclusions on the fraction of AFP present in the cell extracts (optical recrystallometer), as well as to obtain information on samples with low AFP content (nanolitre osmometer).

AFP-independent RI activity was found for BSA and *P. tricornutum* cell extracts with the optical recrystallometer (Fig. 2.1 a). As explained by Knight et al. (1988), molecules, especially large ones, stabilise grain boundaries by reducing the grain boundary energy and disturb grain boundary migration by forcing water molecules to diffuse around them. This results in a weak inhibition of recrystallisation. The RI observed for BSA and *P. tricornutum* thus constitutes a baseline or background activity. AFP independent RI was not observed in the nanolitre osmometer, which thus appears to be a valuable method to verify negative controls.

In samples with high protein concentration and high RI activity we observed an effect of the sample matrix on RI activity. Increasing the protein concentration of *F. nana* cell extract in the calibration did not lead to any further decrease in R (no values below R=2.44

(±0.50)), whereas for other cell extracts and fcAFP we observed values as low as 1.33 (±0.21) and 0.45 (±0.27), respectively (Fig. 2.1, 2.4, 2.6, 2.7, 2.9). Solutes like salts, sugars, amino acids, peptides change the osmolality of a sample, attracting water molecules for the hydration of these solutes that is not included the surrounding ice crystals (Wolfe et al. 2002). This leads to an increased amount of liquid water molecules available for ice restructuration. For samples containing a complex matrix, like cell extracts, this might result in an elevated recrystallisation activity compared to pure samples of single proteins in a defined buffer. To study the effect of matrices in detail, further experiments should include tests of different non-active matrices (e.g. BSA or *P. tricornutum* cell extracts) at fixed protein concentration (e.g. 150 μg mL^{-1}), spiked with changing concentrations of RI active protein (e.g. fcAFP). It is important to consider both effects (AFP independent recrystallisation inhibition activity and the matrix effect) when interpreting the results and to include appropriate negative controls, providing a similar matrix as present in the samples.

2.4.2 Taxonomy and ecology

All Arctic taxa investigated, such as *Nitzschia spp.*, *Navicula spp.*, *Entomoneis spp.* and *Thalassiosira spp.* were reported to commonly occur in Kongsfjord sea ice (Hop et al. 2002). *Thalassiosira nordenskioeldii*, *Fragilariopsis spp.*, *Navicula spp.* and *Nitzschia spp.* were also frequently found in the water column in the Kongsfjord (Hop et al. 2002; Hasle and Heimdal 1998). All Antarctic taxa investigated here were reported to occur in sea ice of the Weddell Sea in different frequencies ranging from regular (*E. antarctica*, *P. glacialis*, *P. inermis*) to dominant (*F. nana*) (Bartsch 1989; Hager 2008). We also identified sequences with high similarities of 97.6% to *P. inermis* and above 99.5% to *E. antarctica* and *F. nana* Ant in an environmental 18S library from East Antarctic sea ice (110-130°E) (J. Kegel, personal communication). Sequences with high similarities (>99.5%) to *F. nana* were also present in an 18S library from Weddell Sea ice (J. Kegel, personal communication).

2.4.3 Physiology and AFP activity under salinity and temperature stress

Physiological data from this study fit well with the ecological observations of the Antarctic species. The species *E. antarctica*, *P. inermis* and *P. glacialis*, which are less frequently found in sea ice (Bartsch 1989), were most severely damaged by the stress conditions, as indicated by arrested cell growth, a severe drop in quantum yield and low total protein concentration (Fig, 2.10, 2.11, 2.12). A similar stress response (reduction of total protein per cell) was also reported for *P. tricornutum* under heat stress (Rousch et al. 2004). The low protein concentrations in several samples of *E. antarcica* and *P. inermis* preclude any conclusions on RI activity regulation, but it is apparent that these species are able to produce AFPs (Fig. 2.10, 2.11). In contrast, *F. nana* Ant, representing a dominant species in Weddell Sea ice (Bartsch 1989), reacted to the temperature and salinity stress with a smaller drop in photosynthetic quantum yield and cell numbers and with an up-regulation of AFPs (Fig. 2.9 and (Bayer-Giraldi et al. 2010)).

T. nordenskioeldii (Fig. 2.8), although not isolated from the ice, coped equally well with the stress conditions compared to the Arctic cultures isolated from ice. *Navicula sp.* I (Fig. 2.2) appeared to be the most robust of all investigated species. The decrease in photosynthetic quantum yield was rather small and the cultures showed positive cell growth after only five days of acclimation to the stress conditions. Cell numbers of treated cultures cannot be statistically distinguished from untreated cultures at any time during the course of the experiment, due to the late exponential phase at the beginning of the treatment and early decline of the control culture.

AFP activity was clearly triggered by temperature and salinity stress in *Entomoneis sp.*, *Navicula sp.* III and *P. glacialis*. For all other species, freezing and salinity stress did not result in a clear pattern of AFP activity. This was probably caused by the differences in growth phases between the species when applying the stress. Moreover, high deviations between the replicates of every species and treatment distort clear trends.

In all control cultures and cultures prior to treatment (non-induced), AFP activity was low for *Entomoneis sp.*, *Navicula sp.* III and *T. nordenskioeldii* (Fig. 2.5, 2.6, 2.8), whereas *Navicula sp.* II and *Nitzschia sp.* (Fig. 2.4, 2.7) showed quite high levels. We did not observe a correlation between higher stress tolerance, with regard to photosynthetic quantum yield or growth, to non-induced AFP activity.

Increasing AFP activity during the experiment in the control treatments (5°C, S=70) at T1 and T2 (Fig. 2.13) can possibly be explained by the late stage of the growth phase. Some cultures had already reached the stationary phase on T0 (Fig. 2.2, 2.3, 2.7). An up-regulation of AFP genes under senescence (due to nutrient limitation) in *F. nana* Ant was already observed in earlier experiments (Uhlig 2006).

2.4.4 Content and function of AFPs in diatoms

Temperature and protease sensitivity of the cell extracts indicate that recrystallisation inhibition activity, i.e. antifreeze activity, is mainly of proteinaceous nature. Control treatments and SDS gels with *F. nana* Ant and *P. tricornutum* cell extracts showed that the digestion was successful. Nevertheless, AFP activities of some isolates were rather resistant to temperature and Pronase E treatments (Fig. 2.14). Doucet et al. (2000) previously reported that antifreeze activity from some plant and lichen samples remained even after proteins were degraded. They hypothesised that some activities might be caused by non-protein components (Doucet et al. 2000). Glycolipids from a beetle were for example recently, shown to produce thermal hysteresis (Walters et al. 2009). Species tested contained a calculated amount of 0.1-5% AFP equivalent of total cell protein, which is rather high. It is comparable to or even higher than the content of the photosystem II proteins PsbA and PsbD in diatoms. Under growth at low light (30 μmol photons m^{-2} s^{-1}) values of 0.15% and 0.42% were reported for *Thalassiosira pseudonana* and 0.07 and 0.08% for *Coscinodiscus radiatus*, respectively (Wu et al. 2011). Total AFPeq amount per cell was found to increase with increasing cell size. Smaller cells like *F. nana* Ant contain about 500 times less AFPeq than the 400 times bigger *Navicula sp.* II cells. Since total protein per cell also increases with diatom cell size (Hitchcock 1982), the fraction of AFPeq per total protein is not affected (Fig. 2.13).

The presence of notable AFP contamination of bacterial origin can be excluded as samples were filtered and washed to reduce bacterial contamination and checked with DAPI staining (data not shown).

Cellular AFP levels estimated in this study indicate high AFP concentrations for some cultures tested. For *F. nana* Ant 20 to 80 fg AFP equivalent per cell were calculated from R_{OR} (index of recrystallisation assessed with the optical recrystallometer) in this study, which is 30 to 120 times higher than AFP content determined by Bayer-Giraldi et al. (2011) using immunoblot (0.7 fg per cell). Several aspects can lead to the discrepancy observed between both methods. Experiments showed that the antibody raised against one AFP isoform binds to several of the of AFP isoforms in *F. nana* Ant, but due to sequence differences between the isoforms it does not bind to all, i.e. two out of three tested recombinant AFPs (Fig. 2.23). The immunoblot will, accordingly, underestimate total AFP concentration. In contrast, RI assessed in this study will encompass all RI active substances, which might be even more single proteins or other compounds than the actual AFP isoforms identified. Also RI measurements will overestimate AFP concentration (in the low concentration range), since some RI is caused by non-AFP compounds, like e.g. observed for *P. tricornutum* cell extracts. The intracellular AFP content is likely to be between a minimum of 0.7 fg per cell (immunoblot) and a maximum of 80 fg per cell (RI measurements). These concentrations (0.016 mg mL^{-1} to 1.8 mg mL^{-1}) are, however, still 5 to 2000 times lower than those reported for fish blood with 10 to 35 mg mL^{-1} (Sönnichsen et al. 1996; Barrett 2001; Davies et al. 2002). Our measurements and calculations addressed the fraction of intracellular AFPs, since cell lysates were prepared from filtered cells and the culture medium discarded. In previous studies it was shown and discussed that diatom AFPs carry signals for subcellular localisation, especially signal peptides for secretion of the AFPs (Janech et al. 2006; Krell et al. 2008). Possible functions of secreted AFPs were proposed by Bayer-Giraldi et al. 2011. In their experiments fcAFP modified the ice microstructure to a more porous mushy texture probably resulting in higher brine retention and surface for diatom attachment, compared to AFP free samples (Bayer-Giraldi et al. 2011). Other isoforms of *F. nana* Ant AFPs do not carry signal

peptides, however, it is not sure if the relevant N-terminus of this sequences is complete due to the isolation of the AFP genes via PCR (Uhlig et al. 2011; Bayer-Giraldi et al. 2011). One isoform, particularly not carrying a signal peptide but an N-terminal sequence of unknown function, was hypothesised to act intracellular or in association with the cell membrane (Uhlig et al. 2011).

It is still unknown if AFPs in diatoms only act as recrystallisation inhibitor, which requires 100 - 500 times less AFP than TH (Ewart et al. 1999). We used a set of data available from this study and from studies on recombinant AFPs from *F. nana* Ant (Bayer-Giraldi et al. 2011; Uhlig et al. 2011) to gain information on the possible function of intracellular AFPs in diatoms. Considering AFP contents of 0.7 fg (Bayer-Giraldi et al. 2011), 20 fg and 80 fg per cell and protein sizes of 25.9 kDa (Bayer-Giraldi et al. 2011), 41.3 kDa and 52.8 kDa (Uhlig et al. 2011), we calculated concentrations of 0.3 to 68.5 μM AFP inside the cells. Thermal hysteresis activity of three recombinant *F. nana* Ant AFP isoforms was reported for concentrations of 1.2 μM or higher (Bayer-Giraldi et al. 2011; Uhlig et al. 2011), whereas RI was detected at concentrations down to 0.012 μM for fcAFP in saline solution (Bayer-Giraldi et al. 2011). At the concentrations calculated (0.3 to 68.5 μM), AFPs in *F. nana* will clearly act as recrystallisation inhibitor. Since the immunoblot is likely to underestimate cellular total AFP content, we assume that AFPs might even account for low thermal hysteresis at intracellular concentrations. Both functions might protect the cells from intracellular ice formation or mechanical damage through ice crystal growth.

The activity of the AFPs might potentially be higher than estimated in this study due to the chemical composition of our extraction buffer. Antifreeze activity (RI as well as TH) was reported to increase with salinity at constant AFP concentration (Bayer-Giraldi et al. 2011; Uhlig et al. 2011). Potential intracellular (Uhlig et al. 2011) as well as extracellular AFPs (Janech et al. 2006; Raymond et al. 1994) will encounter conditions that are iso-osmolar to the surrounding brine. Subjected to elevated salinities, diatoms regulate turgor pressure by accumulation of salts as well as compatible solutes such as glycerol, sorbitol or proline (Kirst 1990; Bartsch 1989; Krell et al. 2007), substances not used in our buffer

composition. Low molecular mass solutes were shown to increase activity of a thermal hysteresis protein from the beetle *Dendroides canadensis*. Even though the effects were small in comparison to the other solutes tested, sodium chloride, sorbitol and proline caused an increase in TH activity (Duman et al. 1993; Li et al. 1998). Activity (ice pitting) of AFP preparations from sea ice samples that were dominated by diatoms was also shown to be solute dependent. All solutes tested (NaCl, LiCl, NaPO3, mannitol, urea) had the same enhancing effect on activity (Raymond 2000). The extraction buffer with a salinity of 8.72 and no low molecular mass solutes used in our study, will most likely result in an underestimation of AFP activity.

Our study confirms that the presence of AFPs in diatoms is a bipolar phenomenon with a broad phylogenetic distribution throughout the entire diatom phylogeny within species from cold habitats. This fact and the high cellular AFP levels highlight the importance of AFPs for polar diatoms. The function of diatom AFPs is dependent on the AFP concentration as well as other ambient conditions and will have to be investigated in more detail.

Acknowledgements

We thank Sebastian Gerland and Mats Granskog from the Norsk Polar Institut, Tomsø for the opportunity to join the field campaing in NyÅlesund and for help with the sampling. Authors would like to thank Rainer Kiko for introduction to the work with the Clifton Nanolitre Osmometer, in particular the RI measurements.

2.5 Supplementary material

Table 2.3: Growth rates (μ) and error (er), as well as R^2 of the correlation of experimental cultures during exponential phase (before the treatment). The growth phases at time of treatment with elevated salinity and decreased temperature (T0) are given.

	5 °C, S=34			-4 °C, S=70			
	μ	er	R^2	μ	er	R^2	Growth phase at T0
E.ant	0.33	0.04	0.99	0.36	0.06	0.99	exponential phase
F.nana Ant	0.68	0.09	0.97	0.61	0.08	0.97	1^{st} day stationary phase
Na.sp. I	0.49	0.06	0.98	0.44	0.08	0.97	end of exponential phase
F.nana Arc	0.49	0.04	0.99	0.55	0.04	0.99	1^{st} day stationary phase
Na.sp II	0.44	0.02	0.996	0.41	0.02	0.99	exponential phase
En.sp	0.49	0.02	0.997	0.48	0.01	0.999	exponential phase
Na.sp III	0.44	0.03	0.99	0.43	0.02	0.997	exponential phase
Ni.sp	0.47	0.03	0.99	0.46	0.04	0.98	1^{st} day stationary phase
P.gla	0.29	0.01	0.996	0.29	0.01	0.997	exponential phase
P.ine	0.45	0.06	0.98	0.5	0.02	0.998	lag phase, end of exponential phase
T.nor	0.55	0.05	0.99	0.49	0.05	0.99	end of exponential phase

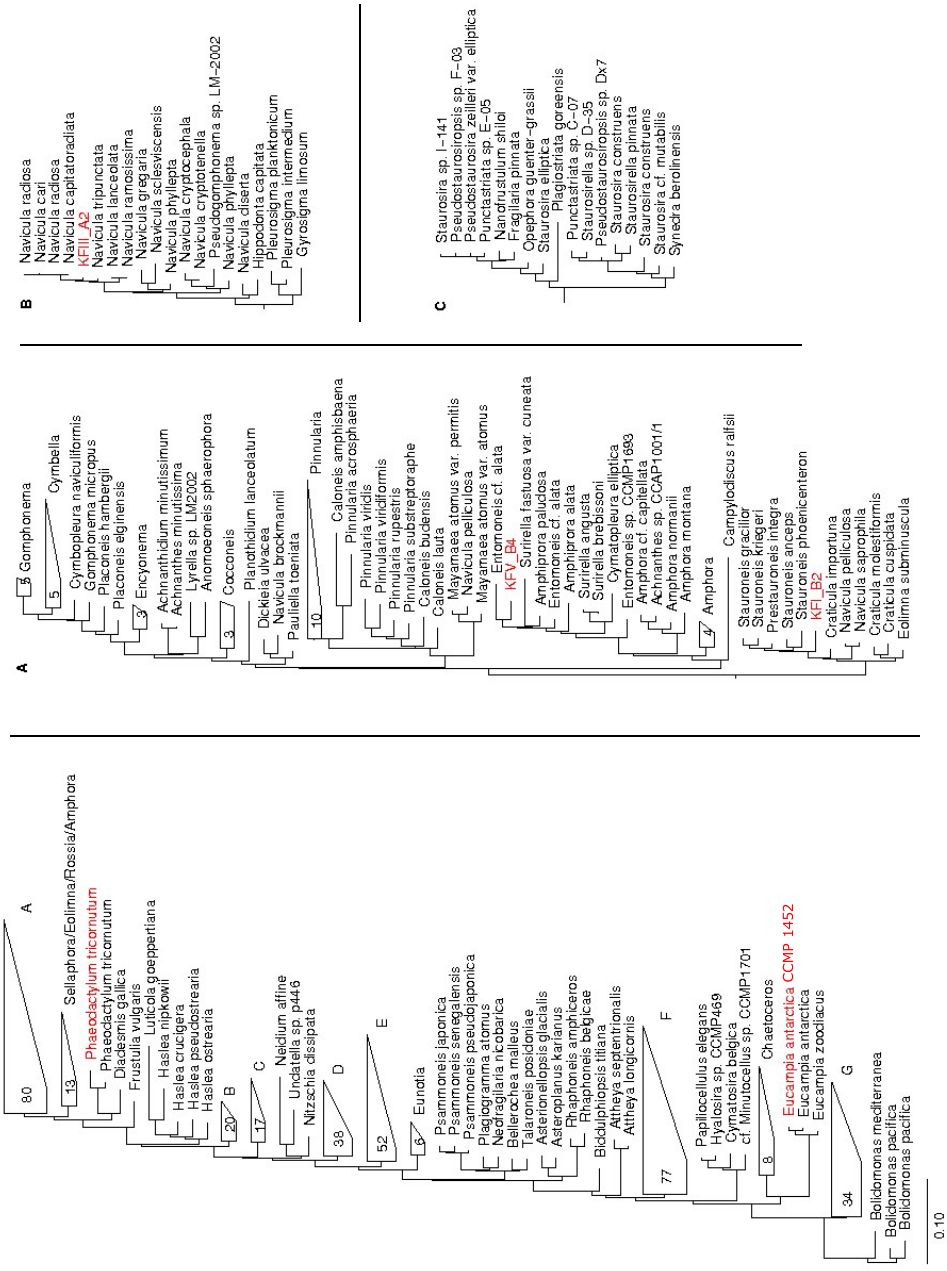

Figure 2.15: Taxonomy of diatoms based on 18S rDNA sequencing - Part 1: Overview of complete tree and close-ups into parts A-C. The species used in the experiments are marked in red.

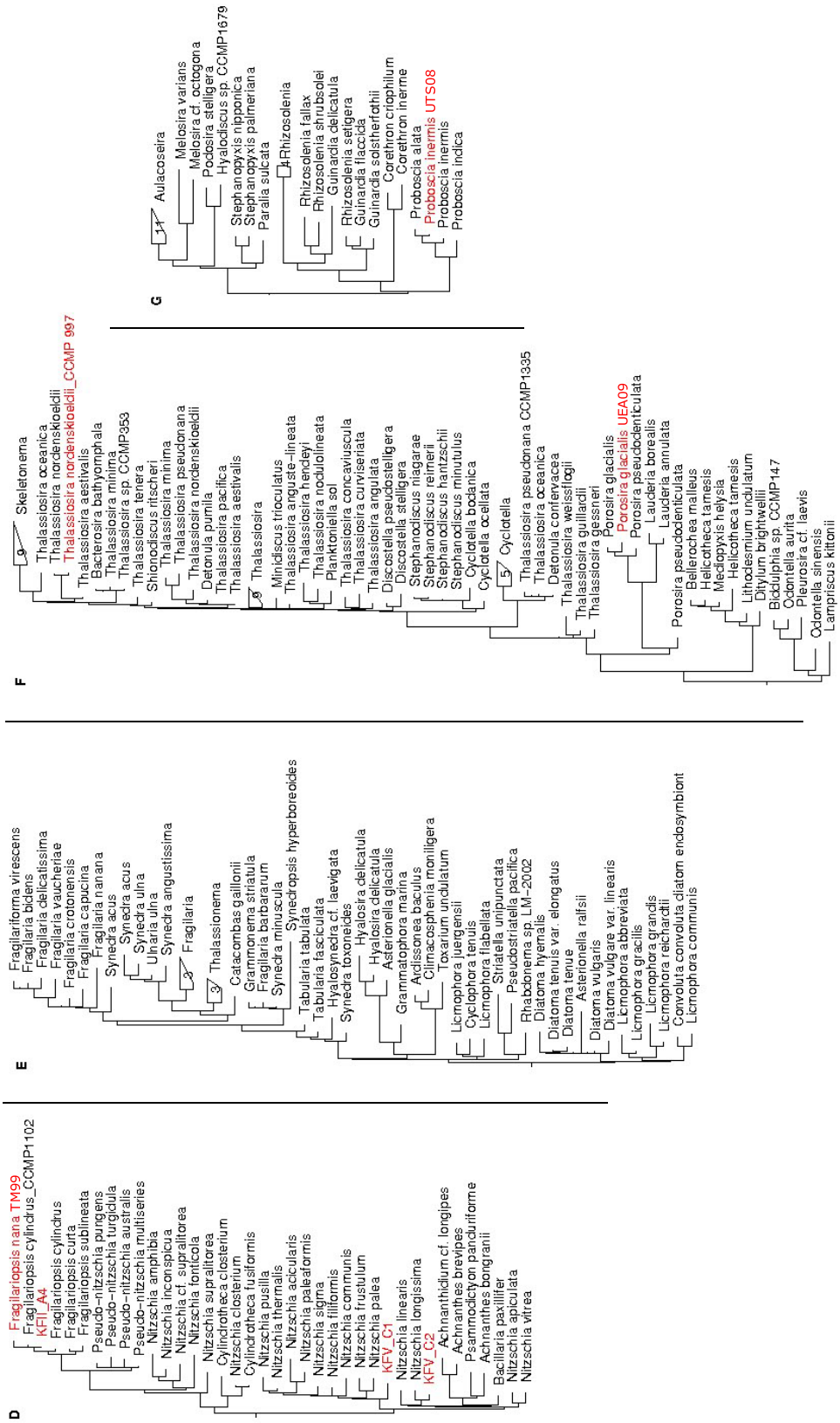

Figure 2.16: Taxonomy of diatoms based on 18S rDNA sequencing - Part 2: Close-ups into parts D-G. The species used in the experiments are marked in red.

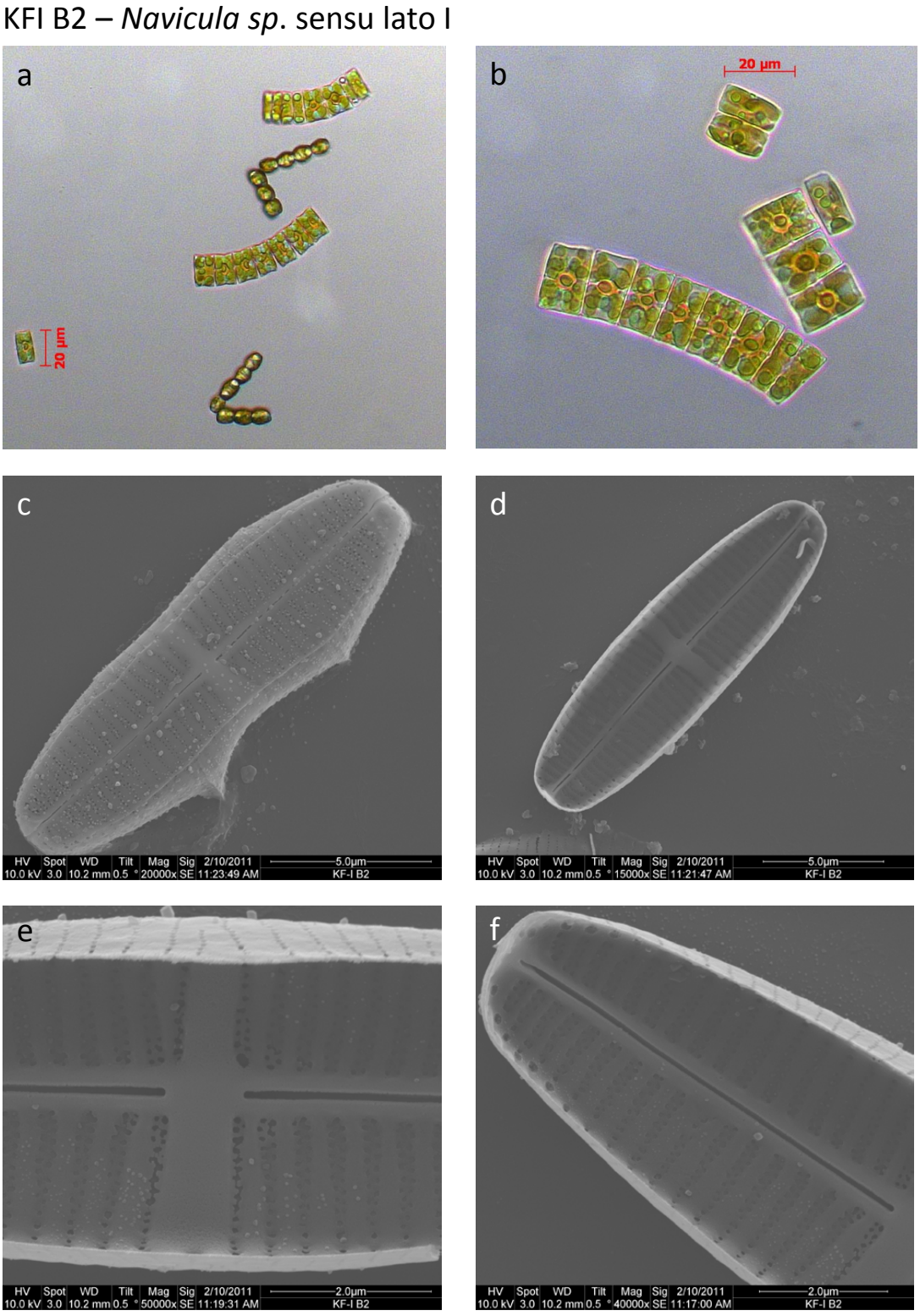

Figure 2.17: KFI B2 - *Navicula sp.* sensu lato I: a and b: light microscopy of chains; c, d, e, f: scanning electron microscopy; c: outer valve view; d: internal valve view; e and f: internal valve views showing raphe endings.

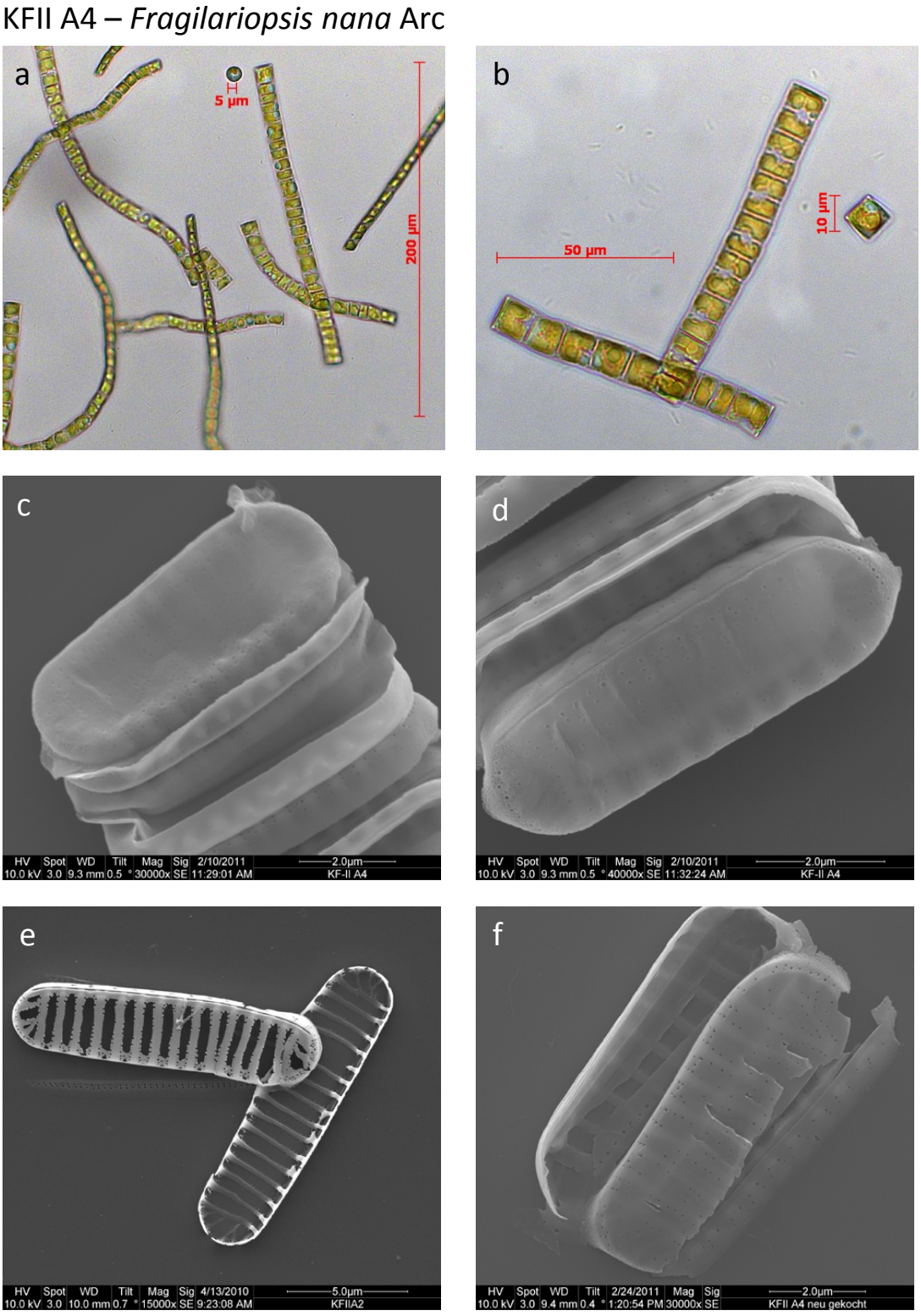

Figure 2.18: KFII A4 - *Fragilariopsis nana* Arc: a and b: light microscopy of chains; c, d, e, f: scanning electron microscopy; c: outer valve view of chain; d: complete cell in outer valve view; e and f: internal and outer valve view of cleaned cells.

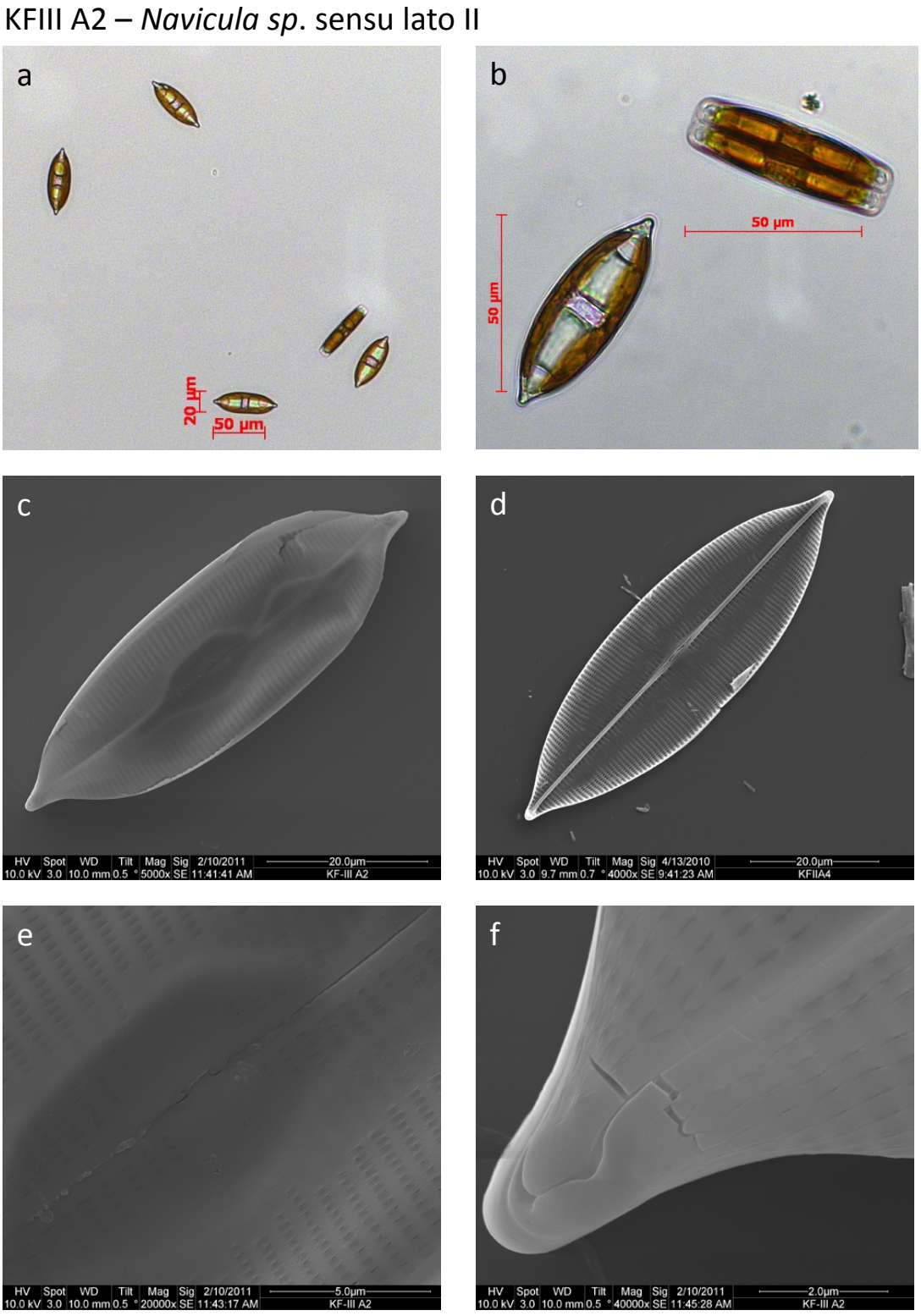

Figure 2.19: KFIII A2 - *Navicula sp.* sensu lato II: a and b: light microscopy of single cells; c, d, e, f: scanning electron microscopy; c: outer valve view; d: internal valve view; e: internal valve view showing raphe endings; f: outer valve view showing raphe ending.

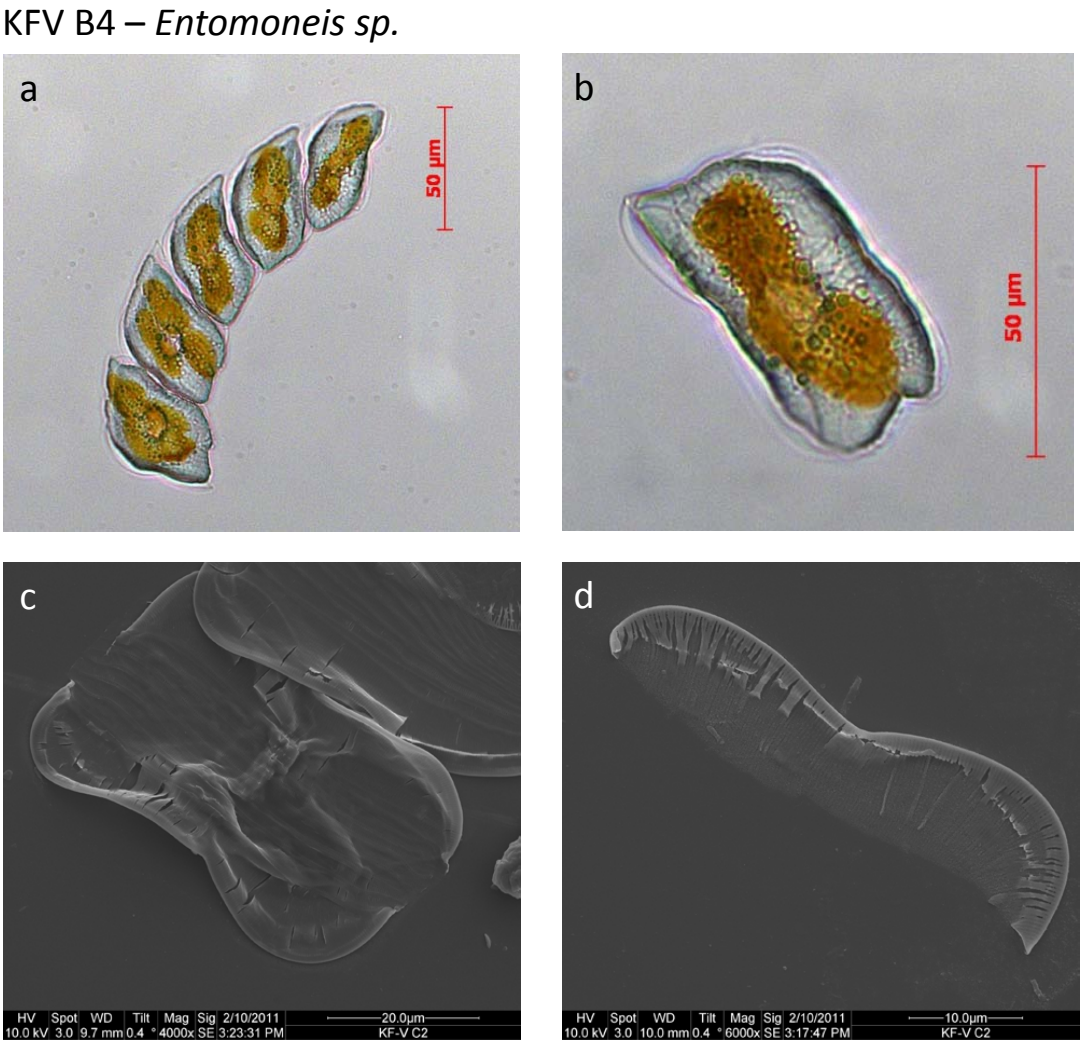

Figure 2.20: KFV B4 - *Entomoneis sp.*: a and b: light microscopy of chain and single cell; c and d: scanning electron microscopy; c: girdle band view of raw preparations; d: fragment of acid cleaned cell.

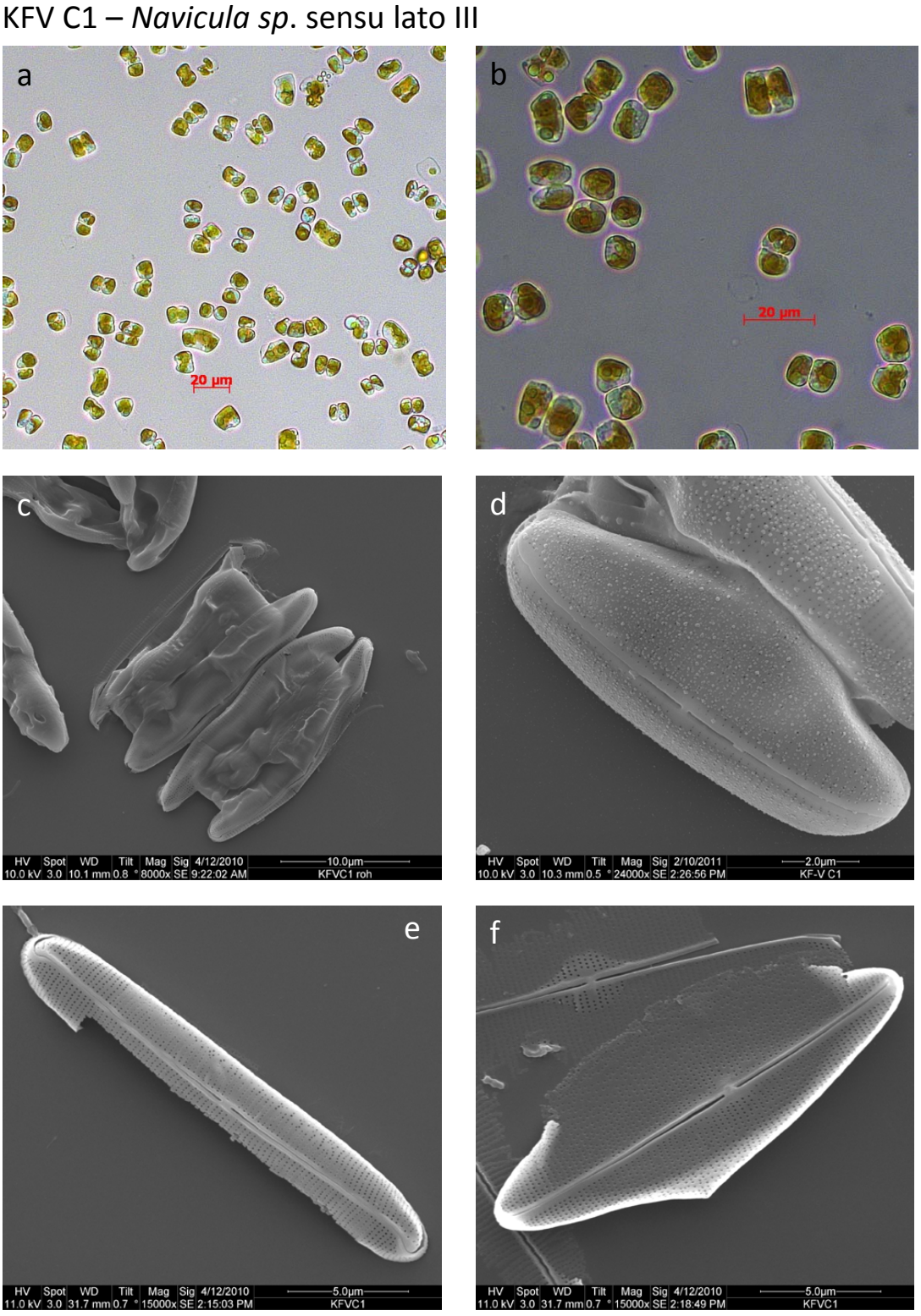

Figure 2.21: KFV C1 - *Navicula sp.* sensu lato III: a and b: light microscopy of single cells and pairs; c, d, e, f: scanning electron microscopy; c and d: girdle band view of raw preparations; e: outer valve view of acid cleaned cell; f: inner valve view of acid cleaned cell.

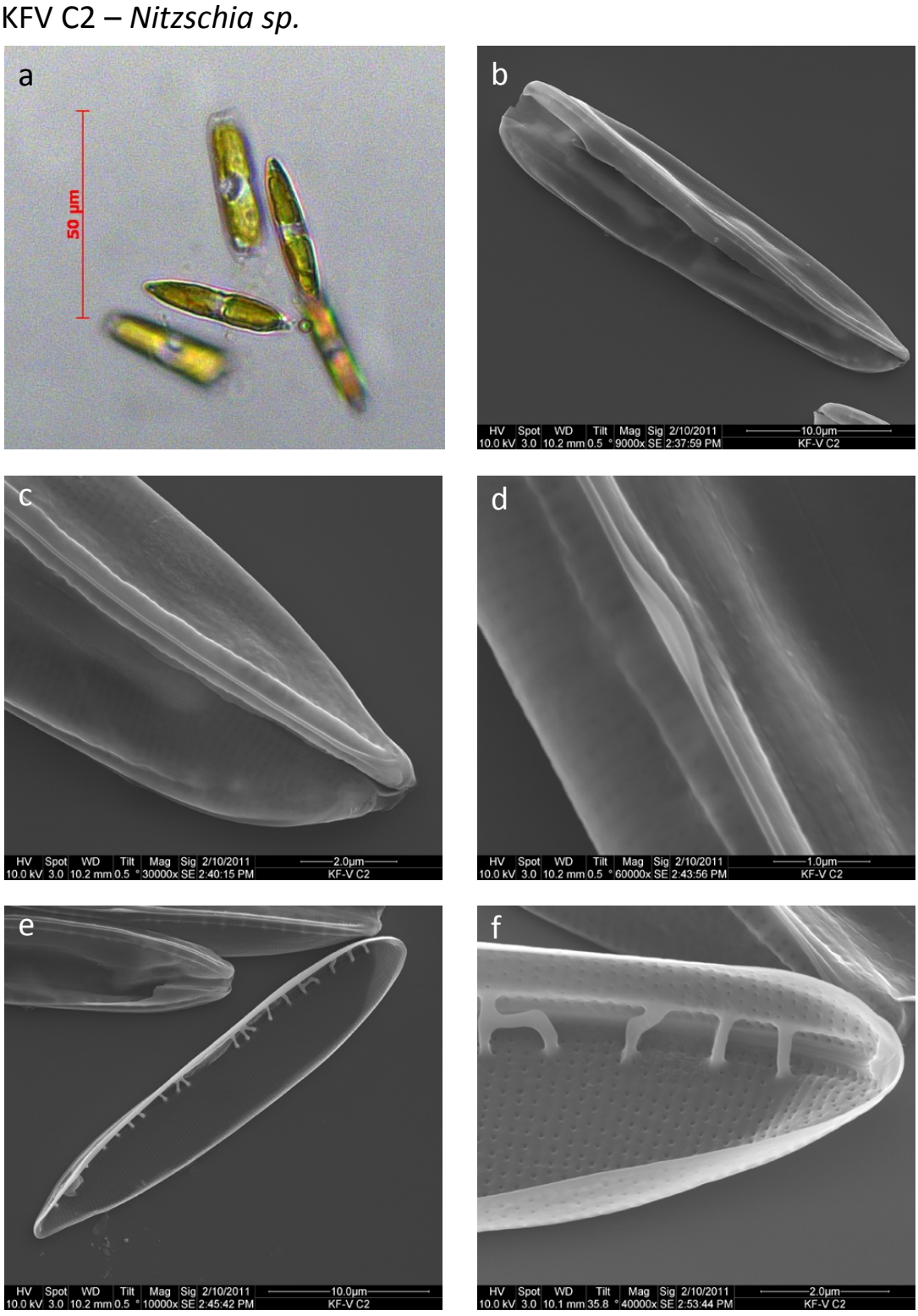

Figure 2.22: KFV C2 - *Nitzschia sp.*: a: light microscopy of single cells; b, c, d, e, f: scanning electron microscopy; b: cleaned cell; c: magnification of c; d: external view of central part of raphe; e: internal valve view; f: internal view on raphe.

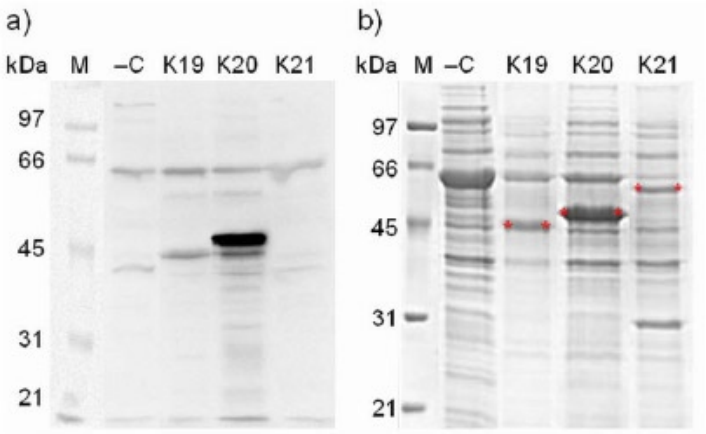

c)

Recombinant AFP	Publication	Sequence name	EST GeneBank Acc. No.
fcAFP	Bayer-Giraldi et al. 2011	Fcyl AFP-11	DR026070
K19	not published	Fcyl AFP-9	EL737280
K20	Uhlig et al. 2011	Fcyl AFP-10	EL737258
K21	Uhlig et al. 2011	Fcyl AFP-12	EL737755

Figure 2.23: a) Immunoblot of anti-AFP IgG against three recombinant *F. nana* AFP isoforms. Polyclonal rabbit IgG raised against *F. nana* Ant AFP isoform 11 (fcAFP) detects the isoforms AFP-11 (Bayer-Giraldi et al. 2011) and K20 (lane 4 - AFP-10), it weakly detects K19 (lane 3 - AFP-9) and fails to detect K21 (lane 5 - AFP-12). Intensity of reaction correlates well with phylogeny of AFP genes. For detailed information on AFP phylogeny, recombinant AFPs and antibody refer to (Bayer-Giraldi et al. 2010; Bayer-Giraldi et al. 2011; Uhlig et al. 2011). Cell lysates of expression cells were separated on 10% SDS polyacrylamide gel and blotted onto PVDF membranes (BioRad) at 50 V for two hours. Immunodetection was performed as described in (Bayer-Giraldi et al. 2011). Lane 1 shows the marker, lane 2 the cell lysate of expression cells without expression plasmid as negative control and lanes 3, 4 and 5 cell lysates of the expression cells with respective expression plasmids. (b) Recombinant expression of AFPs. Cell extracts (20 μl) were separated on 12% SDS polyacrylamide gels and stained with Coomassie. Marked bands were verified by mass-spectrometry to be the desired heterologously expressed AFPs. (c) List of recombinant *F. nana* AFPs and GeneBank Accession Numbers of respective EST sequences.

3 Heterologous expression, refolding and functional characterisation of two antifreeze proteins from *Fragilariopsis cylindrus* (Bacillariophyceae)

Christiane Uhlig, Johannes Kabisch, Gottfried J. Palm, Klaus Valentin, Thomas Schweder, Andreas Krell

Abstract

Antifreeze proteins (AFPs) provide protection for organisms subjected to the presence of ice crystals. The psychrophilic diatom *Fragilariopsis cylindrus* which is frequently found in polar sea ice carries a multitude of AFP isoforms. In this study we report the heterologous expression of two antifreeze protein isoforms from *F. cylindrus* in *Escherichia coli*. Refolding from inclusion bodies produced proteins functionally active with respect to crystal deformation, recrystallisation inhibition and thermal hysteresis. We observed a reduction of activity in the presence of the pelB leader peptide in comparison with the GS-linked SUMO-tag. Activity was positively correlated to protein concentration and buffer salinity. Thermal hysteresis and crystal deformation habit suggest the affiliation of the proteins to the hyperactive group of AFPs. One isoform, carrying a signal peptide for secretion, produced a thermal hysteresis up to 1.53 °C ± 0.53 °C and ice crystals of hexagonal bi-pyramidal shape. The second isoform, which has a long preceding N-terminal sequence of unknown function, produced thermal hysteresis of up to 2.34 °C ±

0.25 °C. Ice crystals grew in form of a hexagonal column in presence of this protein. The different sequences preceding the ice binding domain point to distinct localisations of the proteins inside or outside the cell. We thus propose that AFPs have different functions *in vivo*, also reflected in their specific TH capability.

3.1 Introduction

Ice active proteins have been detected in cold adapted organisms throughout all kingdoms. First reports of these proteins in fish (DeVries and Wohlschlag 1969) were followed by the discovery in insects (Patterson and Duman 1979), plants (Griffith et al. 1992), bacteria and fungi (Duman and Olsen 1993), microalgae (Raymond et al. 1994) and a crustacean (Kiko 2010). Ice active proteins act in different ways: they can for example distort the ice crystal habit (Raymond and DeVries 1977), cause pitting on ice surfaces (Raymond et al. 1989), inhibit recrystallisation, i.e. the growth of larger ice crystals at the expense of smaller ones (Knight et al. 1984), cause thermal hysteresis (TH) (DeVries and Wohlschlag 1969; Duman and DeVries 1976), i.e. non-colligatively depress the freezing point, or exhibit several of these functions (Knight et al. 1984). Due to the different character and effect the nomenclature of these proteins varies. Compliant with Bayer-Giraldi (Bayer-Giraldi et al. 2010) we will use the term antifreeze proteins (AFPs).

According to their potential to depress the freezing point AFPs are classified as "moderate" or "hyperactive" (Scotter et al. 2006). While the moderate fish AFPs depress the freezing point by 0.7 to 1.5 °C (Duman 2001) with about 1 °C TH at 10-40 mg mL^{-1} (Graham et al. 2008), the hyperactive group of mainly insect AFPs is often reported with thermal hysteresis values of 3 to 6 °C (Duman 2001). Additionally, different patterns of crystal deformation in the thermal hysteresis gap and of the bursts at temperatures below the thermal hysteresis gap are observed for moderate and hyperactive AFPs (Scotter et al. 2006). The adsorption inhibition model, which proposes binding of the AFPs to the ice surface (Raymond and DeVries 1977), is accepted for both, moderate and hyperactive AFPs (Graham et al. 1997; Scotter et al. 2006). The difference of activity with respect to thermal hysteresis is so far hypothesised to be caused by binding of the AFPs to different crystal faces (Raymond et al. 1989; Graether et al. 2000; Scotter et al. 2006).

Organisms inhabiting the system of brine channels and pores in sea ice have developed a suite of physiological and biochemical adaptations to cope with this harsh environment (Mock and Thomas 2005). For example diatoms and bacteria produce exopolymeric substances to protect themselves against dehydration stress and the presence of ice crystals (Krembs et al. 2002), two typical traits in sea ice. Sea ice diatoms were additionally reported to excrete proteins, which can influence the crystal growth habit of ice (Raymond et al. 1994; Raymond and Knight 2003). In psychrophilic diatoms AFPs were reported to be acting as recrystallisation inhibitors since they did not cause significant thermal hysteresis (Raymond and Knight 2003). Only recently TH of 0.8 °C at 1 mg mL^{-1} protein concentration was reported for an AFP from *Chaetoceros neogracile* (Gwak et al. 2010).

For *F. cylindrus* several AFP genes have been isolated under salinity stress (Janech et al. 2006; Krell et al. 2008). Additionally, the presence of an AFP multigene family and distinct regulation patterns point towards the importance of these genes for the adaptation of *F. cylindrus* to subzero temperatures and high salinities (Bayer-Giraldi et al. 2010). The presence of a large AFP multigene family in *F. cylindrus* hampers the isolation of single protein isoforms from the diatom by biochemical separation techniques (Raymond et al. 1989; Graham et al. 1997; Marshall et al. 2004) or ice affinity based methods (Kuiper et al. 2003; Raymond 2000) from the diatom itself, e.g. for functional studies.

Detailed analyses on the function and structure of single isoform AFPs, are available for a multitude of fish and insect AFPs comprising moderate and hyperactive ones. Protein structures of different fish AFPs and insect AFPs were resolved by X-ray or nuclear magnetic resonance (NMR) studies (Nishimiya et al. 2008; Liu et al. 2007) and reviewed in (Ewart et al. 1999; Jia and Davies 2002; Doucet et al. 2009). Additionally the protein ice binding sites and in some cases the preferred binding faces at the ice crystals were determined (Nishimiya et al. 2008; Liu et al. 2007) and reviews by (Ewart et al. 1999; Jia and Davies 2002; Doucet et al. 2009). However, for the phylogenetically diverse group of AFPs, which contains the *F. cylindrus* sequences, only limited information on the function is available. Characterisations of AFPs from the bacterium *Colwellia* SLW5

(Raymond et al. 2007), the fungi *Typhula ishikariensis* (Hoshino et al. 2003; Xiao et al. 2010), *Flamminula populicola* and *Lentinula eodes* (Raymond and Janech 2009), the diatoms *C. neogracile* AFP (Gwak et al. 2010) and *Navicula glacei* (Janech et al. 2006) as well as from the crustacean *Stephos longipes* (Kiko 2010) include TH activity, crystal morphology, recrystallisation inhibition (RI) and biochemistry. Information on the ice binding sites and total protein structure of this group of AFPs is lacking.

By screening a set of expression vectors with different promoter/ribosomal binding site (RBS) combinations as well as expression tags and leader peptides (Kraft et al. 2007; Siurkus et al. 2010) we were able to overexpress two *F. cylindrus* AFP isoforms in *E. coli*. Refolding from inclusion bodies resulted in functional active single isoform AFPs. The recombinant AFPs (recAFPs) were used for functional studies and provide the basis for future analyses of the protein structure. The activity was found to be correlated with the buffer salinity and protein concentration. We report for the first time a hyperactive antifreeze protein from a psychrophilic microalga exhibiting a potential to lower the freezing point that might be ecologically significant. The amino acid sequence of this hyperactive protein belongs to a clearly separate group inside the *Fragilariopsis* clade that has a C-terminal antifreeze domain following long N-terminal preceding sequences with unknown function.

3.2 Material and methods

3.2.1 Vector construction

F. cylindrus AFP sequences Fcyl0046a10 and Fcyl0052c02 (GenBank: EL737258, EL737755) retrieved from a salt stress clone library (Krell et al. 2008) were chosen for heterologous expression in *E. coli* (Table 3.1).

The sequences were amplified from the respective *F. cylindrus* cDNA library clones with Phusion polymerase (Finnzymes) in one or two subsequent PCR reactions. Reaction conditions were as follows: One initial denaturation step at 98 °C for 5 min, followed by 30 cycles each comprising denaturation at 98 °C for 30 sec, varying annealing temperatures

Table 3.1: Names of the recombinant AFPs and the corresponding AFP isoforms as well as the EST (expressed sequence tag) names and accession numbers.

Recombinant AFP (recAFP)	Corresponding AFP isoform	EST name	EST GeneBank Acc. No.
K37	Fcyl AFP-10	Fcyl0046a10	EL737258
K20	Fcyl AFP-10	Fcyl0046a10	EL737258
K21	Fcyl AFP-12	Fcyl0052c02	EL737755

in the range of 58 to 61 °C for 30 sec, elongation at 72 °C for 30 sec; and a final elongation step at 72 °C for 5 min. The primers (Supplementary Table 3.3) introduced attB sites (dotted) for Gateway recombination, a TEV (tobacco etch virus) cleavage site (bold) and in some cases a His-Tag (underlined) into the amplicon. The primer sequences, combinations, annealing temperatures and tags introduced into the PCR products are given in Supplementary Tables 3.3 3.4. The products were cleaned up using the minElute Gel Extraction Kit (Qiagen), and introduced into the Gateway pDONR201® vector (Invitrogen) via the BP reaction. The resulting Gateway® entry plasmids were recombined with selected destination vectors (Tab. 3.2) (Kraft et al. 2007; Siurkus et al. 2010) in the LR reaction to generate the expression vector.

The reaction mixes were transformed into electrocompetent *E. coli* DH10B cells (Invitrogen) for amplification of the plasmid. Successful recombination was proven via restriction analysis and sequencing. Resulting expression vectors were transformed into Arctic^{TM}RIL cells (Stratagene) for expression.

3.2.2 Selection of expression constructs and heterologous expression

To select for constructs with strong AFP expression clones were grown overnight at 37 °C under vigorous agitation in 5 mL Plasmid Growth (PG) medium (Genetix) containing 30 μg mL^{-1} Chloramphenicol (Applichem), 30 μg mL^{-1} Gentamycin (Carl Roth) and 75 μg mL^{-1} Streptomycin (Applichem). The following day 30-50 mL PG without antibiotics were inoculated to an optical density at 600 nm (OD600) of 0.1-0.2 and grown

Table 3.2: Destination vectors and their properties chosen from Siurkus et al. (2010) and Kraft et al. (2007) for construction of expression vectors.

Name	Promotor	RBS[a]	Tag/leader peptide	Vector set
pCUlac_SUMO	plac_CU	SD_lac	His + SUMO[b], N-term	CEO[e]
pCTUT7_SUMO	plac_CTU	SD_T7	His + SUMO[b], N-term	CEO[e]
pCUlac_oA	plac_CU	SD_lac	ompA[c]	PEO[f]
pCTUT7_oA	plac_CTU	SD_T7	ompA[c]	PEO[f]
pCUlac_pB	plac_CU	SD_lac	*pelB*[d]	PEO[f]
pCTUT7_pB	plac_CTU	SD_T7	*pelB*[d]	PEO[f]

[a] RBS: ribosomal binding site

[b] SUMO: small ubiquitin-related modifier, SUMO vectors were selected following Bayer-Giraldi et al. (2011)

[c] ompA: leader peptide of the porin A of *Escherichia coli*

[d] *pelB*: leader peptide of pectatlyase B of *Erwinia carotovora*

[e] CEO: cytoplamatic protein expression and optimisation

[f] PEO: periplasmatic protein expression and optimisation

till OD600 reached 0.5-1.0. Expression was induced by addition of a final concentration of 1.0 mM IPTG (isopropyl β-D-1-thiogalactopyranoside, Omnilab) and monitored over 24 h by analysing subsamples of 20 μL of expression media with cells via SDS-PAGE (sodium dodecyl sulfate polyacrylamide gel electrophoresis). Bands of the desired size were excised and verified via mass-spectrometry. For selected constructs expression conditions were further optimised with respect to incubation temperature, IPTG concentration and expression time after induction. The constructs pCTUT7_pB_K15 (K37), pCTUT7_SUMO_K20 (K20) and pCTUT7_K21 (K21) were chosen for up-scaling (Supplementary Fig. 3.6). Cultures of these constructs were then grown in 400 mL PG without selection antibiotics at 37 °C. When OD600 reached about 0.6 (for construct K37) or 0.8 (for K20, K21) expression was induced by addition of IPTG to a final concentration of 1.0 mM, respectively 1.5 mM. After 17 h cells were harvested by centrifugation at 3200g and 4 °C for 30 min.

3.2.3 Inclusion body purification

Inclusion bodies were isolated and solubilised according to Rudolph et al. (Rudolph et al. 1997). Briefly, cells were resuspended in 0.1 M Tris-HCl, pH 7, 1 mM EDTA, incubated with lysozyme and disrupted by 5 cycles of 5 min sonication at settings cycle 4x10% and power 50% with a Sonopuls HD 2070 sonicator (Bandelin). The cell debris was treated with DNase (Omnichem) and incubated with EDTA, Triton X-100 and NaCl. The inclusion bodies were spun down at 17,000 rpm and 4 °C in a Beckman Ultracentrifuge Rotor Type 70Ti for 10 min and washed 6 times with each 20 mL of 0.1 M Tris-HCl, pH 7, 20 mM EDTA.

Inclusion bodies were then solubilised to a final concentration of 10 mg pellet per mL 6 M GdmCl, 0.1 M Tris-HCl pH 8, 100 mM Dithiotreithol, 1 mM EDTA. The pH was lowered to 3-4 by addition of HCl and insoluble cell debris removed by centrifugation at 10,000g, 4 °C for 10 min. Soluble proteins were concentrated over 15 mL 10 kD Amicon filtration devices (Millipore) according to the manufactures recommendations at 4 °C and 3220g for 20 to 45 min. For K21 dithiothreitol (DTT) was removed by dialysis against 4 M GdmCl, 10 mM HCl twice at 25 °C for 2 h and again overnight at 0 °C. Precipitate was spun down at 10,000g for 10 min at 4 °C.

3.2.4 Refolding and purification of recombinant AFPs

In order to refold the proteins, the protein solutions were quickly diluted into 50 mM Tris, 0.5 mM EDTA, 1 M Arginine, pH 8.0 (K20, K37) or 50 mM Tris, 0.5 mM EDTA, 1 M Arginine, 3 mM GSH (Glutathione), 1 mM GSSG (Glutathione disulfide), pH 9.0 (K21) to a final concentration of 0.05 mg mL^{-1} and incubated for 24 h at 4 °C. Proteins were concentrated in Amicon filtration devices as described for the solubilised proteins. The buffer was exchanged by dialysis against 50 mM Tris, pH8, 150 mM NaCl at 0 °C, twice for two hours and a third time overnight. Precipitations were removed by centrifugation at 31,000 rpm in a Beckmann Ultracentrifuge Rotor Type 70Ti for 30 min at 4 °C.

To reduce ionic strength the protein solutions were diluted 1:2 with deionised water and the recombinant AFPs purified by anion-exchange chromatography on Poros HQ 20 media (Applied Biosystems, column dimensions 4.6 x 50 mm). Proteins were eluted with a 20 mL gradient of 10 mM to 1 M NaCl in 50 mM Tris pH8.0, 1 mM EDTA and 0.02% NaN_3.

3.2.5 Determination of protein concentration and gel electrophoresis

Protein concentrations were determined with a modified Bradford assay described by Zor and Selinger (Zor and Selinger 1996), measuring at wavelengths of 450 and 600 nm (instead of 590 nm) in a Synergy HT plate reader photometer (BioTek). Standard curves were prepared with BSA (bovine serum albumin, Merck). Dilutions were made in the buffers of the respective purification step. Routine monitoring of the protein expression and purification procedure was done by 12% SDS-PAGE (Laemmli 1970) and Coomassie staining.

3.2.6 Antifreeze assays

Antifreeze activity was analysed using a nanolitre osmometer (Clifton Technical Physics) set up with a Leica M125 stereomicroscope, a Leica DFC295 camera and the Leica Application Suite V3.5.0 software. To obtain detailed information on the function of the proteins and a high sensitivity in the measurements each sample was analysed in respect to thermal hysteresis (TH), recrystallisation inhibition (RI) and crystal morphology.

Samples were each loaded in two opposite positions of the sample holder and quickly frozen to -40 °C. For the recrystallisation assay the samples were incubated at a temperature of -4 °C for 20 min, if not stated differently. In the Clifton nanolitre osmometer a sample appears turbid and dark immediately after freezing due to the formation of a multitude of small crystals. When the crystals grow bigger due to recrystallisation the scatter inside the sample decreases and the sample appears brighter. In the presence of

a recrystallisation inhibitor the turbidity does not or barely decrease. The turbidity at the end of the incubation period in comparison to the beginning was visually observed and taken as a measure for recrystallisation (similar to Kiko 2010). Thermal hysteresis was calculated as the difference of the melting point and hysteresis freezing point, which were determined as described previously (Kiko 2010). Accordingly, the melting point was defined as the temperature when the last small crystal melts, the hysteresis freezing point as the temperature when visible growth of a small remaining (2-5 μm) crystal occurs when slowly lowering the temperature. Melting and hysteresis freezing temperatures were calculated from the calibration curve prepared with ultrapure water and a standard of 3000 mOsm (95.9 g NaCl kg^{-1} ultrapure water). Additionally the morphology of the growing ice crystals was recorded. All samples were put on ice and assayed directly after the incubation procedures described below.

3.2.7 Functional characterisation

The effect of temperature, protease and dithiothreitol on antifreeze activity was assayed in recAFP solutions of 200 μg mL^{-1} (K20: 4.8 μM; K37: 6.5 μM; K21: 3.8 μM) in 50 mM Tris, 150 mM NaCl, pH 8.0 at 0 °C (salinity 11). Temperature stability was assessed by incubation at temperatures ranging from 0 °C to 50 °C for 30 min, and incubation at 20 °C from 30 to 180 min. Protease (Pronase E, Sigma) was added to a final concentration of 1 mg mL^{-1} and samples were incubated for 30 to 180 min at 20 °C. Negative controls were run with 1 mg mL^{-1} BSA instead of Pronase E. Possible formation of intra- or intermolecular disulfide bridges was assayed for K21, the only protein in this study containing cystein residues. The effect of reducing agents was determined by adding a final concentration of 5 mM DTT and incubation at 20 °C for 60 and 180 min.

The function of the recAFPs was also assayed in a range of salinities of approx. 4 to 93 (salinity describes the concentration of dissolved ions in seawater and approximately corresponds to g L^{-1} NaCl in water). For this purpose 2 μL of 1 mg mL^{-1} recAFP solutions were diluted into 8 μL of buffers of different salinities and incubated for 10 min on ice before measurements. The buffers were 50 mM Tris, pH 8.0 at 0 °C and contained

different amounts of NaCl to adjust salinities. Buffers and buffers with 200 μg mL^{-1} BSA (3.0 μM) were run as negative controls to estimate colligative effects of the different salt concentrations in the buffers. For salinities above 58 the incubation temperature for the RI assay was set to an appropriate temperature ranging down to -7.38 °C.

Additionally, recAFPs were diluted to concentrations ranging from 1.8 to 32.4 μM AFP in the above described buffers with resulting salinities of approx. 11 and 72 ± 2 incubated for 10 min on ice and assayed.

3.2.8 Phylogeny

A phylogenetic analysis of AFP sequences was performed as described in Bayer-Giraldi et al. (2010). Analysis comprised amino acid sequences of the AFP domains used in the prior analysis (Bayer-Giraldi et al. 2010) and additionally the AFP domain of *F. cylindrus* AFP sequence Fcyl0052c02 retrieved from a salt stress clone library (Krell et al. 2008). Furthermore *F. cylindrus* AFP sequences were analysed with respect to signal peptides using SignalP (Nielsen et al. 1997).

3.3 Results

3.3.1 Expression and cleanup

SDS-PAGE screening (Fig. 3.1 a) revealed strongest expression of recombinant *F. cylindrus* AFPs in pCTUT7 vectors (strong promoter/RBS combination, Table 3.2) in combination with the leader peptide *pelB* or a SUMO tag. The promoter/RBS combination pCUlac or the ompA leader peptide did not yield substantial expression of the proteins (Fig. 3.1 a). Although a multitude of different expression vectors was screened, recAFPs were found for all constructs with a notable expression in the insoluble fraction after cell lysis (compare lanes of lysates (3), cleared lysates (4) and IB pellets (5) in Fig. 3.1 b, c, d).

For further cleanup and refolding three proteins were selected (Table 3.1). Expression of gene Fcyl0046a10 (Fcyl AFP-10) in vector pCTUT7_SUMO (K20) and in vec-

tor pCTUT7_*pelB* (K37) resulted in products with predicted molecular weights of approx. 41.3 kDa (K20) and of approx. 30.9 kDa (K37), respectively. Expression of gene Fcyl0052c02 (Fcyl AFP-12) in vector pCTUT7_SUMO (K21) yielded a protein with a predicted molecular weight of approx. 52.8 kDa (K21). In the SDS/PAGE all proteins appeared at slightly higher sizes than predicted. Functionally active recAFPs (K20, K37 and K21) were obtained by solubilisation and refolding of the recAFPs from inclusion bodies (lanes 6; Fig. 3.1 b, c, d). All three proteins demonstrated recrystallisation inhibition and deformation of ice crystals. Thermal hysteresis was not assayed at this stage. Purity of the proteins was increased by anion-exchange chromatography (lanes 7; Fig. 3.1 b, c, d). AFPs K20, K37 and K21 eluted in the fractions of 160-190 mM NaCl, 100-180 mM NaCl and 130-190 mM NaCl, respectively.

3.3.2 Functional characterisation

Temperature, protease and DTT stability

Stability of the recAFPs (K20, K37, K21) was assessed with respect to temperature, protease, as well as to reduction with dithiothreitol (DTT). All proteins (K20, K37, K21) lost thermal hysteresis (TH) activity and recrystallisation inhibition (RI) activity after incubation at 30 °C for 30 min, whereas crystal shapes were still deformed to stars (K20, K37) or hexagons (K21) (3.2 q). After incubation at 40 °C for 30 min a slight deformation of the crystals to weak hexagons remained which was absent after incubation at 50 °C for 30 min.

During incubation at 20 °C for up to 180 min thermal hysteresis activity decreased slightly for all three proteins with rates of 0.023 °C h^{-1} ± 0.022 °C (K20), 0.015 °C h^{-1} ± 0.012 °C (K21) and 0.024 °C h^{-1} ± 0.015 °C (K37). Recrystallisation inhibition activity and deformation of ice crystals remained unchanged during the whole incubation period. We observed aggregation during thawing and short periods at room temperature during the cleanup procedure (K20: 14.5 μM, K21: 19.0 μM).

In respect to Pronase E treatment at 20 °C K21 was most sensitive and lost thermal hysteresis activity after 30 min incubation (Fig. 3.2 g). Activity was completely abolished

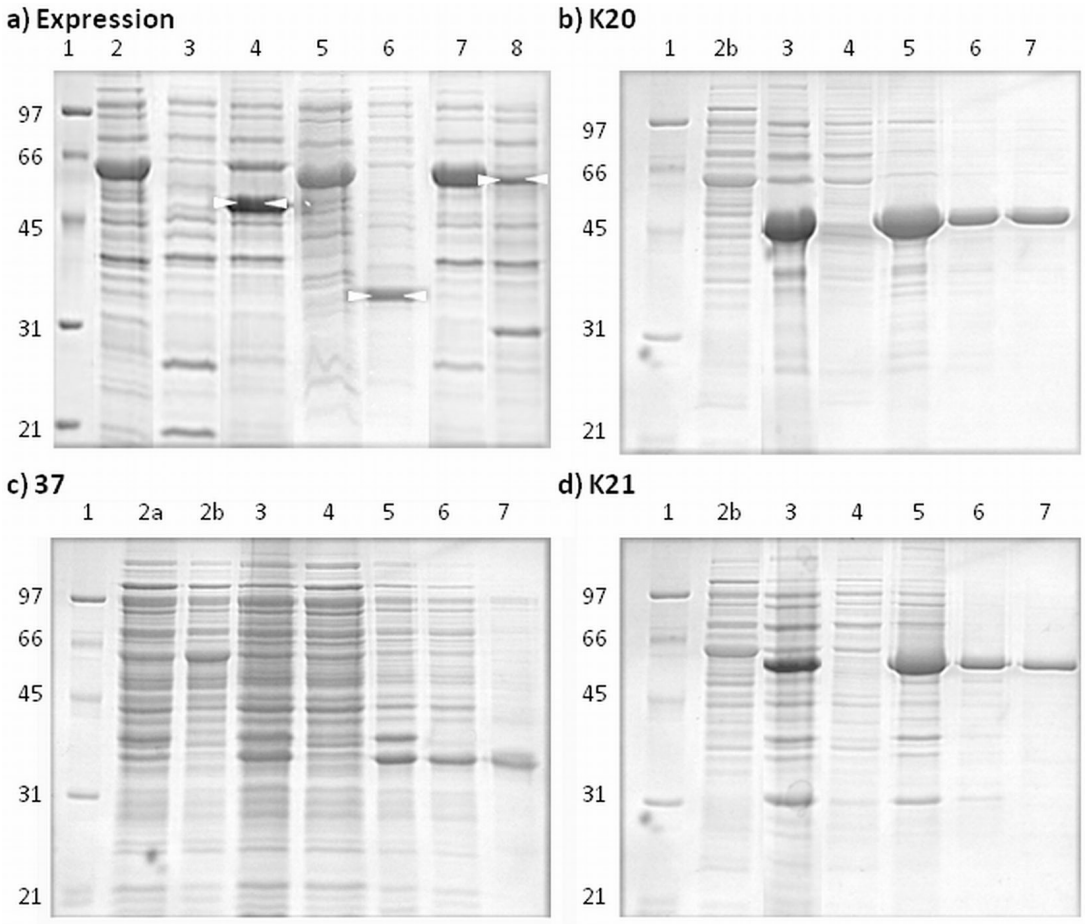

Figure 3.1: Recombinant AFP expression and purification. Expression strength in different expression vectors 18 h to 20 h after induction. (a): 1: Marker, 2: Arctic RIL cells without expression plasmid, 3: pCUlac_SUMO_K20, 4: pCTUT7_SUMO_K20 (K20), 5: pCTUT7_oA_K15, 6: pCTUT7_pB_K15 (K37), 7: pCUlac_SUMO_K21, 8: pCTUT7_SUMO_K21 (K21), 20 μL of culture were mixed with 4 μL loading buffer and boiled for 10min. Arrowheads indicate recombinant AFPs (K20, K37, K21). Expression and cleanup of recAFP constructs K20 (b), K37 (c) and K21 (d): 1: Marker, 2a: Arctic RIL cells, lysate, 2b: Arctic RIL cells, cleared lysate, 3: Lysate, 4: cleared lysate, 5: inclusion body pellet, 6: AFP after refolding, 7: AFP after cleanup.

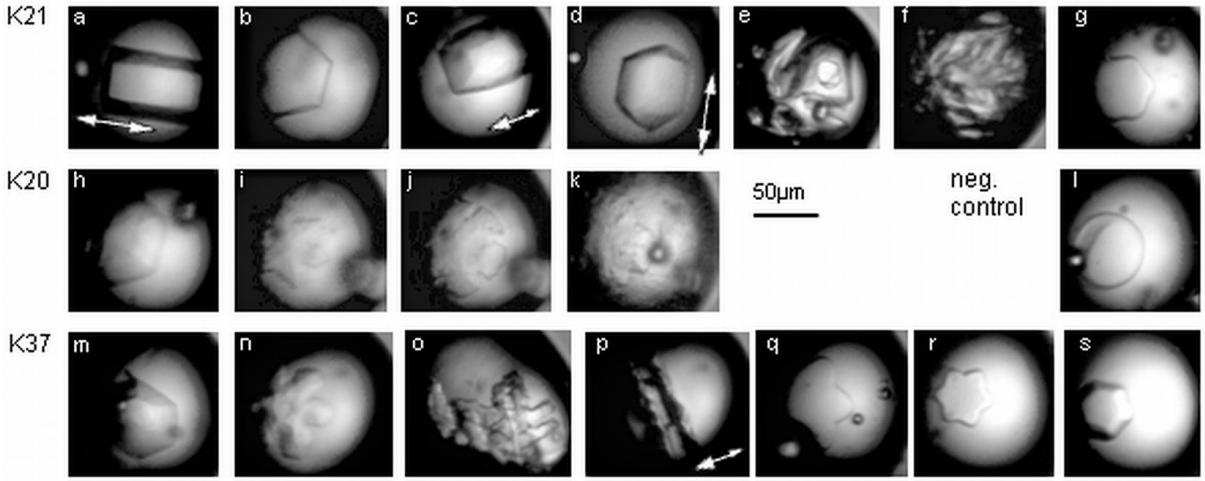

Figure 3.2: Crystal morphology in the presence of recombinant AFP at respective buffer salinity (S) and treatment. K21 (a-g) a, b, c: S=11; d: S=11, 20 °C, 30 min; e: S=30; f: S=70; g: 20 °C, 60 min, Pronase E; K20 (h-k) h: S=11; i, j: S=70; k: S=93; negative control BSA (l) S=11; K37 (m-s) m: S=11; n: S=70, 200 μg mL^{-1}; o: S=80, 200 μg mL^{-1}; p: S=70, 200 μg mL^{-1}; q: S=11, 30 °C, 30 min; r, s: 180 min, Pronase E. The recAFP concentration was 200 μg mL^{-1}. The *c*-axis orientation is perpendicular to the paper plane except for a, c, d and p, where arrows indicate the direction of the *c*-axis.

after 120 min showing round crystals in the crystal deformation assay. For K20 and K37 TH and RI activity only disappeared after incubation for 120 min, yet both proteins caused deformation of crystals after incubation for 180 min (Fig. 3.2 r, s).

Incubation of K21 with 5 mM DTT at 20 °C for 60 and 180 min did not result in any loss of activity compared to the samples incubated at 20 °C without DTT addition. This indicates that the two cystein residues are not forming a disulfide bridge essential for the antifreeze activity measured in the described assays.

Buffer salinity

Total buffer salinity influenced the performance of the recAFPs (Fig. 3.3). At protein concentrations of 200 μg mL^{-1} K20 and K37 (4.8 and 6.5 μM respectively) showed TH of approx. 0.1 °C ± 0.02 °C at a salinity of 11 whereas TH values are about two to three times higher with maximum values of 0.47 °C ± 0.15 °C at higher salinities (46 to 93).

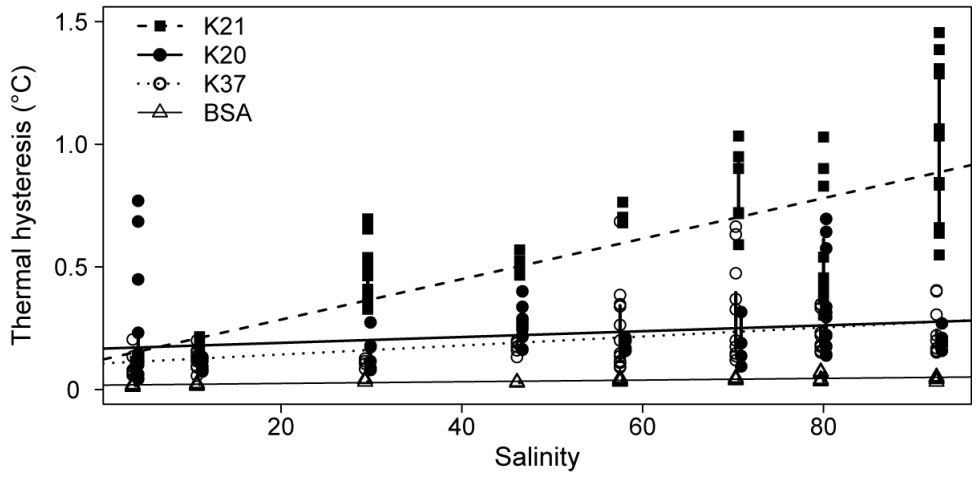

Figure 3.3: Thermal hysteresis (TH) vs. buffer salinity for different recombinant AFPs: K21 (filled squares), K20 (filled circles) and K37 (open circles) and bovine serum albumin (BSA) (open triangles) at a protein concentration of 200 μg mL^{-1}. Vertical lines indicate the 25% and 75% quanitles. Linear models are included: K21: $y = 0.0083(\pm 0.007) \cdot x + 0.1201(\pm 0.0479)$; K20: $y = 0.0012(\pm 0.0006) \cdot x + 0.1667(\pm 0.0314)$; K37: $y = 0.0018(\pm 0.0005) \cdot x + 0.1062(\pm 0.0283)$; BSA: $y = 3.437e^{-04}(\pm 3.813e^{-05}) \cdot x + 1.810e^{-02}(\pm 2.190e^{-03})$.

For K21 (3.8 μM) the effect of salt on the function of the recAFP is even more prominent. This protein produces TH of 0.16 °C ± 0.04 °C at salinity 11 and TH 0.98 °C ± 0.31 °C at salinity 93. Negative controls (buffer (data not shown) and buffer with 3.0 μM BSA (Fig. 3.3)) show TH between 0.021 ± 0.003 (salinity 11) to 0.046 ± 0.008 (salinity 93). For all proteins the scatter of TH values increases with higher salinities. For K20 there is also a high scatter at a salinity of 4. In general, single outstanding TH values were measured, when the remaining crystal was very small before growth was induced.

Linear models calculated in R V2.7.2 (R Development Core Team 2008) indicate significant differences of all the recAPFs in comparison to the negative control (BSA). In addition, K21 differs significantly from K20 and K37. The latter two cannot be distinguished.

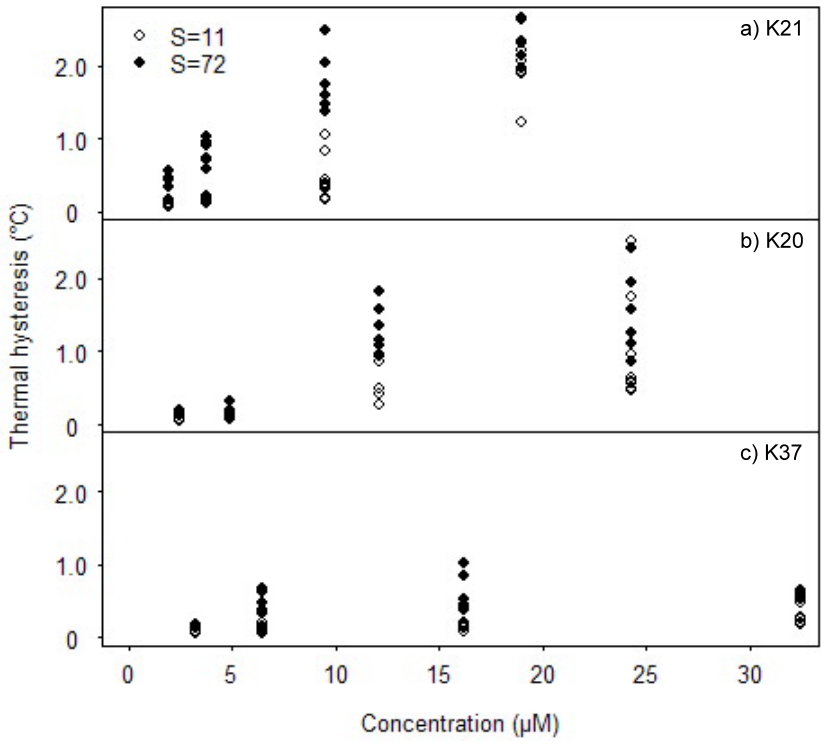

Figure 3.4: Thermal hysteresis (°C) vs. recombinant AFP concentration (μM) in buffers of salinity 11 (open circles) and 72±2 (filled circles) (a) K21, (b) K20, (c) K37 .

Concentration of recAFP

Antifreeze activity was assayed for recAFP concentrations up to 32.4 μM in buffer salinities of 11 and 72 ± 2 (Fig. 3.4). For all three proteins TH was detectable from the lowest concentration assayed with values of 0.09 °C ± 0.01 °C for K21, 0.06 °C ± 0.01 °C for K20 and K37 (1.9, 2.4 and 3.2 μM respectively). TH increased for all three proteins concomitant with higher recAFP concentration and higher buffer salinity. Maximum values were 2.34 °C ± 0.25 °C for K21 at 19.0 μM, 1.53 °C ± 0.53 °C for K20 at 24.2 μM and 0.60 °C ± 0.24 °C for K37 at 16.2 μM.

Comparing the activity in the two buffers, K20 caused 1.5 to 2.5 times higher TH in the buffer with salinity 72 ± 2 than in the buffer with salinity 11. For K37 the factors range from 2.6 to 3.8. For K21 the effect of salt concentration on the TH was dependent upon protein concentration. In the lower concentrations (up to 9.5 μM) the factors ranged

from 4.4 to 5.1 and in the higher concentrations it was 1.2.

Best fits were obtained by fitting the square root of the protein concentration in μM against TH (data not shown) as described in Kristiansen and Zachariassen (2005). Nevertheless the power of the model is limited since for K21 salinity of 11 and K20 salinity of 11 and 72 a sigmoidal correlation between TH and protein concentration was observed.

Crystal morphology in recAFP solution

The shape of ice crystals growing in recAFP solution was strongly dependent on protein concentration and salinity. In the respective assays protein integrity also influenced the resulting shapes. In solutions with bovine serum albumin (BSA), as negative control, crystals appear as circular disks in this assay (Fig. 3.2 l).

In the presence of K20 or K37 (4.8 μM and 6.5 μM) at low salinities (e.g. 11) crystals grew in the direction of the *c*-axis to form a bi-pyramid with hexagonal cross-section. The bi-pyramids often did not grow to a complete pyramid, but the tip was usually missing, exhibiting a hexagonal surface (Fig. 3.2 h, m, s). At higher salinities (70 to 93) crystals in the presence of K20 were star-shaped with some depth in *c*-axis direction (Fig. 3.2 i, n), or snowflake-like (Fig. 3.2 j, k). In the presence of K37 crystals grew dendritic, which was mostly combined with an explosive growth below the hysteresis freezing point (Fig. 3.2 o, p). Dendritic growth developing very fine dendrites was observed for K20 and K37 at high protein concentrations. With higher concentration the explosive growth effect got more pronounced, hindering photographic documentation. When protein integrity is diminished by protease treatment or incubation at 30 °C the star and hexagonal shapes become smoother and more 2-dimensional (Fig. 3.2 q, r, s).

In the presence of K21 (3.8 μM) and a salinity of 11 crystals grew to hexagonal columns with predominant growth in the direction of the *c*-axis (Fig. 3.2 a, c). The basal plane formed a clear hexagonal-shape. Since the diameter of the column did not diminish during growth the hexagonal flat surface remained at the end of the column (Fig. 3.2 b). After incubation for 30 min at 20 °C the development of a cylinder with a pyramid at each end was occasionally observed (Fig. 3.2 d). At a salinity of 30 the crystal shapes resembled

leaves (Fig. 3.2 e) and developed to an explosive dendritic growth at higher salinities (Fig. 3.2 f). For higher protein concentrations of K21 similar effects as described for K20 and K37 were observed.

3.3.3 Phylogeny

The overall topology of the calculated phylogenetic tree is identical to that described by Bayer-Giraldi et al. (2010) showing three groups (data not shown). Inside the *Fragilariopsis* sequences (Supplementary Fig. 3.7) it is possible to distinguish three clades. Clades A and B contain several *F. cylindrus* and *F. curta* sequences. The AFP domain of sequence Fcyl AFP-12 (Fcyl0052c02) clearly groups separately in the *Fragilariopsis* AFP phylogeny (clade C). This clade is supported by five other sequences from the *F. cylindrus* genome (pers. comm. Thomas Mock, University of East Anglia, UK). The full AFP sequence available on the EST (expressed sequence tag) clone Fcyl0052c02 contains a 131 amino acid sequence of unknown function preceding the AFP domain.

Half of the other *F. cylindrus* AFP sequences were predicted to carry signal peptides. Since Fcur AFP and Fcyl AFP sequences were isolated by PCR or from ESTs Bayer-Giraldi et al. (2010), sequences might be truncated at the N-terminus and signal peptide sequences might be cut off.

3.4 Discussion

3.4.1 Quality and characteristics of recAFPs

The multitude of different but very similar AFP isoforms in *F. cylindrus* hinders the isolation of a single natural AFP isoform from this diatom. Employing heterologous expression in *E. coli* we were able to produce active single isoform recombinant AFPs for functional studies. We were able to identify recAFPs in the inclusion body fraction, as earlier reported for heterologous expression of spruce budworm AFP (Gauthier et al. 1998) and fish type III AFP (Chao et al. 1993), yet expression did not result in a soluble AFP fraction.

Refolding of the denatured proteins from inclusion bodies produced active recAFP that displayed functions assigned to AFPs like crystal deformation, recrystallisation inhibition and thermal hysteresis.

Unlike the AFP EST and genome sequences the recAFPs in this study carry a His-tag and a SUMO-tag (K20, K21) or a leader peptide (K37) at the truncated N-terminus. These peptides might alter the AFP activity compared to a native protein. Tags can enhance AFP activity due to increased size of the AFP leading to a larger ice surface covered by the AFP and a bulkier residue to be overgrown by addition of new water molecules to the ice surface. The TH activity of a 7 kDa fish type III AFP was increased by two to three times due to addition of a 12 kDa thioredoxin residue or a 42 kDa maltose-binding-protein, resulting in a protein size approximately three and seven times larger than the native protein (DeLuca et al. 1998). For isoform Fcyl AFP-10 we observed higher activity for the large SUMO-tag construct (K20) than for the construct with the smaller *pelB* leader peptide (K37) (Fig. 3.4). Whereas in the low concentration range the activity of both proteins Fcyl APF-10 plus SUMO-tag (K20) and plus *pelB* (K37) is similar, in the high concentration range they show considerable differences (Fig. 3.4). Nevertheless we assume that the enhancing effect of the SUMO-tag and leader peptide is rather small since the increase in size of the fusion-proteins is only 1.2 (K37) and 1.6 times (K20) for isoform Fcyl AFP-10 and 1.4 for isoform Fcyl AFP-12 (K21).

On the other hand the tag and leader peptide might change the tertiary structure or sterically hinder the interaction of the AFP with the ice surface and thus reduce AFP activity. The SUMO-fusion proteins (K20 and K21) carry a GS-sequence which provides a flexible linker avoiding sterical interference of the SUMO-tag with the rest of the recAFP (Argos 1990). The leader peptide does not carry a GS-linker but was supposed to be cleaved off at the signal peptidase I cleavage site (Dalbey et al. 1997). Due to the formation of inclusion bodies the protein was not transported to the periplasm, hindering the cleavage of the leader peptide. Sterical interference of the leader peptide might hinder the interaction of the AFP with the ice surface, leading to a negative effect on TH.

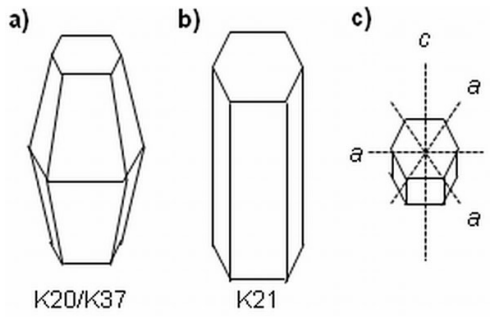

Figure 3.5: Schematic drawings of crystal shapes grown in the presence of recAFP: a) hexagonal bi-pyramid without tips for proteins K20 and K37, b) hexagonal column for protein K21, c) designation of crystal axes.

Thermal hysteresis of recAFPs presented here might thus differ from the potential of the native *F. cylindrus* AFPs. Crystal deformation was not influenced by the type of tag or leader peptide (DeLuca et al. 1998), since K20 and K37 show the same deformation patterns, e.g. hexagonal bi-pyramid (Fig. 3.4 m, n ,3.5 a).

3.4.2 TH potential

Maximal thermal hysteresis values for the *F. cylindrus* recAFPs K20 (1.53 °C ± 0.53 °C at 24.2 μM (1 mg mL^{-1})) and K37 (0.60 °C ± 0.24 °C at 16.2 μM (0.5 mg mL^{-1})) are in the same range as reported for mature *C. neogracile* AFP (0.80 ± 0.03 °C, 38.2 μM (1 mg mL^{-1})) (Gwak et al. 2010). The activity was found to be approximately ten fold higher than that of fish AFPs where values of 0.7 to 1.5 °C (Duman 2001) are common with about 1 °C TH at 10-40 mg mL^{-1} (Graham et al. 2008). Maximal TH values measured for K21 (2.34 °C ± 0.25 °C at 19.0 μM (1.0 mg mL^{-1})) are the highest reported for diatom AFPs to date. The group of hyperactive AFPs defined by Scotter et al. (2006), comprising several bacterial, insect and fish AFPs, is one to two orders of magnitude more active than moderately active fish AFPs. Albeit the *F. cylindrus* recAFPs did not reach TH values of up to 5.5 °C reported for hyperactive insect AFPs (Scotter et al. 2006) they fall well within the hyperactive group at concentrations assayed in this study. Higher concentrations of recAFPs were not tested due to limits in the expressed protein concentration process.

Thermal hysteresis is known to increase complementarily with AFP concentration in solution. However, the correlation varies according to different models proposed for antifreeze proteins and antifreeze glycoproteins (Raymond and DeVries 1977; Feeney et al. 1986; Kristiansen and Zachariassen 2005). In our study the recAFPs' TH is linear with the square root of the protein concentration for K37 at both salinities and K21 at salinity of 72 (data not shown), which suggests a similar kinetic as described in Kristiansen and Zachariassen (2005). In contrast K20 at both salinities and K21 at a salinity of 11 follow a sigmoidal correlation (Fig. 3.4) already reported for a Ca^{2+}-dependent bacterial AFP (Gilbert et al. 2005) and smaller antifreeze glycoproteins (Feeney et al. 1986), indicating cooperative interaction (Feeney et al. 1986). At constant concentration of recAFP the addition of NaCl enhances the TH activity of the recAFPs like reported for one other *F. cylindrus* AFP (Bayer-Giraldi et al. 2011) as well as for *Berkeleya sp.* and *Amphiprora sp.* AFP preparations (Raymond 2000). The correlation is linear and most pronounced for K21 (Fig. 3.3). In the natural environment of sea ice diatoms it is highly efficient to couple the antifreeze function to salinity since lower temperatures in the brine pockets are accompanied by higher salinities (Cox and Weeks 1983). Thus additionally to the up-regulation of AFP gene expression (Bayer-Giraldi et al. 2010), the proteins themselves exhibit a higher activity, when temperatures drop and salinity inevitably increases.

Since AFP function and activity is dependent on AFP concentration, it is important to estimate their concentration in the natural system to infer which function the diatom AFPs fulfil *in vivo*. Raymond et al. (1994) suggest a concentration of 50 μg mL^{-1} AFP in seawater for full recrystallisation inhibition activity. Extrapolating from TH values obtained for K21 at a salinity of 93, K21 could cause TH up to 0.25 °C at a concentration of 50 μg mL^{-1} (0.9 μM K21), adding to the colligative freezing point depression caused by elevated salinity. The additional small TH, in combination with other exudates, e.g. exopolymeric substances, might ensure a liquid layer around the diatom cell (Krembs et al. 2002), avoiding freezing damage. K20 and K37 would probably not account for any TH at a concentration of 50 μg mL^{-1}.

If natural concentrations of the diatom AFPs fall short of the minimal AFP concentration required for thermal hysteresis, diatom AFPs will probably act as recrystallisation inhibitors. This function requires 100-500 times less AFP than thermal hysteresis (Ewart et al. 1999). RI was proposed to be an important function of diatom AFPs since AFP preparations from natural sea ice samples containing high amounts of diatoms (Raymond and Knight 2003) showed low TH. The recAFPs studied here have the ability to inhibit recrystallisation. Mechanical damage of cells by large ice crystals can thus be avoided (Thomashow 1998).

We observed that TH values and crystal deformation results were dependent on the size of the initial crystal and additionally on the position in the sample holder. For the beetle *Ragium inquisitor* it was stated that measured TH values were inversely proportional to the ice crystal size in the TH assay (Zachariassen and Husby 1982). In our study this effect caused considerable scatter in the data. Nevertheless, single values of extraordinary high TH are important since they reflect the potential of the proteins to inhibit crystal growth if the starting crystal is small. If the diatom AFPs also act inside the cell and there are no nucleation seeds present, they might be able to protect the cell from internal freezing by supercooling. Supercooling can be substantially higher than the TH activity measurable with the nanolitre osmometer (Zachariassen and Husby 1982).

3.4.3 New crystal deformation shape

At low concentrations of K21 and low salinities ice crystals grow in form of a hexagonal column (Fig. 3.5 b). This shape (designated also as columnar spicule) has so far only been reported for a TH-inactive mutation of a herring type II antifreeze (Liu et al. 2007, figure 7, panel 4). In contrast K21 shows high potential of freezing point depression. It is likely that K21 binds to different faces on the ice crystal than K20 and K37. The latter cause hexagonal bi-pyramidal shapes frequently reported for moderate AFPs indicating AFP binding to the nonbasal or pyramidal planes (Raymond and DeVries 1977; Davies and Hew 1990; Knight et al. 1991; Wen and Laursen 1992). In any case, the missing tips of the bi-pyramids grown in the presence of K37 and K20 suggest binding also to the

basal planes (Fig. 3.5 a). Binding to the basal plane is evident for K21, which produces prominent hexagonal surfaces at the end of the hexagonal columns (Fig. 3.5 b). The observation of pyramids at the ends of a hexagonal column after incubation at 20 °C for 30 min (Fig. 3.2 d) indicates that the affinity to the basal planes is diminished when the protein is subjected to conditions that lead to protein degradation. K21 probably binds to the basal plane and to the primary prism faces as previously described for the spruce budworm AFP (Graether et al. 2000). In contrast to the spruce budworm AFP, for all recombinant *F. cylindrus* AFPs the main growth direction at low concentration is along the *c*-axis (Fig. 3.5).

Even though we were not able to clearly determine the crystal axes in small crystals, we conclude that bursts occurred parallel to the *a*-axes. Burst patterns of crystals in recombinant Fcyl AFP solutions showed radial symmetry and resembled those described for hyperactive AFPs (Scotter et al. 2006). Occasionally, growth of two parallel layers was observed (Fig. 3.2 q). Spicular bursts, which are typical for moderate AFPs (Scotter et al. 2006), did not occur. Concluding, the binding patterns as well as TH potential observed for the recAFPs in this study suggests classification into the hyperactive group proposed by Scotter et al. (2006).

3.4.4 Phylogeny and function of *F. cylindrus* AFP sequences

Showing high thermal hysteresis potential and distinct crystal morphology K21 (Fcyl AFP-12), additionally groups into a phylogenetically separate clade (C) (Fig. 3.7). The long preceding sequence clearly distinguishes this sequence from the other *F. cylindrus* AFP sequences. Whereas AFP sequences from clades A and B (Fig. 3.7) carry signal peptides at the N-term that suggest a secretory pathway (Janech et al. 2006), no information is available on the function of the long preceding sequence of Fcyl AFP-12. This part of the protein shows no similarity to known proteins, it could be involved in AFP function, subcellular localisation, or other yet not recognised functions of AFPs. It is known from the winter flounder *Pleuronectes americanus* that multiple isoforms of AFPs are located in distinct organs (blood, skin) and carry different functions (plasma antifreeze, intracel-

lular antifreeze) (Gong et al. 1996). We assume that in the sea ice diatom *F. cylindrus* the secretory isoforms are acting uncoupled from the cell in the brine and most probably as recrystallisation inhibitors. The non-secretory AFPs might function as intracellular antifreeze or associated to the cell. It was suggested previously for plants and insects that AFPs in association with plasma membranes might act as antifreeze to prohibit seeding of crystallisation over the cell membrane (Urrutia et al. 1992; Duman 2001). However, it was not specified whether these proteins are integrated inside the membrane with transmembrane domains, or whether they are associated differently to the surface of the cells.

3.5 General remarks to strain classification

According to Lundholm and Hasle (2008) the *Fragilariopsis* strain used in our lab, which was isolated from the Weddell Sea in 1999, is *F. nana* and not *F. cylindrus*, as previously referred to. The same holds true for the sequenced *Fragilariopsis* strain CCMP 1102, which is actually *F. nana*. To avoid confusion we followed the preceding reports (Krell et al. 2008; Bayer-Giraldi et al. 2010) denoting the sequences as Fcyl, but we suggest to correct the nomenclature in following studies to Fnana.

Acknowledgements

Research for this project was partially funded by a scholarship of the German National Academic Foundation to Christiane Uhlig. Johannes Kabisch and Thomas Schweder were financially supported by the German Federal Ministry of Education and Research (BMBF) (0315400A/B). We thank Hauke Lilie for advice on the refolding protocol and Thomas Mock for information on AFP sequences of the *F. cylindrus* genome. Stephan Frickenhaus helped with preparation of the figures. We thank Sven Kranz and Jim Raymond for helpful comments on the manuscript and Gerhard Dieckmann for support.

3.6 Supplementary material

Table 3.3: Names and sequences of the primers used for amplification of the AFP genes from cDNA library clones. Sequences introducing attB sites (small caps) for Gateway recombination, His-Tag (brackets) and TEV restriction sites (bold) are shown.

Name	Sequence
CU0018	GGGGACAAGTTTGTACAAAAAAGCAGGCTtatgctacctgtcctcgtagtccc
CU0024	GGGGACAAGTTTGTACAAAAAAGCAGGCTtatgctacctgtagcccccgtag
CU0029	GGGGACCACTTTGTACAAGAAAGCTGGGTa[catcaccatcaccatcac] **gaaaacctgtattttcagggc**atgcacgaagaaacaacaacagatg
CU0032	GGGGACAAGTTTGTACAAAAAAGCAGGCTtatgcttcagtgattgcattgctc
CU0035	accatcaccatcac**gaaaacctgtattttcagggc**aataatccatctccccctgctgtcg
CU0036	GGGGACCACTTTGTACAAGAAAGCTGGGTa[catcaccatcaccatcac]gaaaacctg
CU0038	accatcac**gaaaacctgtattttcagggc**gcatccatcaacgtccaacccgtc
CU0040	GGGGACAAGTTTGTACAAAAAAGCAGGCTtc[gaaaacctgtattttcagggc]
CU0041	cGAAAACCTGTATTTTCAGGGCgcatccatcaacgtccaacccgtc
CU0042	cGAAAACCTGTATTTTCAGGGCaataatccatctccccctgctgtcg
CU0043	cGAAAACCTGTATTTTCAGGGCatgcacgaagaaacaacaacagatg
CU0044	GGGGACCACTTTGTACAAGAAAGCTGGGTttatgctacctgtagcccccgtag
CU0045	GGGGACCACTTTGTACAAGAAAGCTGGGTttatgctacctgtcctcgtagtccc
CU0046	GGGGACCACTTTGTACAAGAAAGCTGGGTttatgcttcagtgattgcattgctc

Table 3.4: Destination vectors and their properties chosen from Siurkus et al. (2010) and Kraft et al. (2007) for construction of expression vectors.

Name	Clone from cDNA library	Primer fw ($1^{st}/2^{nd}$ reaction)	Primer rev	Annealing temp. °C ($1^{st}/2^{nd}$ reaction)	Tag	Protein restriction	Vector set
K13	Fcyl0052c02	CU0029	CU0032	58	His, N-term	TEV[a]	PEO[b]
K15	Fcyl0046a10	CU0035/CU0036	CU0018	60	His, N-term	TEV[a]	PEO[b]
K20	Fcyl0046a10	CU0042/CU0040	CU0045	61/58	none	TEV[a]	CEO[c]
K21	Fcyl0052c02	CU0043/CU0040	CU0046	61/68	none	TEV[a]	CEO[c]

[a]TEV: tobacco etch virus

[b]PEO: periplasmatic protein expression and optimisation,

[c]CEO: cytoplamatic protein expression and optimisation.

>K20_pCTUT7_SUMO_K20

m[hhhhhh]GSGLVPRGSASMSDSEVNQEAKPEVKPEVKPETHINLKVSDGSSEIFFKIKKTTPLRRLM
EAFAKRQGKEMDSLRFLYDGIRIQADQTPEDLDMEDNDIIEAHREQIG*ggggs*astslykkagf**enlyfqg**n
npsppavdlgtaedfvilakagvtnvpggyitgdigvspiaasamtgfnlimdssnefststeasgsfyapdymsptgtklttav
sdmltayndaaarpvtggpfdnslsgetytnlgageiggltltpgvytydisvgitgsdvtfdgdgnedsvfiiktsksvlqaagt
evilqngakaenifwsvaqevnvgagahmkgillvktavkfitgssfegrvlsatavtlqeatikqptassarrglrgqva

>K21_pCTUT7_SUMO_K21

m[hhhhhh]GSGLVPRGSASMSDSEVNQEAKPEVKPEVKPETHINLKVSDGSSEIFFKIKKTTPLRRLM
EAFAKRQGKEMDSLRFLYDGIRIQADQTPEDLDMEDNDIIEAHREQIG*ggggs*astslykkagf**enlyfqg**m
heetttdgetfkkvnvghcvssediasmwvanekgsdarlviadtdtvssiepvttgraswnddhivmggmtfvpnqqctd
snrrklhdtpsfdsisihralkervdflggrrlidrvledggsyatnqlinnpnkvnlgtagnyvilgktgitggagsdvngdmgv
spitsaavtgfglikqvadgfstssvvngkiyaadynteatpaklttaignmqaaytdsqsrlasngaynnigggeiggldlgrgv
ytfntpvsitssmtftggpddvfiiktskglkqaaatkvilaggakaenifwsvagtvyvgatahmegiilvatsatfitgsslngri
lsqtavnlqsnaitea

>K37_pCTUT7_pelB_K15

MKSLLPTAAAGLLLLAAQPAMAsdhfvqeswv[hhhhhh]**enlyfqg**nnpsppavdlgtaedfvilakagvtnvpg
gyitgdigvspiaasamtgfnlimdssnefststeasgsfyapdymsptgtklttavsdmltayndaaarpvtggpfdnslsget
ytnlgageiggltltpgvytydisvgitgsdvtfdgdgnedsvfiiktsksvlqaagtevilqngakaenifwsvaqevnvgagah
mkgillvktavkfitgssfegrvlsatavtlqeatikqptassarrglrgqva

Figure 3.6: Protein sequences of the constructs selected for refolding and functional analysis. His-Tag (brackets) and TEV restriction sites (bold) SUMO-tag/pelB peptide (small caps) and GS-linker (cursive) are shown. The AFP protein sequences start directly after the TEV restriction sites.

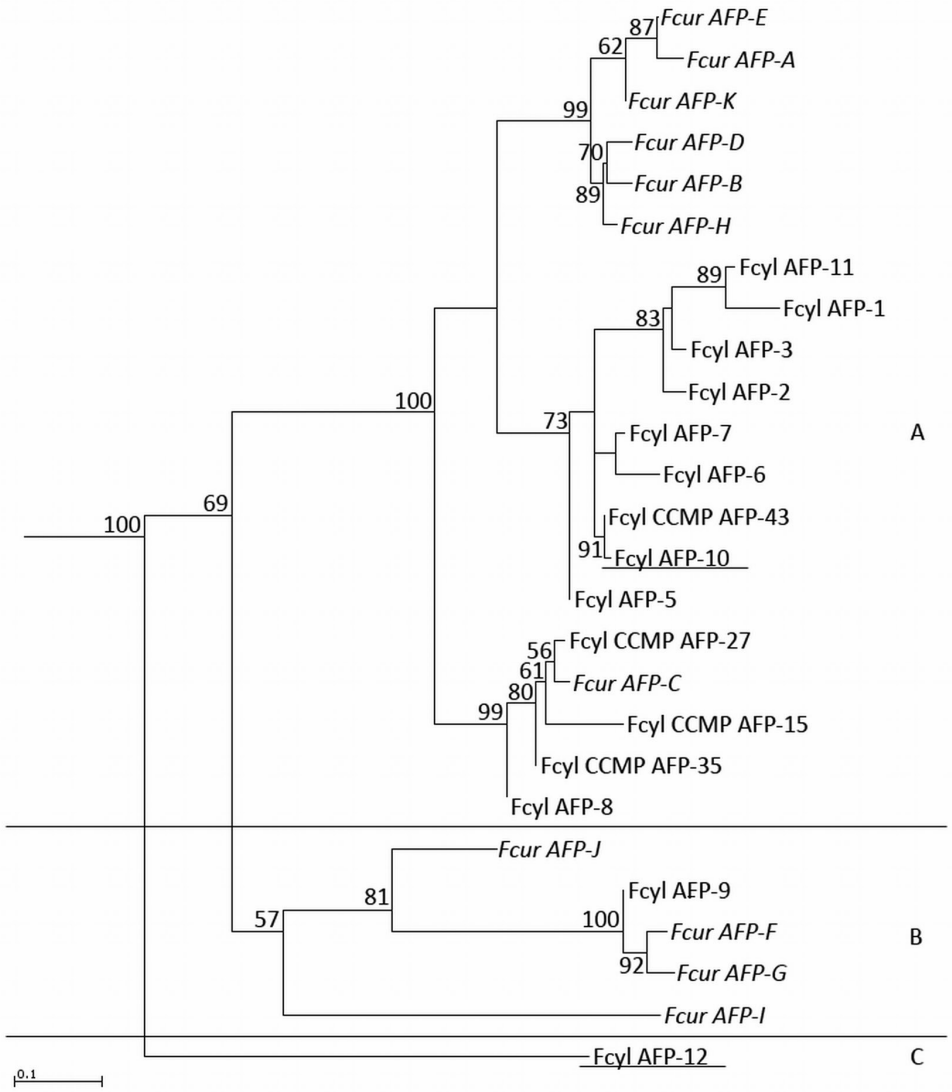

Figure 3.7: Close up into the phylogeny of *Fragilariopsis* AFP domains estimated with PhyML. PhyML algorithm v3.0 was applied with the following settings: model for amino acid substitution WAG, initial tree: BioNJ, 100 bootstraps (modified after Bayer-Giraldi et al. 2010). Nodal support values greater than 55 are shown. *F. curta* (Fcur) sequences are shown in italics. Sequences used for heterologous expression are underlined (Fcyl AFP-10, Fcyl AFP-12).

4 Differential abundance and phylogenetic diversity of AFP transcript fragments in environmental transcriptomes from polar sea ice

Christiane Uhlig, Fabian Kilpert, Klaus Valentin, Jessica Kegel, Andreas Krell, Thomas Mock, Bánk Beszteri

Abstract

Antifreeze proteins (AFPs) are known as an adaptation mechanism of organisms subjected to subzero temperature and freezing conditions. They have been found and studied from organisms inhabiting sea ice, particularly diatoms. Information on the presence and phylogeny of AFP sequences isolated from environmental samples is lacking up to date. We analysed AFP sequences from five transcriptomes of eukaryotic communities from Arctic and Antarctic sea ice for functional expression and phylogenetic relationship. AFP transcripts were found in all cDNA libraries with abundances ranging from 115 to 1824 AFP sequences per 100,000 reads. Phylogenetic placement assigned 90% of the sequences to a clade of AFPs from the diatoms *Navicula glacei*, *Chaetoceros neogracile* and the crustacean *Stephos longipes*. The remaining 10% belong to a separate clade of *Fragilairopsis* AFP sequences. These findings show that AFPs play an important role in eukaryotic sea ice organisms in their natural habitat and that the *Navicula*/*Chaetoceros* clade is more prominent than the *Fragilariopsis* clade under the investigated conditions.

4.1 Introduction

Sea ice constitutes one of the largest ecosystems in the world, accommodating a vast community of organisms including viruses, bacteria, microalgae and small metazoans (Thomas and Dieckmann 2002). Despite permanent changes in abiotic conditions as well as subzero temperatures the organisms inside the brine channels and pores of sea ice thrive and proliferate due to a whole suite of physiological and biochemical adaptations (Mock and Thomas 2005). One of these is the production of antifreeze proteins (AFPs), also called ice-active substances or ice-binding proteins (Raymond and Knight 2003; Raymond et al. 2007).

AFPs have been demonstrated to be present and active in sea ice diatoms (Raymond et al. 1994; Raymond 2000). First evidence of AFP genes from diatoms was reported for *Navicula glacei* and *Fragilairopsis cylindrus* (Janech et al. 2006; Krell et al. 2008). A follow-up study showed that *F. cylindrus* and *F. curta* have a multitude of AFP isoforms (Bayer-Giraldi et al. 2010). These also display different transcription patterns, which indicate functional differentiation between the isoforms (Bayer-Giraldi et al. 2010). Phylogenetically diatom AFPs cluster in two separate groups (Bayer-Giraldi et al. 2010). The first group formed by the *Fragilariopsis* sequences is rather distantly allied to the second containing the *N. glacei* and *C. neogracile* sequences. The former clade is more closely related to fungal AFP sequences, the latter to Archeal ones, than both are to each other (Bayer-Giraldi et al. 2010). This tree topology indicates horizontal gene transfer events for the acquisition of AFP genes (Bayer-Giraldi et al. 2010) as previously speculated for an AFP sequence from the crustacean *Stephos longipes* that clusters with the *Navicula* and *Chaetoceros* AFPs (Kiko 2010).

Functional analyses of heterologously expressed diatom AFP isoforms from *Fragilariopsis cylindrus* and *Chaetoceros neogracile* revealed strong activity with respect to thermal hysteresis (i.e. freezing point depression) and recrystallisation inhibition (Gwak et al. 2010; Bayer-Giraldi et al. 2011; Uhlig et al. 2011). Recrystallisation describes the process of small ice crystals growing into larger ones by grain boundary migration, which can lead

to deleterious effects for organisms, as membranes can be damaged by lager ice crystals (Thomashow 1998). *F. cylindrus* AFP and a glycoprotein fraction of extracellular polymeric substances (EPS) from *Melosira arctica* have been described to alter ice structure and brine pore morphologies (Bayer-Giraldi et al. 2011; Krembs et al. 2011). A mushy ice structure and increased brine retention was observed, in presence of these substances, which was hypothesised to create a more favourable microenvironment for the organisms (Krembs et al. 2002; Krembs et al. 2011; Bayer-Giraldi et al. 2011).

Our current knowledge on AFPs primarily comes from studies on unialgal laboratory cultures. Shotgun sequencing of environmental genomic DNA or mRNA now provides tools to analyze the presence and activity of genes in the environment and can give insight on gene evolution, e.g. horizontal gene transfer events (reviews by Heidelberg et al. 2010; Mock and Kirkham 2011). Especially for microorganisms and in marine environments metagenome and metatranscriptome data have already contributed significantly to the understanding of microbial community composition and function (e.g. Venter et al. 2004; Rusch et al. 2007; Yooseph et al. 2007; Frias-Lopez et al. 2008). Studies like the Global Ocean Sampling (GOS)-Expedition and others have so far, however, mainly focused on procaryotes (e.g. Venter et al. 2004; Rusch et al. 2007; Yooseph et al. 2007; Frias-Lopez et al. 2008). One reason is that metagenomic approaches are difficult to apply for eukaryotic communities, e.g. due to the large genome size of eukaryotes compared to prokaryotes, and the presence of introns (Heidelberg et al. 2010; Grant et al. 2006). For eukaryotes transcriptomic studies are more applicable since introns and non-coding regions (which constitute the majority of eukaryotic genomes) are absent in mRNA. Furthermore, metatranscriptomes provide information on the actual gene activity of communities in a habitat under certain environmental conditions (John et al. 2009), a type of information that is not gained from metagenomes. First studies on environmental transcriptomic activity of eukaryotic communities are now available from algal mats of hot springs in China, and also from a marine habitat, Tampa Bay in Florida, USA (Grant et al. 2006; John et al. 2009). Metagenomic and -transcriptomic data can also be employed to analyse the presence, activity and phylogeny of single gene classes in the environment in comparison

with cultured organisms, as done for phosphatase genes from marine bacteria (Sebastian and Ammerman 2009).

In this study we identify AFP genes from randomly sequenced cDNA libraries and a shotgun cDNA pyrosequencing dataset from sea ice community mRNA. We assess the diversity and phylogenetic distribution of AFP fragments thus found using phylogenetic placement and interpret the relative AFP fragment abundance as a rough measure of *in situ* transcriptional activity. This study provides first metatranscriptomic insights into AFP diversity and transcriptional activity from eukaryotic sea ice communities.

4.2 Material and Methods

4.2.1 Sampling

Sea ice samples from the Southern Ocean were collected on cruise ANTXXIII-7 of RV Polarstern in the Weddell Sea in 2006 (sampling sites G and S) and on the SIPEX cruise of RV Aurora Borealis in the Dumot d´Urville Sea in 2007 (sampling sites A and J). The Arctic sample was retrieved from Kongsfjord, Svalbard, in spring 2009 (sampling site KF) (Table 4.1).

Ice samples were retrieved by collection of biomass rich ice pieces which were freshly broken by passage of the ship (ice fishing, for station G), or by drilling (Kovacs drill 9 cm diameter, all other samples). From the cores, the lower biomass rich sections (1 - 10 cm) were taken, cut in slices, crushed, washed with cold sterile brine or sea water and filtered at 4 °C under vacuum not exceeding -200 mbar onto polycarbonate filters with pore size 1.2 μm for Kongsfjord (KF) and Weddell Sea (G, S) samples and 0.2 μm for SIPEX (A, J). Filters were either treated with RNAlater® (Applied Biosystems) (0.5 to 1.5 mL) and stored at -80 °C (A, J, KF) or frozen dry and stored in liquid nitrogen (G, S) until RNA extraction.

Table 4.1: List of sampling sites including sampling date and position and physical properties of sea ice. Data of stations A and J were adapted from (Meiners et al. 2011) and for station G and S from (Haas et al. 2009).

Station		Date	Latitude	Longitude	Ice thickness (m)	Salinity (range or mean)	Temp (°C)	Ice type at lower section	Age of ice
Antarctic									
Weddell Sea	G[a]	060923	60°07.150 S	47°54.550 W	1.46 (±0.05)	n.d.	n.d.	n.d.	1^{st} year ice
	S	061008	65°06.117 S	57°23.551 W	1.51 (±0.57)	5.66	n.d.	columnar	1^{st} year ice
Dumont d´Urville Sea	A	070911	64°13.773 S	127°57.132 E	0.59 (0.52—0.70)	5.0 – 11.4	-5.7 (-9.7 to -2.3)	granular-columnar -granular	1^{st} year pack ice
	J	071003	65°01.496 S	117°42.015 E	1.08 (1.05-1.09)	2.1 – 8.1	-4.5 (-6.8 to -2.0)	columnar	1^{st} year pack ice
Arctic									
Kongsfjord	KF	090504	78°57.550N	12°20.023 E	0.50	5.4 – 9.9	-2.01 (-2.1 to -1.6)	n. d.	1^{st} year ice (spring melt)

[a] due to the sampling method (ice fishing) no information on physical ice properties is available for station G, ice thickness and age were assumed to be similar to an other station from 060923 and values adapted

4.2.2 RNA preparation

For samples stored in RNAlater®, RNAlater® solution was removed by repeated centrifugation for 10 min at 10,000 g to 16,000 g and 4 °C. RNA was isolated using TRIreagent® (Sigma) according to the manufacturer's recommendations except the following modifications. TRIreagent® was heated to 60 °C before addition to the cell pellet, and glass beads (diameter 212 - 600 μm) were used to facilitate homogenisation of the cells. Isopropanol precipitation was carried out at -20 °C and for samples stored in RNAlater®, 200 μL RNAse-free water was added to improve mixing of the aqueous phase and the isopropanol. DNA was digested using the RNAse-Free DNase Set (Qiagen) and RNA purified either by using the RNeasy kit (Qiagen) or by ammonium acetate precipitation.

4.2.3 Construction of cDNA libraries and 454 sequencing

Construction of cDNA libraries for all stations was accomplished by vertis Biotechnologie AG (Munich, Germany) (see Table 4.2 for samples used for cDNA library establishment). First strand synthesis from total RNA was conducted using an oligo(dT)-linker primer and cDNA was further amplified with high fidelity polymerase. The plasmid vector pBS II sk+ was used for ligation of cDNA. For cloning, the ligations were electroporated into T1 Phage resistant TransforMax™EC100™-T1R (Epicentre) electro-competent cells. Sanger sequencing of the complete cDNA libraries was performed by the Max-Planck-Institute for Molecular Genetics (Berlin, Germany) using the M13 forward primer (TGT AAA ACG ACG GCC AGT).

Additionally, 454 sequencing was performed for a pooled sample of G3 and S3 (Weddell Sea) (Table 4.2). Messenger RNA (mRNA) was purified twice using the Oligotex mRNA mini kit (Qiagen) to reduce the amount of rRNA and bacterial mRNA. Pooled mRNA was used in the SuperSmart cDNA synthesis kit (Clontech) for generation of double-stranded cDNA in 30 PCR cycles with the standard protocol. 10 μg of the cDNA was used for library construction at the NERC sequencing facility in Liverpool (GS-FLX), UK and 454 Roche (GS-Titanium), US. Both sequencing facilities prepared the libraries according

Table 4.2: Environmental RNA samples investigated in this study and respective sequencing method.

Sample/ dataset	Station (see Table 4.1)	Reference in text	Processing and sequencing
G3/S3	One samples each from station G and S (pooled)	metatranscriptome G3/S3	mRNA cleanup, cDNA synthesis, 454 sequencing of cDNA
G5	G	cDNA library G5	1^{st} strand synthesis from RNA with oligo(dT)-primer, cDNA library construction, Sanger sequencing of the entire library
S5	S	cDNA library S5	
A4	A	cDNA library A4	
J4	J	cDNA library J4	
KF1	KF	cDNA library KF1	

to standard 454 Roche protocols but specifically for either FLX or Titanium sequencing. Sequencing was performed according to the protocols for the GS-FLX platform (Liverpool) and the 454 Roche GS-Titanium (US). For assembly of 454 sequence reads, Newbler (Roche, version 2.6) was applied with default parameters for transcriptomic sequences.

4.2.4 Sequence retrieval and phylogenetic placement

For retrieval of AFP sequences, the sea ice cDNA libraries and the metatranscriptome were filtered against a reference AFP set. This set included all AFP protein sequences used by Uhlig et al. (2011) and additionally bacterial ice nucleation protein sequences as well as *Chlamydomonas*, fish, plant and insect AFPs. TBLASTX was run with the environmental datasets as database and the reference AFP sequences as queries with a cutoff e-value of 10^{-3}. BLAST analysis for the metatranscriptome was only done with the contigs. BLAST runs for the cDNA libraries were done with the contigs as well as with the singletons (i.e. sequences that were not assembled to a contig). Potential AFP candidates were retrieved from the datasets either manually or using mothur (Schloss et al. 2009). Resulting sequences were cross-checked manually versus the non-redundant protein

database (*nr*) at NCBI with the BLASTX algorithm. Sequences retrieving no AFP hits or other than AFP sequences as top hits were discarded. AFP candidates were translated to amino acids in the respective reading frame resulting from the BLAST search.

For phylogenetic placement a reference alignment was calculated as reported previously (Bayer-Giraldi et al. 2010) applying the ClustalW algorithm in Mega 4.1 (Tamura et al. 2007) with all sequences used in Uhlig et al. (2011). A reference phylogeny was built with PhyML 3.0 (Guindon and Gascuel 2003) including bootstrap analysis with 100 replicates. A profile HMM was calculated from the reference alignment with HMMER 2.3.2 (Durbin et al. 1998). All translated AFP candidate sequences were aligned to the reference alignment with HMMER 2.3.2 (Durbin et al. 1998) and placed into the reference tree with pplacer 1.0 (Matsen et al. 2010). Graphical output was generated using placeviz and the trees were displayed and modified in Archaeopteryx (Han and Zmasek 2009). Taxonomy assignments were chosen according to the best placement (pplacer output parameter maximum likelihood weight ratio (MLratio)). Additionally, the quotient MLratios 1^{st} hit/2^{nd} hit was calculated to assess robustness of the placement. The placement was considered robust when the ratio was $\geq$5. When the ratio was smaller, it was analysed if the 2^{nd} hit hit belonged to another AFP group than the 1^{st} hit (for grouping see Fig. 4.1). Phylogenetic placement (Fig. 4.2) was conducted both with singletons and contigs. For the cDNA libraries (see Table 4.2), calculation of the numbers of AFP sequences per 100,000 reads (Fig. 4.3) was based on the unassembled reads (i.e. contigs were weighted according to the number of reads belonging to them). In case of the metatranscriptome (see Table 4.2), these calculations took only into account the number of reads that were grouped into contigs. Due to high error rate in 454 sequencing and short read lengths (Margulies et al. 2005), sequences that were not assembled into contigs were discarded.

For comparison, taxonomy was also assigned to each AFP candidate according to the best BLAST hit running BLASTP against *nr* at NCBI. Calculations were done as described for the phylogenetic placement.

4.3 Results

4.3.1 AFP candidates

To identify AFP sequences in eukaryotic communities from sea ice, we searched five cDNA libraries and one metatranscriptome from five different sampling sites (Tables 4.1, 4.2) for AFP sequences. BLAST analysis resulted in six unassembled reads for the Arctic cDNA library KF1 (Table 4.3). The Antarctic cDNA libraries revealed 16 (A4), 10 (J4), 19 (G5) and 106 (S5) AFP reads, whereas the metatranscriptome G3/S3 had 22 AFP sequence fragments (Table 4.3). All potential AFP candidates were similar to AFP sequences previously known from sea ice diatoms and a crustacean and related to the sequences published by Bayer-Giraldi et al. 2010. No significant hits were found for any of the other groups (i. e. bacterial ice nucleation proteins or *Chlamydomonas*, fish, plant and insect AFPs). Although TBLASTX searches with sequences from the latter groups yielded in some hits from our datasets, none of these hits passed the reverse check against *nr* at NCBI, since all were resulting in much better alignment scores with non-AFP sequences.

Relative abundance of AFP fragments (AFP sequences per 100,000 reads) varied considerably among different samples. Four of the cDNA libraries contained between 115 (KF1) and 329 (G5) AFP sequences per 100,000 reads. Sample S5 stood out with an approximately 10 times higher AFP abundance (1824 AFPs per 100,000 reads). Surprisingly the metatranscriptome of samples G3/S3 (parallel samples to cDNA libraries G5 and S5, see Table 4.2) only revealed a number of 14 AFP sequences per 100,000 reads.

4.3.2 Phylogeny of environmental AFP sequences

Two thirds (50 out of 69) of the candidate AFP singletons and contigs were placed with high robustness (MLratios 1^{st} hit/2^{nd} hit ≥ 5) (Fig. 4.2, Supplementary Fig. 4.4, 4.5, 4.6). Half (10 out of 19) of the insecure placements showed the 2^{nd} hit in a different group from the 1^{st} hit (Fig. 4.2, Supplementary Fig. 4.4, 4.5, 4.6). This was especially often observed when the 1^{st} hit was not placed inside a clade but at the node defining that clade (e.g. sequence awiA4P0002O06, Fig. 4.2).

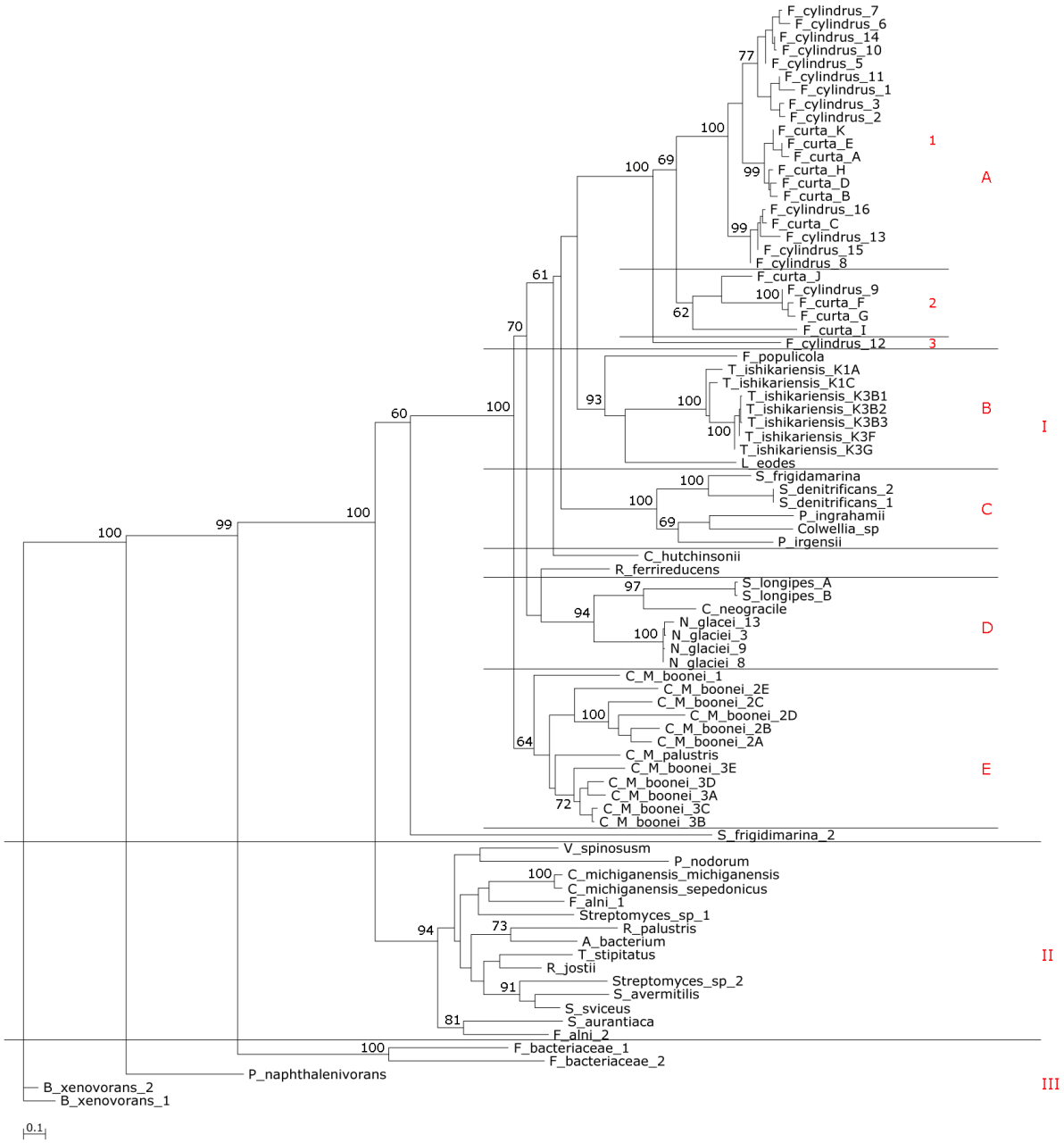

Figure 4.1: Reference tree for phylogenetic placement of environmental AFP sequences based on the maximum likelihood criterion calculated with PhyML. Bootstrap supports higher than 60 are shown for the main nodes. Grouping was chosen similar to (Bayer-Giraldi et al. 2010; Uhlig et al. 2011) and used in further analysis. Sequence names that differ from previous publications are listed in supplementary Table 4.4. Branch lengths show substitutions per site (see scale bar).

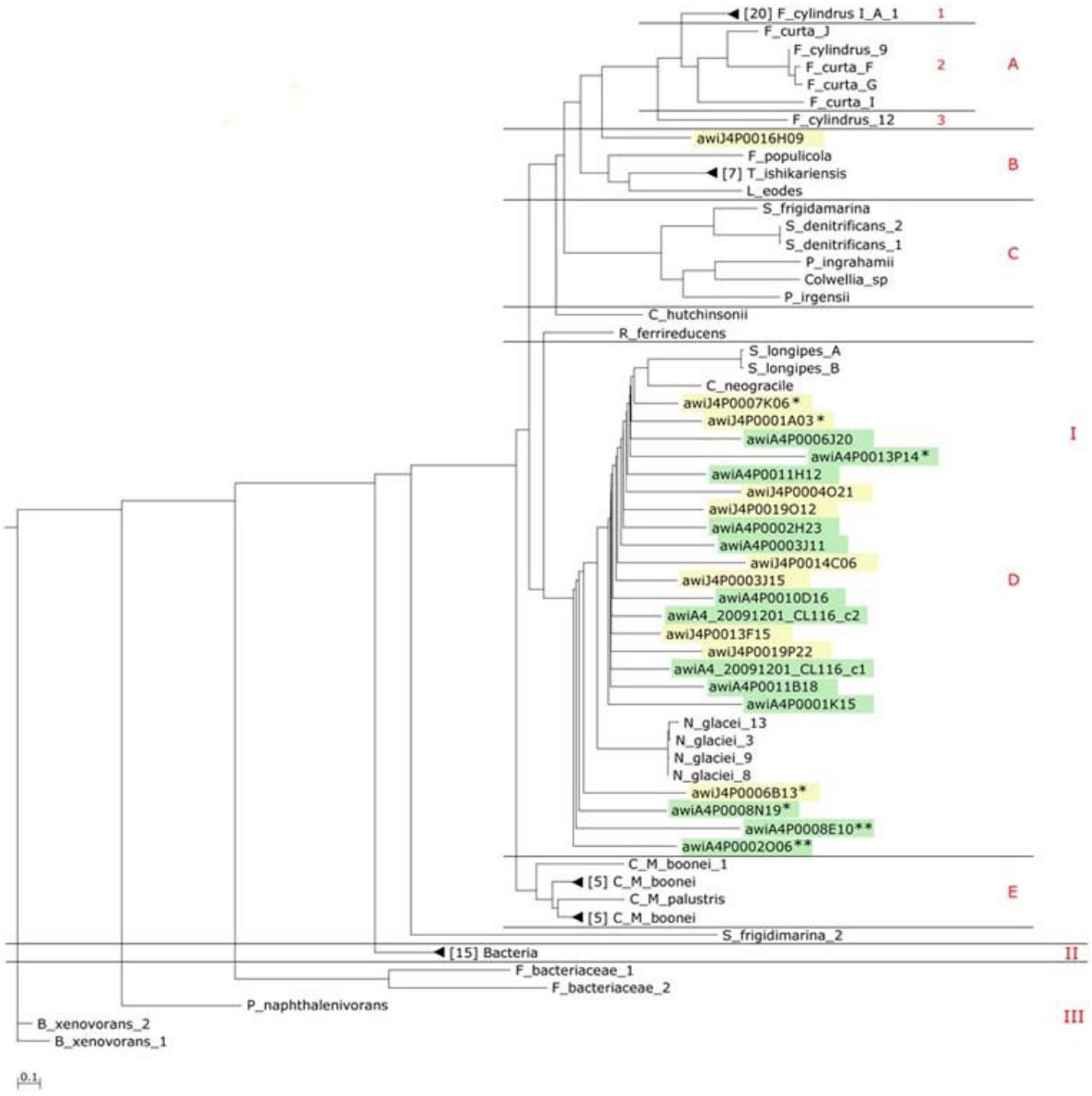

Figure 4.2: Phylogenetic placement of AFP sequences from samples A4 and J4. Sequences are coloured according to the sample (yellow J4 and green A4). Low placement security (ML ratios 1^{st} hit/2^{nd} hit <5) is indicated by stars. Hits placed in the same group are marked with one star (*), whereas hits with the 2^{nd} hit in another group are marked with two stars (**). Note that contigs contain several unassembled reads (see Supplementary Table 4.6). Groups not containing hits are collapsed and the number of sequences therein shown in brackets. The reference tree was calculated with PhyML. Branch lengths show substitutions per site (see scale bar).

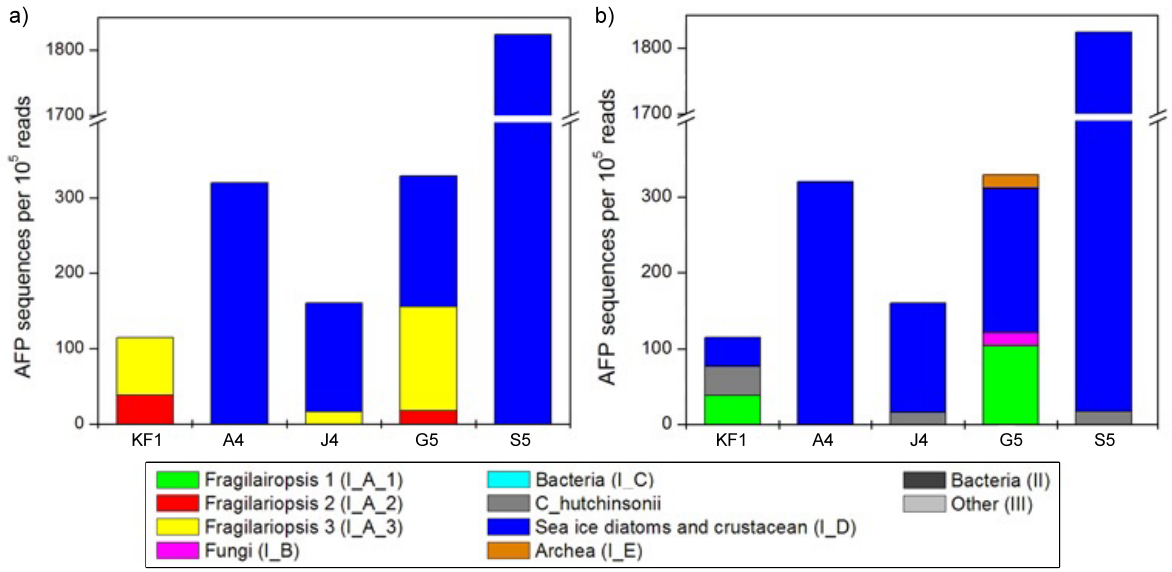

Figure 4.3: Number of AFP sequences in AFP groups of reference tree for phylogenetic placement (a) and best BLAST (b). Calculations are based on numbers of unassembled reads.

All AFP candidate sequences retrieved from the Arctic cDNA library KF1 were placed to the *Fragilariopsis* sequences (clade I_A) (Fig. 4.3 a, Table 4.3, Supplementary Fig. 4.4). In contrast, when assigning the taxonomy using BLAST, two sequences each were assigned to the *Fragilariopsis* (clade I_A_1), *C. hutchinsonii* (no clade) and sea ice diatoms and crustacean (clade I_D) sequences (Fig. 4.3 b, Supplementary Table 4.5). All sequences from cDNA library A4 were affiliated to the sea ice diatom and crustacean clade (I_D) in both, the phylogenetic placement and the best BLAST hit analysis (Fig. 4.2, Fig. 4.3, Table 4.3, Supplementary Table 4.5). For sequences from sample J4 results of both analyses matched for the majority of sequences, which belonged to the sea ice diatom and crustacean clade (I_D) (Fig. 4.2, Fig. 4.3, Table 4.3, Supplementary Table 4.5). Only one sequence diverged, which was placed to the *Fragilariopsis* sequences (clade I_A_3), but had *C. hutchinsonii* as best BLAST hit (Fig. 4.2, Fig. 4.3, Table 4.3, Supplementary Table 4.5). Half of the sequences of cDNA library G5 were affiliated to the sea ice diatom and crustacean clade (I_D) in both analyses (Fig. 4.3, Table 4.3, Supplementary Fig. 4.5, Supplementary Table 4.5). The remaining sequences were placed

Table 4.3: Total number of AFP reads in the respective AFP group resulting from phylogenetic placement, additionally the total number of unassembled reads for each dataset and the average read length in base pairs (bp) are given.

AFP-Group	Clade	cDNA library					454[a]
		KF1	A4	J4	G5	S5	G3/S3
Total		6	16	10	19	106	22
F_cylindrus 1	I_A_1						
F_cylindrus 2	I_A_2	2			1		
F_cylindrus 3	I_A_3	4		1	8		
Fungi	I_B						
Bacteria	I_C						
Sea ice diatom and crustacean	I_D		16	9	10	106	22
Archea	I_E						
Bacteria + Fungi	II						
Other	III						
No. of unassembled reads		5228	5002	6245	5773	5812	157553
Average read length (bp)		645	665	699	815	790	176

[a]454: 454 sequencing of cDNA

to the *Fragilariopsis* sequences (clade I_A), whereas BLAST resulted in six best hits for *Fragilariopsis* sequences (clade I_A) and one hit each for Fungi (I_B) and Archaea (I_E) (Fig. 4.3, Table 4.3, Supplementary Fig. 4.5, Supplementary Table 4.5). All sequences from cDNA library S5 were placed to the sea ice diatom and crustacean sequences (clade I_D) (Fig. 4.3, Table 4.3, Supplementary Fig. 4.5). When using BLAST, one of those sequences had *C. hutchinsonii* as best hit (Fig. 4.3, Supplementary Table 4.5). For the metatranscriptome G3/S3 the single contig containing all 22 AFP reads was affiliated in the sea ice and crustacean clade (I_D) with both methods (Table 4.3, Supplementary Fig. 4.6, Supplementary Table 4.5).

4.4 Discussion

4.4.1 Abundance of AFP sequences

Five cDNA libraries and one metatranscriptome from eukaryotic sea ice communities (Table 4.2) were screened for the presence of AFP sequences, by filtering the datasets against reference AFP sequences. All datasets revealed AFP sequences but we observed a large discrepancy of the relative abundance of AFP sequences between the metatranscriptome G3/S3 and the parallel cDNA libraries G5 and S5 (Table 4.2). Whereas the metatranscriptome G3/S3 had only 14 sequences per 100,000 reads, the parallel cDNA libraries G5 and S5 had 329 and 1824 AFP sequences per 100,000 reads, respectively (Table 4.3). The metatranscriptome shows a low complexity as, from a total of 212,301 original reads, 157,553 were assembled to only 670 contigs. Of those 279 were large contigs with length $\geq$500 base pairs. The AFP contig, however, was 793 base pairs (bp) in length and thus comparable to the Sanger reads with an average length of 645 to 815 bp. Placement of the short original reads (only 176 bp in average) showed similar results with most of the hits in the sea ice diatom and crustacean clade (data not shown). Also a less stringent BLAST analysis (with e-value=10 instead of e-value=10^{-3}) did not result in more putative AFP fragments, since none of the sequences found in addition passed the reverse BLASTX check against the non-redundant database at NCBI. In conclusion, it is likely that the lower quality, i.e. higher error rate and shorter read length of the 454 reads in comparison to Sanger reads (Margulies et al. 2005), leads to the discrepancy in the numbers of AFP fragments between the parallel samples from stations G and S (Table 4.2).

In search of an explanation for the striking multitude of AFP sequences from cDNA library S5 compared to all other samples, we analysed the data on physical properties of sea ice at the time of sampling. Data from stations KF, A, J and S do not indicate any emergent differences (unpublished data and Haas et al. 2009; Meiners et al. 2011) explaining the much higher number of AFP sequences in sample S. No data is available for station G, thus a detailed comparison between the two Weddell Sea samples is not feasible. Unfortunately, no metagenomic studies have been conducted on the samples

investigated in the present work. Metagenomic data can be used to normalise transcript numbers to the copy number of genes in the genomic dataset (Frias-Lopez et al. 2008). If few genes are present in the genomic set, fewer transcripts can be expected, than if many were present. High representation of transcripts might solely be caused by the dominance of a single species or group that then influences the transcript numbers of particular genes (Sebastian and Ammerman 2009). 18S data indicate, however, that at least at class or genus level this is probably not the reason for the strong presence of AFP sequences in station S. Both, stations S and G, are dominated by Bacillariophyta or rather *Fragilariopsis* species (J. Kegel personal communication, Haase 2007).

4.4.2 Identification of target genes - pplacer versus BLAST

Comparison of the taxonomy assignment with pplacer and BLAST shows, that the classification of sequences from the sea ice diatom and crustacean clade (e.g. for samples A4, J4, S5) reach agreement (Fig. 4.3). In contrast samples KF1 and G5 show more inconsistencies between both analyses (Fig. 4.3). Sequences assigned to *Fragilariopsis* clades 2 and 3 (I_A_2, I_A_3) by pplacer often have the best BLAST hit in *Fragilariopsis* clade 1 (I_A_1). Analyses with BLAST, however, have shown to be error prone in phylogenetic assignments (Koski and Golding 2001; Hanekamp et al. 2007) and can be difficult to interpret, depending on the search results (Matsen et al. 2010). For sequences, for which no close relatives are represented in the database, BLAST will result in some best hit, which might be far away from the true related sequences (Koski and Golding 2001). In the phylogenetic placements this case is easier to detect, since the hits will appear deep in the tree, the likelihood ratios of the best placements will be similar, and the best placements will be far apart, i.e. not on adjacent nodes. In the subsequent discussion we will thus refer to the results of phylogenetic placement with pplacer only.

Sequences with low placement security (about 20% of all sequences), were usually placed before a node defining a clade. For those sequences taxonomy assignment either by pplacer or BLAST have to be particularly interpreted with caution, since, closely related sequences are lacking. In addition, the phylogeny of AFPs does not overlap with

the phylogeny of the respective species. For example, AFP sequences from the diatoms *Fragilariopsis sp.* are more closely related to fungal and bacterial AFP sequences than to the other diatom AFPs from *Navicula glacei* and *Chaetoceros neogracile* (Fig. 4.1) (Bayer-Giraldi et al. 2010). This incongruence between AFP and species phylogenies was previously hypothesised to be caused by multiple horizontal gene transfer events (Kiko 2010; Bayer-Giraldi et al. 2010).

4.4.3 Presence of AFP genes *in situ* versus molecular biodiversity

By studying Arctic and Antarctic environmental cDNA libraries we show that AFPs are expressed *in situ* in both Polar Regions. The Arctic dataset KF1 differs from the other datasets in having AFP sequences placed into the *Fragilariopsis* clade (I_A), whereas nearly all AFP sequences from Antarctic samples were placed exclusively to the sea ice diatom and crustacean sequences (clade I_D). Only half of the sequences of sample G5 (Antarctic) were affiliated to the *Fragilariopsis* clade.

For the Antarctic stations J, G and S the eukaryotic biodiversity was previously assessed based on 18S rDNA sequences (J. Kegel personal communication). Stations G and S are clearly dominated by Bacillariophyta (diatoms); over 80% and over 90% of 18S sequences, respectively, were assigned to this taxon. Station J is dominated by Dinophyceae (dinoflagellates), with over 70% of the reads versus only 17% diatoms (J. Kegel personal communication). AFP sequence distribution, however, is more similar for stations J and S both dominated by AFP clade I_D (sea ice diatoms and crustacean). In contrast, station G has approximately equal amounts of AFP sequences from the *Fragilariopsis* clade (I_A) and the sea ice diatom and crustacean (clade I_D). The sample from the dinoflagellate-rich station J shows a similar amount of AFP sequences to the diatom dominated stations. For the tropical dinoflagellate *Karina brevis* an EST library revealed one sequence with similarity to antifreeze-glycoproteins from the polar cod (*Boreogadus saida*) (E=10^{-6}) and the black-legged tick (*Ixodes scapularis*) (E=10^{-4}) (Monroe et al. 2010). BLAST searches of those sequences against cDNA library J4 did not result in any significant

hits. Investigations on other polar microalgae taxa like dinoflagellates and prymnesiophytes (e.g. *Phaocystis antarctica*) might identify more AFP sequences from microalgae than currently known. It is possible that also dinoflagellates acquired AFP-like genes by lateral gene transfer, either from bacteria or fungi or even from diatoms.

4.4.4 Importance of clade I_D

The dominance of sequences placed to the sea ice diatom and crustacean sequences (clade I_D) indicates that this clade might be of particular importance for eukaryotic sea ice organisms, especially microalgae (diatoms, dinoflagellates) dominating the assemblages in these samples. It is possible that genes from this clade might also be present and active in *Fragilariopsis* species. At least two stations (G and S) were additionally shown to be dominated by *Fragilariopsis* species (with over 80% and 90% of 18S sequences, respectively) (Haase 2007). Despite the dominance of *Fragilariopsis sp.* in the two stations, relatively few of the AFP sequences (50% for station G and none for station S) were grouped with the *Fragilariopsis* AFPs. It is surprising that none of the environmental sequences were placed in the large *Fragilariopsis* subclade 1 (I_A_1) (Fig. 4.1). Sequences from this clade were previously shown to be differentially expressed under salinity and temperature stress in *Fragilariopsis cylindrus* and *F. curta* and thought to be important due to their multitude of isoforms (Bayer-Giraldi et al. 2010). Inside this group an E/G point mutation at amino acid position 18 was observed that correlated with up-regulated and down-regulated isoforms, respectively (Bayer-Giraldi et al. 2010). It was speculated that a successive activation of several AFP isoforms might take place, when the cells are subjected to elevated salinity and subzero temperature (Bayer-Giraldi et al. 2010). The previous study investigated conditions resembling the freezing of diatoms into the ice in autumn and the subsequent several days. In contrast, the organisms investigated in the present study had been incorporated in the sea ice for the entire winter, since sampling took place in early to late spring. It might thus be possible, that genes from clade I_A_1 are activated as short term stress response to decreasing temperature and ice formation, whereas genes from clades I_A_2, I_A_3 and I_D are activated for long term protection.

Acknowledgements

We would like to thank Stephan Frickenhaus for assembly of the metagenome data. This work was supported by the Deutsche Forschungsgemeinschaft (DFG) through grant VA 105/13-1 and 2 to KV.

4.5 Supplementary material

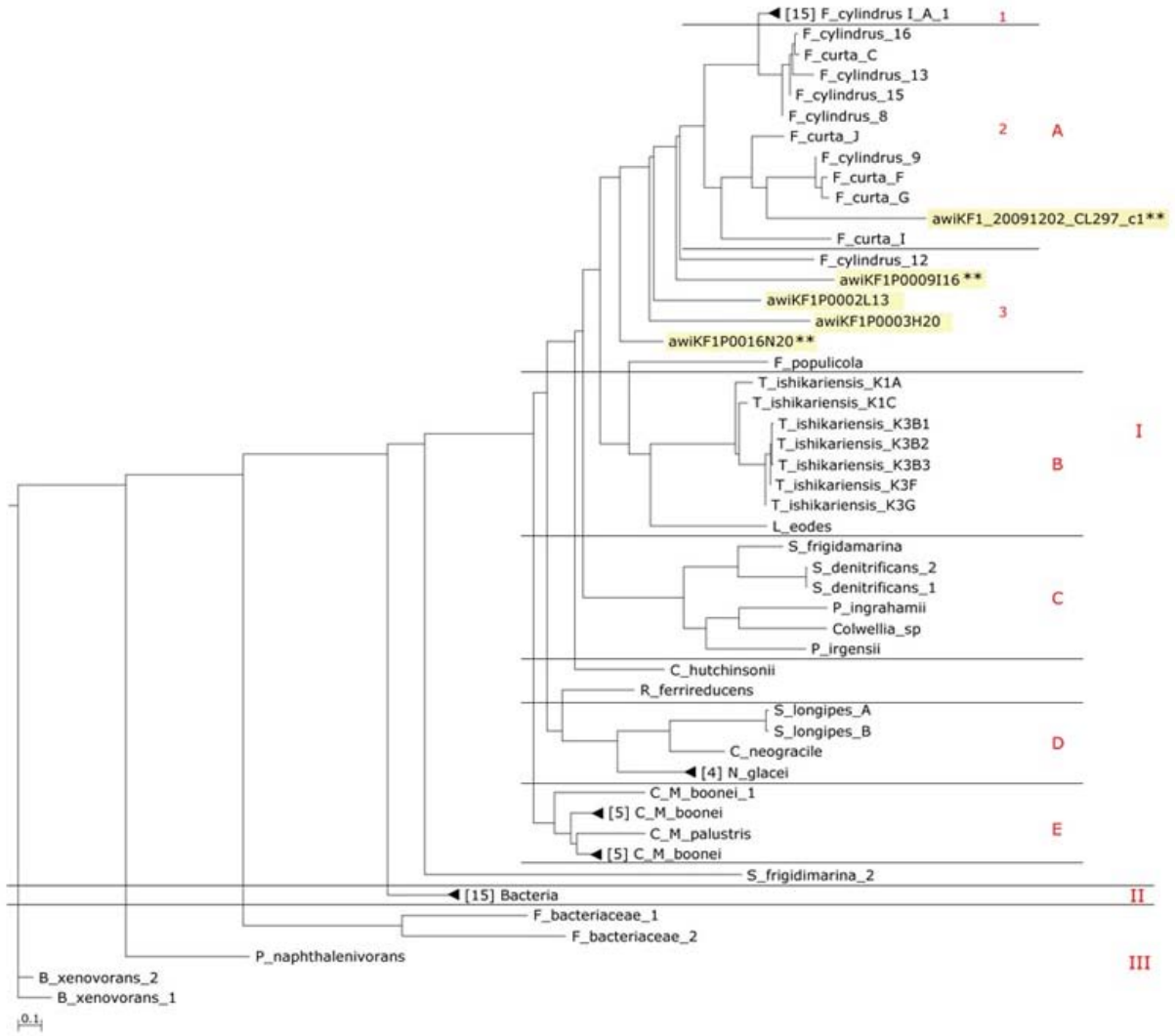

Figure 4.4: Phylogenetic placement of AFP sequences from sample KF1. Sequences are marked in yellow. Low placement robustness (ML ratios 1^{st} hit/2^{nd} hit <5) is indicated by stars. Hits placed in the same group are marked with one star (*), whereas hits with the 2^{nd} hit in another group are marked with two stars (**). Note that contigs contain several unassembled reads (see Supplementary Table 4.6). Groups not containing hits are collapsed and the number of sequences therein shown in brackets. The reference tree was calculated with PhyML. Branch lengths show substitutions per site (see scale bar).

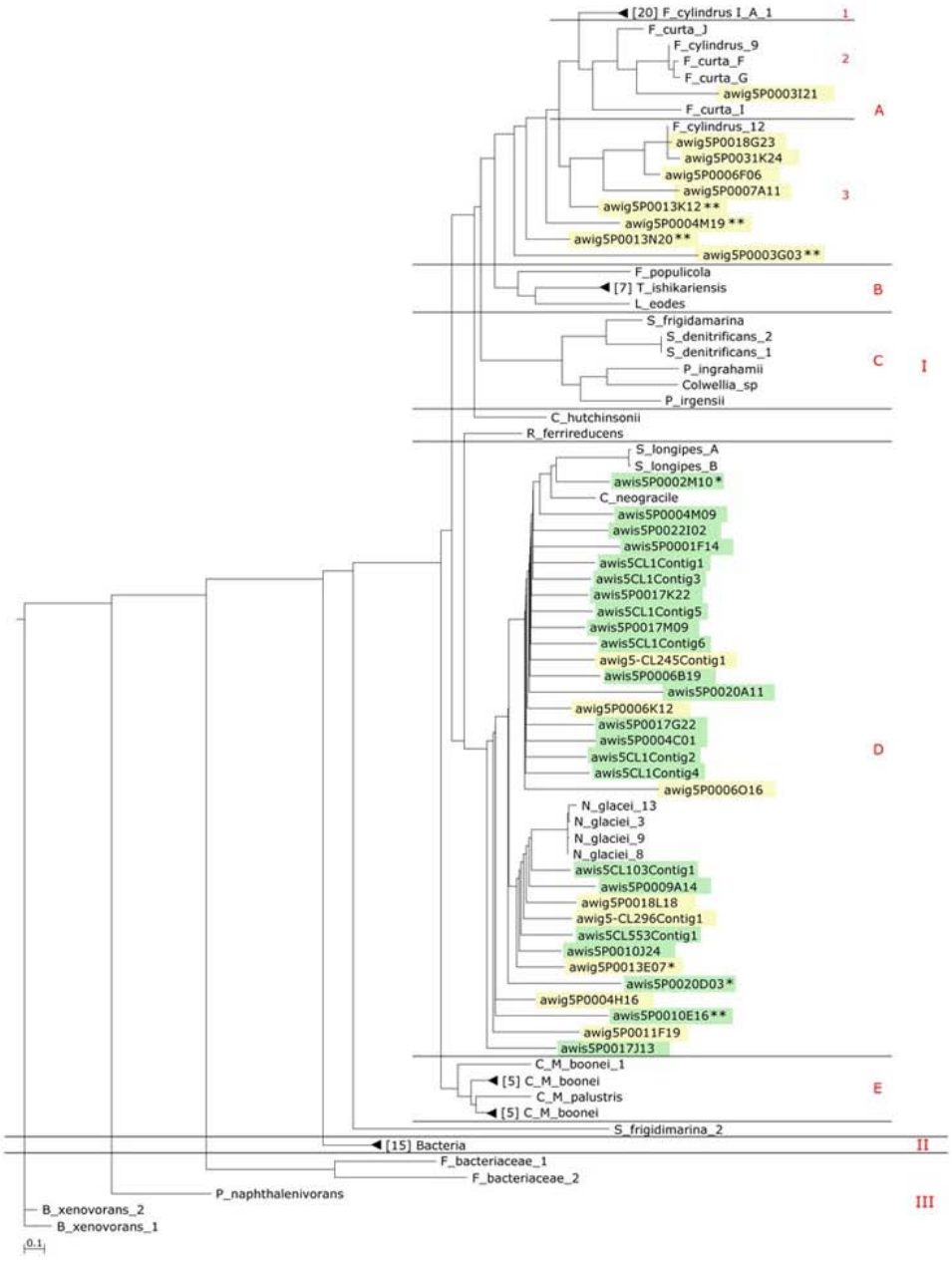

Figure 4.5: Phylogenetic placement of AFP sequences from samples G5 and S5. Sequences are coloured according to the sample (yellow G5 and green S5). Low placement robustness (ML ratios 1^{st} hit/2^{nd} hit <5) is indicated by stars. Hits placed in the same group are marked with one star (*), whereas hits with the 2^{nd} hit in another group are marked with two stars (**). Note that contigs contain several unassembled reads (see Supplementary Table 4.6). Groups not containing hits are collapsed and the number of sequences therein shown in brackets. The reference tree was calculated with PhyML. Branch lengths show substitutions per site (see scale bar).

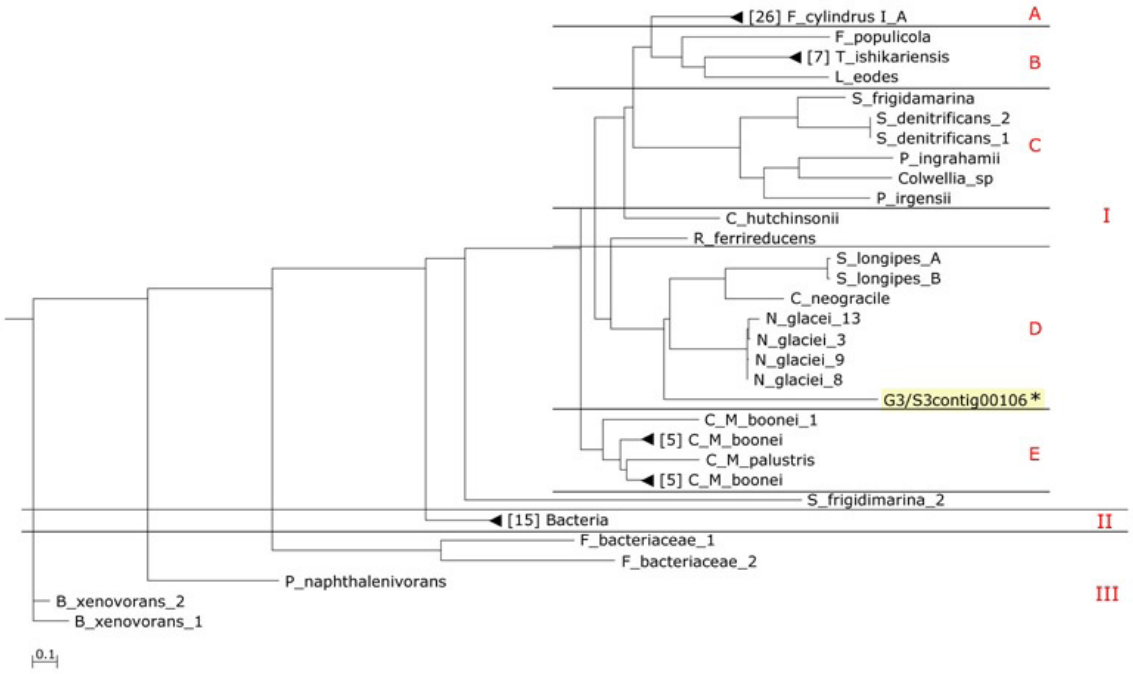

Figure 4.6: Phylogenetic placement of AFP sequences from sample G3/S3. Sequences are marked in yellow. Low placement robustness (ML ratios 1^{st} hit/2^{nd} hit <5) is indicated by stars. Hits placed in the same group are marked with one star (*), whereas hits with the 2^{nd} hit in another group are marked with two stars (**). Note that contigs contain several unassembled reads (see Supplementary Table 4.6). Groups not containing hits are collapsed and the number of sequences therein shown in brackets. The reference tree was calculated with PhyML. Branch lengths show substitutions per site (see scale bar).

Table 4.4: List of the sequences named differently than in previous publications

This study	Bayer-Giraldi et al. (2010)	NCBI	Accession no.
Fcylindrus_13	CCMP-15	IBP 2	GU001149
Fcylindrus_14	CCMP-43	IBP 3	GU001150
Fcylindrus_15	CCMP-35	IBP 4	GU001151
Fcyldinrus_16	CCMP-27	IBP 5	GU001152

Table 4.5: Total number of AFP reads in the respective AFP group resulting from best BLAST (compare to reference tree), additionally the total number of unassembled reads for each dataset and the average read length in base pairs (bp) are given.

AFP-Group	Clade	cDNA library					454[a]
		KF1	A4	J4	G5	S5	G3/S3
Total		6	16	10	19	106	22
F_cylindrus 1	I_A_1	2			6		
F_cylindrus 2	I_A_2						
F_cylindrus 3	I_A_3						
Fungi	I_B				1		
Bacteria	I_C						
C_hutchinsonii		2		1		1	
Sea ice diatom and crustacean	I_D	2	16	9	11	105	22
Archea	I_E				1		
Bacteria + Fungi	II						
Other	III						
No. of unassembled reads		5228	5002	6245	5773	5812	157553
Average read length (bp)		645	665	699	815	790	176

[a]454: 454 sequencing of cDNA

Table 4.6: Contig names shown in Figures 4.2, 4.4, 4.5, 4.6 and respective number of members of unassembled reads.

Contig name	No. of members
awiKF1_2009-12-02-CL297_c1	2
awiA4_2009-12-01-CL116_c1	2
awiA4_2009-12-01-CL116_c2	3
awig5-CL245Contig1	2
awig5-CL296Contig1	2
awis5-CL103Contig1	2
awis5-CL1Contig1	11
awis5-CL1Contig2	21
awis5-CL1Contig3	26
awis5-CL1Contig4	2
awis5-CL1Contig5	7
awis5-CL1Contig6	20
awis5-CL553Contig1	2
G3/S3contig00106	22

5 General discussion

Sea ice constitutes one of the largest biomes on earth (Thomas and Dieckmann 2002), a habitat that is permanently at subzero temperatures. Organisms throughout several kingdoms of life have developed antifreeze proteins (AFPs) as an important adaptation mechanism to live successfully in sea ice (DeVries and Wohlschlag 1969; Raymond et al. 1994; Raymond et al. 2007; Kiko 2010). In this thesis I have shown the widespread distribution of AFPs throughout the order of *Bacillariophyta*, by investigating AFP activity from mainly Arctic diatom species (**chapter 2**), which were underrepresented in previous studies. Further, detailed functional analyses of two recombinant AFPs from *Fragilariopsis nana* (refer to footnote 1 on page 11) in combination with estimates on the intracellular AFP concentration enabled me to propose possible functions of AFPs in diatoms (**chapter 2 and 3**). The described presence and high abundance of active AFP genes in environmental samples proves their importance for eukaryotic sea ice communities (**chapter 4**). In the following, the main findings are summarised and discussed with focus on the distribution and phylogeny of AFPs in diatoms and the potential functions of diatom AFPs. Finally, future research themes are proposed covering the areas of diatom AFP evolution, *in situ* function and potential applications.

5.1 Distribution and phylogeny of diatom AFPs

5.1.1 Distribution of AFP activity and genes in diatoms

To further the knowledge on the distribution of AFPs in polar diatoms, Arctic and Antarctic diatom species were tested for the presence of AFPs by assessing the recrystallisation inhibition (RI) activity of cell lysates (**chapter 2**). The study revealed RI activity in three *Navicula sp.* cultures as well as in cultures of *Fragilariopsis nana*, *Entomoneis sp.*, *Nitzschia sp.* and *Thalassiosira nordenskioeldii* from the Arctic and cultures of *F. nana*,

Table 5.1: Number of species investigated for AFP activity in this and previous studies (Raymond et al. 1994; Raymond 2000; Janech et al. 2006) in the respective diatom families. All polar species showed activity, whereas all temperate species did not show activity. Families where sequence information on AFPs is available are shown in bold.

Order (No. of species polar/temperate)	Family	No. of polar species (Arctic/Antarctic)	No. of temperate species (marine/freshwater)
Achnanthales (0/1)	Achnanthaceae		1 (1/0)
Bacillariales (7/1)	**Bacillariaceae**	**7 (2/5)**	1 (0/1)
Chaetocerotales (2/0)	**Chaetocerotaceae**	**1 (0/1)**	
	Attheyaceae	1 (1/0)	
Coscinodiscales (1/0)	Coscinodiscaceae	1 (0/1)	
Hemiauales (1/0)	Hemiaulaceae	1 (0/1)	
Fragilariales (1/0)	Fragilariaceae	1 (1/0)	
Navicuales (8/1)	Amphipleuraceae	2 (0/2)	
	Berkeleyaceae	1 (0/1)	
	Peurosigmataceae	1 (0/1)	
	Naviculaceae	**4 (1/3)**	
	Phaeodactylaceae		**1 (1/0)**
Rhizosoleniales (1/0)	Rhizosoleniaceae	1 (0/1)	
Suriellales (1/0)	Entomoneidaceae	1 (1/0)	
Thalassiosirales (3/3)	**Thalassiosiraceae**	3 (1/2)	**2 (2/0)**
	Stephanodiscaceae		1 (0/1)
Thalassiophysales (1/0)	Catenulaceae	1 (1/0)	

Eucampia antarctica, *Porosira glacialis* and *Proboscia inermis* from the Antarctic. Regardless if they were isolated from the ice or water column, all polar species showed RI activity under experimental conditions, and were thus able to produce AFPs or other components that produce similar effects (Walters et al. 2009). By merging data from this and previous reports (Raymond et al. 1994; Raymond 2000; Janech et al. 2006), it can be shown that AFP activity is present in a wide range of polar diatom species isolated from the sea ice or from the water column from both Polar Regions (Table 5.1, see also Tables A.1 and A.2 in Appendix A).

Reports on the presence of AFPs in sea ice assemblages, are summarised in Table 5.2. The presence of AFPs was assessed either by functional measurements of AFP activity, i.e. ice pitting studies (Raymond et al. 1994; Raymond 2000), or the sequencing approach presented in **chapter 4**. By using independent techniques, AFPs were shown to be present in Arctic and Antarctic sea ice from various regions and under different environmental conditions, e.g. ice type and age. Like in the sequencing study (**chapter 4**), most of the investigations by Raymond were done on 1^{st} year ice, or ice of younger age (Raymond et al. 1994; Raymond 2000). One sample was explicitly defined as 2^{nd} year ice, which showed lower activity than the samples from younger ice (Raymond 2000). It was hypothesised that the production of AFPs is stimulated by ice formation and for that reason lower in the slower growing 2^{nd} year ice than in the faster growing 1^{st} year ice (Raymond 2000).

Most of the species tested (Raymond et al. 1994; Raymond 2000; Janech et al. 2006, **chapter 3**) belong to the orders Bacillariales, Navicuales and Thalassiosirales (23 out of 32 species) and include both, polar and temperate, species (see Table 5.1). None of the temperate species tested showed AFP activity (**chapter 2**, Table A.3 in Appendix A, and Raymond et al. 1994), indicating that the presence of AFPs is unique to diatom species experiencing freezing conditions (Raymond et al. 1994; Janech et al. 2006). Reports on AFP activity or genes in mixed diatom assemblages *in situ* are so far restricted to the Polar Regions (Table 5.2). Corresponding results were reported from a study on AFP activity in cyanobacteria and mosses from the Antarctic as well as temperate regions, in which also only samples from cold habitats showed antifreeze activity (Raymond and Fritsen 2000). In addition, the lack of AFP sequences in the genomes of the temperate species *Thalassiosira pseudonana* and *Phaeodactylum tricornutum* (Janech et al. 2006; Armbrust et al. 2004; Bowler et al. 2008) implicates that AFPs are in fact an adaptation exclusively to the diatoms in polar areas or cold regions.

Table 5.2: Reports on presence of AFP activity or genes in mixed diatom assemblages from sea ice in this (chapter 4) and previous studies (Raymond et al. 1994; Raymond 2000). For further information on the samples of the sequencing study refer to chapter 4.

Sampling site	Sampled ice type	Further comments	Reference
Antarctic - ice pitting activity			
McMurdo Sound (1994, 1995, 1998)	platelet ice (1994), congelation ice (1995, 1998)	October to December, mostly 1^{st} year ice, 2^{nd} year ice had low activity	Raymond et al. 1994, Raymond 2000
Ross and Bellinghausen Seas (1995)	n.d.	May/August, less than two month old, strong activity	Raymond 2000
Ross sea	darkly coloured chunk from the underside of an ice floe	November, mostly *Berkeleya*, very strong activity	Raymond 2000
Weddell Sea	coloured chunks floating in pancake ice	April/May, strong activity	Raymond 2000
Antarctic - sequencing study			
Weddell Sea, station G	n.d.	September, 1^{st} year ice	this study
Weddell Sea, station S	columnar	Oktober, 1^{st} year ice	this study
D´Urville Sea, station A	granular/columnar	September, 1^{st} year pack ice	this study
D´Urville Sea, station J	columnar	October, 1^{st} year pack ice	this study
Arctic - ice pitting activity			
Resolute, Canada	underside of sea ice	June, mostly pennate diatoms, good activity	Raymond 2000
Arctic - sequencing study			
Kongsfjord	congelation ice	May, just before melt, 1^{st} year ice	this study

5.1.2 Phylogeny of AFP genes from diatom isolates and environmental samples

Information on AFP genes is only available for four Antarctic diatom isolates (*Fragilariopsis nana*, *Fragilairopsis curta*, *N. glacei*, *C. neogracile*) (Krell et al. 2008; Bayer-Giraldi et al. 2010; Janech et al. 2006; Gwak et al. 2010). As analysed by Bayer-Giraldi et al. (2010) and in **chapter 3**, *Fragilariopsis* species contain a multitude of AFP isoforms that group into one phylogenetic clade. A second clade contains the *N. glacei* and *C. neogracile* sequences. The former clade is more closely related to fungal AFP sequences, the latter to Archeal ones, than both are to each other (Bayer-Giraldi et al. 2010). This tree topology indicates that AFPs might be transferred in between species via horizontal gene transfer (HGT) (Bayer-Giraldi et al. 2010; Kiko 2010). HGT was also proposed for an AFP sequence found in the Antarctic copepod *Stephos longipes*, this gene is similar to the AFPs from *N. glacei* and *C. neogracile* (Kiko 2010).

In **chapter 4** the phylogenetic analysis of AFP genes retrieved from environmental cDNA libraries of five sea ice diatom assemblages is described. AFPs were found to be expressed *in situ*, in samples from both Polar Regions (Table 5.2), however, the phylogenetic relationship of the AFP genes from the Antarctic sample differs from that of the Arctic samples. Mainly AFP sequences similar to the *Navicula/Chaetoceros* clade were present in the samples from the Antarctic. In contrast, the Arctic dataset contained only AFP sequences from the *Fragilariopsis* clade. Surprisingly, no divergence in the phylogenetic affiliation of AFP sequences was observed for samples in which different taxonomic groups of microalgae were dominant. The *Navicula/Chaetoceros* clade of AFP sequences was dominant in several samples, although one of those was dominated by dinoflagellates, whereas the others were dominated by diatoms (J. Kegel, personal communication). One sample showed a striking dominance in terms of the abundance of AFP sequence as the abundance was one order of magnitude higher than in the other samples. This sample was dominated by diatoms belonging to *Fragilariopsis* species (J. Kegel, personal communication, Haase 2007). All AFP sequences found in this sample were placed in the

Navicula/Chaetoceros clade. These data indicate that AFP sequences, which are closely related to the *Navicula/Chaetoceros* clade, might also be present in *Fragilariopsis* species, in addition to the already known *Fragilariopsis* sequence (Bayer-Giraldi et al. 2010, **chapter 3**). Alternatively, *Navicula* and *Chaetoceros* species might have been the only species expressing AFPs in the respective samples.

The dominance of the *Navicula/Chaetoceros* clade in nearly all samples indicates that this clade is of special importance for the eukaryotic sea ice assemblages under the given *in situ* conditions. Studies using quantitative reverse-transcription PCR on *Fragilairopsis* cultures revealed differential expression of several AFP isoforms from the *Fragilairopsis* clade under salt and salinity stress (Bayer-Giraldi et al. 2010). The experimental conditions in that study resembled the freezing of the diatoms into the ice column and the subsequent sea ice development. Bayer-Giraldi et al. (2010) proposed that the successive activation of several isoforms represents early responses as well as later acclimation to stress. As the eukaryotic communities investigated in **chapter 4** had been incorporated in the sea ice for the entire winter, genes from the *Navicula/Chaetoceros* clade might be activated for long-term protection.

This first study on environmental AFP sequences indicates that there are variations in the AFP genes active in different communities. Whether these variations were caused by dissimilar species composition or other factors (e.g. ice type, age of ice, temperature) could not be completely resolved, as information on species composition and environmental conditions was not available for all samples. In future studies, care should be taken to gain comprehensive information on environmental conditions and species composition to answer these unresolved questions. In addition, functional measurements should be combined with molecular tools, to deduce the connection between *in situ* AFP activity, gene expression and phylogeny.

In summary, the presence of AFPs, either measured as activity or determined as AFP genes, is spread throughout the diatom phylogeny, yet is restricted to polar diatom species. AFPs are found in species isolates as

well as in natural assemblages in the Arctic and in the Antarctic, in several regions, and in ice of different type and age. AFP genes of different phylogenetic affiliation are active in different assemblages in situ and the amount of active AFP genes varies between assemblages. Parameters causing the observed variations could not be determined in the present study.

5.2 Functional characterisation of AFPs from sea ice diatoms and their ecological significance

5.2.1 Functional characterisation of recombinant AFP isoforms

Detailed functional characterisation of AFPs provides the basis to deduce the *in situ* function of AFPs. In **chapter 3** the recombinant expression and functional characterisation of two *F. nana* AFP isoforms is presented. The two isoforms studied are phylogenetically separated within the *Fragilariopsis* clade and showed distinct characteristics. The recombinant protein of isoform *F. nana* AFP-10 showed maximal thermal hysteresis (freezing point depression) of 1.5 °C at 24.2 μM protein, whereas maximal thermal hysteresis of recombinant protein of isoform *F. nana* AFP-12 was higher with 2.3 °C at 19.0 μM protein. These values are 2 to 3 times higher than reported for mature *C. neogracile* AFP (0.8 °C, 38.2 μM) (Gwak et al. 2010). Another recombinant *F. nana* AFP also showed maximal thermal hysteresis of 2.5 °C, but at an approximately ten times higher concentration of 345 μM (Bayer-Giraldi et al. 2011). Thermal hysteresis activity of the recombinant *F. nana* AFPs studied in **chapter 3** is higher than that reported for moderate fish AFPs, with about 0.5 to 1 °C at millimolar concentrations (Davies and Hew 1990), and is close to the values reported for hyperactive AFPs with the same activity at micromolar concentrations (Scotter et al. 2006). For both *F. nana* isoforms thermal hysteresis activity increased with increasing AFP concentration as well as with increasing buffer salinity (**chapter 3**). In the natural environment of sea ice diatoms it is highly efficient to couple the antifreeze function to salinity since lower temperatures in the brine pockets are accompanied by higher salinities (Cox and Weeks 1983).

Furthermore, different molecular functions of the two recombinant AFPs were shown by studying ice crystal deformation patterns. Ice crystals growing in solutions of recombinant *F. nana* AFP-10 or *F. nana* AFP-12 formed hexagonal bi-pyramids or hexagonal columns, respectively. The first pattern indicates AFP binding to the non-basal planes (see Fig. 1.6 j on page 8), which is typical for moderate AFPs (Scotter et al. 2006). The second indicates binding to the basal and non-basal planes, known for hyperactive insect AFPs (Graether et al. 2000). At high protein concentration or high buffer salinity, crystal burst of radial symmetry in directions of the *a*-axes were observed. A radial burst pattern and a burst pattern parallel to the *a*-axis was described for recombinant AFPs from *Tyhula ishikariensis* and another *F. nana* AFP, respectively (Xiao et al. 2010; Bayer-Giraldi et al. 2011). Both sequences are closely related to the AFP sequences studied in **chapter 3**. Radial burst patterns parallel to the *a*-axis are typical for hyperactive AFPs (Scotter et al. 2006). In conclusion, the binding and burst patterns as well as thermal hysteresis potentials observed for the recombinant *F. nana* AFPs in **chapter 3** classify both isoforms into the group of hyperactive AFPs.

5.2.2 Subcellular localisation and function

As observed in the characterisation of recombinant AFPs, the *in situ* function of AFPs will strongly depend on the protein concentration (**chapter 3**, Bayer-Giraldi et al. 2011). Intracellular AFPs most likely occur in higher concentrations than extracellular AFPs, thus the localisation will influence AFP function. The presence of intracellular AFPs in diatoms was demonstrated in **chapter 2**, where AFP activity, i.e. recrystallisation inhibition, was found in cleared cell lysates of several polar diatom species. For *F. nana* intracellular concentrations of 0.3 to 68.5 μM AFP equivalent were calculated (AFP equivalent refers to the calibration of the measurements using a recombinant AFP). Lowest AFP concentration of a recombinant *F. nana* AFP required for RI was reported with 0.012 μM AFP in saline solution (Bayer-Giraldi et al. 2011). Thermal hysteresis was observed for protein concentrations of 1.2 μM AFP and higher (Bayer-Giraldi et al. 2011, **chapter 3**). The intracellular concentrations calculated for diatoms thus confirm that diatom AFPs will

act as recrystallisation inhibitor, but the estimates also lie in the range of concentrations required for thermal hysteresis (**chapter 3**). Intracellular inhibition of recrystallisation was proposed as a cryoprotective function by reducing mechanical disruption of cells or organelles in freeze-thaw cycles caused by growing ice crystals (Raymond 2000). Isoform *F. nana* AFP-12 is potentially an intracellular antifreeze, as it does not carry a signal peptide that indicates secretion. Sequence analysis, however, revealed that it has a 131 amino acid sequence of unknown function preceding the antifreeze domain (**chapter 3**). The respective sequence shows no similarity to known proteins and might be involved in AFP function, in subcellular localisation, or other not yet recognised functions of the AFP. Alternative to the intracellular localisation, *F. nana* AFP-12 could also be associated with the cell membrane. Membrane associated antifreeze components (AFPs or antifreeze glycolipids) are present in plants and insects and were suggested to inhibit spreading of extracellular ice into the cytosol or to stabilise cell membranes at low temperature (Urrutia et al. 1992; Duman 2001; Walters et al. 2009). Except for the gene sequence for isoform *F. nana* AFP-12, which groups into a phylogenetically distinct clade (see Supplementary Fig. 3.7 in **chapter 3**), all *F. nana* AFP isoforms group into two clades, of which most of the sequences carry signal peptides, indicating the extracellular secretion of the AFPs (Janech2006, Krell2008, **chapter 3**). The different signals for subcelluar localisation indicate that the different AFP isoforms fulfil different functions. From the winter flounder *Pleuronectes americanus* it is known that multiple isoforms of AFPs are located in distinct organs (blood, skin) and carry different functions (plasma antifreeze, intracellular antifreeze) (Gong et al. 1996). The other isoform studied in **chapter 3**, *F. nana* AFP-10, carries a signal peptide and is thus probably secreted to the extracellular space (Krell et al. 2008). AFPs, that are secreted into the brine, surrounding the diatom cells, were proposed to modify the surface and optical properties of ice thus enhancing algal attachment or light scatter (Raymond et al. 1994). In addition, it was hypothesised that AFPs maintain the fine brine channels providing habitable space for ice diatoms (Raymond 2000). Modification of ice texture and brine channel morphology was observed for a recombinant *F. nana* AFP as well as a glycoprotein fraction of *Melosira arctica* exopolymeric substance

(EPS), resulting in more porous ice structure and a angular and convoluted structure of the brine channels, respectively (Bayer-Giraldi et al. 2011; Krembs et al. 2011). These structures create a favourable environment for the ice alga since more liquid is retained and not drained during sea ice formation and aging (Bayer-Giraldi et al. 2011; Krembs et al. 2011). In addition, EPS were proposed to protect diatoms from being damaged by ice crystals (Krembs et al. 2002). It is probable, that the glycoprotein fraction described by Krembs et al. (2011) is a proteinaceous antifreeze component (Raymond 2011), which would have caused AFP activity as assessed in the measurements in **chapter 2**. AFPs might accumulate in the EPS layer found around diatom cells in sea ice (Krembs et al. 2002), acting more effectively in this microenvironment, than when dissolved in brine. Microbial EPS for example provide a hydrated microenvironment maintaining extracellular enzymes in close vicinity to the cells (Decho and Herndl 1995). In a similar manner, secreted AFPs might be concentrated in EPS around diatom cells, accumulating to the concentrations required for RI or even thermal hysteresis. AFP activity in some sea ice diatoms was shown to be rather robust against elevated temperature (20 °C) and proteolytic treatment (**chapter 2**), implicating that AFPs are stable enough for adequate accumulation in a given time. The combination of EPS and embedded AFPs might protect the cells very effectively from potential damage by ice crystals.

In summary, the two F. nana AFP isoforms studied in chapter 3 show crystal deformation patterns and a thermal hysteresis potential that affiliates these sequences to the group of hyperactive AFPs. Different AFP isoforms carry different signals of subcellular localisations, i.e. are found intracellular, maybe associated to membranes, or are excreted. Intracellular AFP concentrations demonstrate that AFPs will act as recrystallisation inhibitor and likely also as thermal hysteresis protein. Extracellular AFPs might accumulate in EPS providing protection against ice crystal damage.

5.2.3 Further considerations on the ecological significance of diatom AFPs

The capability of sea ice diatoms to survive and grow within sea ice provides the advantage that cells are positioned in a stable matrix that guarantees maximal light availability (Eicken 1992). In ice covered regions of Polar Oceans, light availability decreases with depth in the ice and is even lower in the underlying water column (Eicken 1992). Light fuels photosynthesis, which provides the first energy source for photoautotrophic organisms, allowing for growth and reproduction. AFP protected diatom species (**chapters 2 and 4**) can populate sea ice as favourable ecological niche compared to the underlying water column with respect to the light availability. AFPs furthermore modify the brine pore morphology to smaller, more convoluted pores compared to AFP free ice (Krembs et al. 2011; Bayer-Giraldi et al. 2011). This will lead to a reduced accessibility for grazers in sea ice and protect the microalgae from being grazed, while situated in the fine ice pores. Grazers, however, have access to sea ice diatoms as important food source (Lizotte 2001) at the ice water interface, where the ice structure is characterised by lager channels and pores (Weissenberger et al. 1992). While feeding on diatoms they will also ingest the AFPs and might profit from the AFP function. Similar to the uptake of polyunsaturated fatty acids by organisms that cannot produce polyunsaturated fatty acids themselves (Thomas and Dieckmann 2002), AFP could serve as secondary antifreeze for these organisms after ingestion. Krill feeds on ice algae and eventually scrapes of the algae directly from the ice surface (Stretch et al. 1988; Hamner and Hamner 2000). In this process the krill might also ingest small ice crystals that would damage the tissues when growing inside the gut. One could envisage that the ingested diatom AFP, if not digested in the gut, would maintain its activity inside the grazer. Our measurements from **chapter 2** indicate some resistance of the diatom antifreeze components against proteolytic treatment, thus AFPs might retain activity at least for a while after ingestion. In the gut of Antarctic fishes, antifreeze glycoproteins are present in high concentrations (O'Grady et al. 1982), preventing the growth of ice crystals that are ingested with the diet (O'Grady et al. 1983). To my

knowledge, no reports on thermal hysteresis or AFPs from krill are presently available. Another crustacean, the copepod *Stephos longipes*, exhibits thermal hysteresis of the haemolymph, which was attributed to AFP expression detected via *in situ* hybridisation (Kiko 2010). The ingested diatom AFPs might thus, in case of the krill, be the only proteinaceaous antifreeze in the gut, whereas in *Stephos longipes* it might complement the existing AFPs. Reabsorption of the antifreeze gylcoproteins from the gut into the blood of the fishes was not observed (O'Grady et al. 1983).

Next to the effects on crystal growth and ice restructuring, diatom AFPs might also influence the melting process of sea ice. AFPs from insects, bacteria and fishes were shown not only to lower the freezing point of a solution, but also to increase the melting point (Celik et al. 2010). A hyperactive AFP from an Antarctic lake bacterium increased the melting point of ice by up to 0.44 °C (Celik et al. 2010). The recombinant diatom AFPs studied in **chapter 3** were classified as hyperactive AFPs as they showed similar molecular characteristics, i.e. crystal deformation, burst patterns and thermal hysteresis, and thus might also increase the melting point of ice. During the melting of sea ice, diatoms encounter hyposmotic conditions as meltwater dilutes the brine in the pores inhabited by the diatoms. Hyposmotic conditions can be harmful for sea ice diatoms slowing cell growth and even leading to cell death (e.g. Vargo et al. 1986; Ryan et al. 2004; Garrison and Buck 1986). A delayed and thus maybe slower melting process of the ice enclosing the brine pockets might lead to a slower salinity shift and thus higher survival of the diatoms during sea ice melt.

Sea ice diatoms invest high amounts of energy in the production of AFPs. Intracellular AFP concentrations in cells are at high levels of 0.1 - 5% of the total protein concentration (**chapter 2**), which is comparable to or even higher than the amount of photosynthetic protein PsbD (e.g. 0.08-0.42% of total protein for *Coscinodiscus radiatus* and *Thalassiosira pseudonana*, respectively, at 30 μmol photons cm^{-2} s^{-1} (Wu et al. 2011)). Taking into account the fraction of AFP that is excreted the values are even higher. Measurements of primary productivity rates indicate that dissolved organic carbon, which also includes the fraction of secreted AFPs, accounts for 1-10% of the carbon

uptake for *F. nana* (M. Fernï¿½ndez-Mï¿½ndez, personal communication). Regarding the broad distribution of AFPs in polar diatom species and assemblages, the multitude of highly and differentially expressed AFP genes, and the cell biological expenses diatoms invest in AFPs, these proteins seem to be an important factor for diatom success the sea ice habitat.

In summary, the ability to produce AFPs provides the advantage for diatoms to survive in sea ice under more favourable light conditions compared to the water column. The smaller brine channel morphology caused by diatom AFP might result in an exclusion of grazers, and thus protect the diatoms. Higher trophic levels will ingest AFPs while grazing on diatoms and might profit from the antifreeze functions. In addition to crystal formation and restructuring, AFPs might influence the melting of sea ice, slowing down the salinity breakdown inside brine pockets during melting. The high amounts of energy sea ice diatoms invest for the production of AFPs indicate that AFPs are an important factor required for survival in the sea ice habitat.

5.3 Future research and perspectives

Results from this thesis contribute significantly to the knowledge on AFPs from polar diatoms. A broad view of the large scale distribution of AFP activity in diatom isolates and communities down to the function of the single AFP molecule is shown. Research on diatom AFPs is relatively young (Raymond et al. 1994) compared to the research on fish AFPs (DeVries et al. 1970), thus plenty of questions arising from this study have yet to be answered.

The presence of AFP activity in several new diatom species (**chapter 2**) confirms the widespread distribution of AFPs in polar diatoms. AFP phylogeny, however, deviates from diatom taxonomy in the current analysis. Related temperate species and species providing evolutionary junctions should be screened for AFP activity and the presence of AFP genes. As information on diatom AFP genes up to date is only available from Antarctic species, complementary studies, e.g. on Arctic strains of *F. nana* might give valuable information to deduce the evolution of AFPs in diatoms. **Chapter 4** shows that analysis of AFP genes from environmental datasets can provide information on AFP presence, phylogeny and activity. There is a wealth of metagenome and metatranscriptome data already available and the amount of data is expected to increase in the near future. Comparing data from different habitats and organisms (e.g. viral, prokaryotic and eukaryotic) could provide information on the distribution of AFPs as well as their acquisition and evolutionary processes, e.g. horizontal gene transfer. For evolutionary questions further insight could be gained by studying eukaryotic non-diatom algae that are also found associated with the sea ice habitat, such as dinoflagellates or *Phaeocystis* species.

AFP function has been studied in laboratory experiments to obtain information on the molecular function of AFPs from diatoms (chapters 2 and 3). In future studies one focus could be on the question of the *in situ* function of AFPs in the cell or in brine channels. This includes studies on the localisation of different AFP isoforms relative to the cell compartments (i.e. in cytoplasm, in organelles, in membrane or excreted) e.g. by immunolocalisation. For extracellular AFPs the interplay of AFPs with EPS

should be studied. Complementary, differential expression and subsequent activation of AFP isoforms should be investigated to resolve potential short-term acclimation from long-term protection. Quantification of intracellular and excreted AFP concentrations is crucial, since protein function correlates with protein concentration (**chapter 3**). The heterologous expression of single AFP isoforms (**chapter 3** and Bayer-Giraldi et al. 2011) provides the opportunity to study the proteins on the molecular level. Single isoform AFPs can be used to resolve the protein structure via X-ray or nuclear magnetic resonance to gain information on the molecular protein-ice interaction as shown for fish and insect AFPs (e.g. Sönnichsen et al. 1996; Graether et al. 2000). Structural and functional units of proteins, e.g. transmembrane domains and ice binding sites, can be determined.

Finally, there are many scopes for the application of AFPs, for example in medicine and food sciences. In cryopreservation the specific characteristics of AFPs, e.g. potential of thermal hysteresis and recrystallisation inhibition as well as crystal burst pattern, make one AFP suitable for an application whereas others can be unsuitable (see review by Brockbank et al. 2011). If diatom AFPs have suitable characteristics remains to be tested. Diatom AFPs might especially be of interest for food sciences, since the application of genetic modified material in food products is controversial. Due to optional large-scale cultivation of microalgae, harvesting AFPs from microalgae might be more feasible than from fish and circumvents the need of genetic engineered production of AFPs.

I do not care ´bout cold or sneeze,
as long as I have antifreeze.

Klaus Valentin

6 References

Argos, P. (1990). "An investigation of oligopeptides linking domains in protein tertiary structures and possible candidates for general gene fusion". *Journal of Molecular Biology* 211.4, pp. 943 –958. DOI: 10.1016/0022-2836(90)90085-Z.

Armbrust, E. V., J. A. Berges, C. Bowler, B. R. Green, D. Martinez, et al. (2004). "The genome of the diatom *Thalassiosira pseudonana*: ecology, evolution, and metabolism". *Science* 306.5693, pp. 79–86. DOI: 10.1126/science.1101156.

Arrigo, K. R. and D. N. Thomas (2004). "Large scale importance of sea ice biology in the Southern Ocean". *Antarctic Science* 16.04, pp. 471–486. DOI: 10.1017/S0954102004002263.

Assur, A. (1958). "Composition of sea ice and its tensile strength". *National Research Council Publications* 598, 106–138.

Barrett, J. (2001). "Thermal hysteresis proteins". *The International Journal of Biochemistry & Cell Biology* 33.2, pp. 105–117.

Bartsch, A. (1989). "Die Eisalgenflora des Weddellmeeres (Antarktis): Artenzusammensetzung und Biomasse sowie Ökophysiologie ausgewählter Arten". Vol. 63. Berichte zur Polar- und Meeresforschung. Alfred-Wegener-Institut für Polar- und Meeresforschung, Bremerhaven.

Bayer-Giraldi, M., C. Uhlig, U. John, T. Mock, and K. Valentin (2010). "Antifreeze proteins in polar sea ice diatoms: diversity and gene expression in the genus *Fragilariopsis*". *Environmental Microbiology* 12.4, pp. 1041–1052. DOI: 10.1111/j.1462-2920.2009.02149.x.

Bayer-Giraldi, M., I. Weikusat, H. Besir, and G. Dieckmann (2011). "Characterization of an antifreeze protein from the polar diatom *Fragilariopsis cylindrus* and its relevance in sea ice". *Cryobiology*, pp. –. DOI: 10.1016/j.cryobiol.2011.08.006.

Bluhm, B. A., R. R. Gradinger, and S. B. Schnack-Schiel (2010). "Sea ice". Ed. by D. N. Thomas and G. S. Dieckmann. Wiley-Blackwell. Chap. Sea ice Meio- and Macrofauna, pp. 357–394.

Bowler, C., A. E. Allen, J. H. Badger, J. Grimwood, K. Jabbari, et al. (2008). "The *Phaeodactylum* genome reveals the evolutionary history of diatom genomes". *Nature* 456.7219, pp. 239–244.

Bravo, L. A. and M. Griffith (2005). "Characterization of antifreeze activity in Antarctic plants". *Journal of Experimental Botany* 56.414, pp. 1189–1196. DOI: 10.1093/jxb/eri112.

Brockbank, K. G. M., L. H. Campbell, E. D. Greene, M. C. G. Brockbank, and J. G. Duman (2011). "Lessons from nature for preservation of mammalian cells, tissues, and organs". *In vitro cellular & developmental biology-animal* 47.3, 210–217. DOI: 10.1007/s11626-010-9383-2.

Celik, Y., L. A. Graham, Y.-F. Mok, M. Bar, P. L. Davies, and I. Braslavsky (2010). "Superheating of ice crystals in antifreeze protein solutions". *Proceedings of the National Academy of Sciences* 107.12, pp. 5423–5428. DOI: 10.1073/pnas.0909456107.

Chao, H., P. L. Davies, B. D. Sykes, and F. D. Sönnichsen (1993). "Use of proline mutants to help solve the NMR solution structure of type III antifreeze protein". *Protein Science* 2.9, pp. 1411–1428.

Cheng, C.-H. C. (1998). "Evolution of the diverse antifreeze proteins". *Current Opinion in Genetics & Development* 8.6, pp. 715–720. DOI: 10.1016/S0959-437X(98)80042-7.

Comiso, J. C. and F. Nishio (2008). "Trends in the sea ice cover using enhanced and compatible AMSR-E, SSM/I, and SMMR data". *J. Geophys. Res.* 113.C2, C02S07–.

Cox, G. F. N. and W. F. Weeks (1983). "Equations for determining the gas and brine volumes in sea-ice samples". *Journal of Glaciology* 29.102, pp. 306–316.

Dalbey, R. E., M. O. Lively, S. Bron, and J. M. V. Dijl (1997). "The chemistry and enzymology of the type I signal peptidases". *Protein Science* 6.6, pp. 1129–1138.

Davies, P. and C. Hew (1990). "Biochemistry of fish antifreeze proteins". *FASEB Journal* 4.8, pp. 2460–2468.

Davies, P. L., J. Baardsnes, M. J. Kuiper, and V. K. Walker (2002). "Structure and function of antifreeze proteins". *Philosophical Transactions of the Royal Society of London. Series B: Biological Sciences* 357.1423, pp. 927–935. DOI: 10.1098/rstb.2002.1081.

DeLuca, C. I., R Comley, and P. L. Davies (1998). "Antifreeze proteins bind independently to ice". *Biophysical Journal* 74.3, 1502–1508.

DeVries, A. L. (1983). "Antifreeze Peptides and Glycopeptides in Cold-Water Fishes". *Annual Review of Physiology* 45.1, pp. 245–260. DOI: 10.1146/annurev.ph.45.030183.001333.

DeVries, A. L. and D. Wohlschlag (1969). "Freezing resistance in some Antarctic fishes". *Science* 163, pp. 1073–1075.

DeVries, A. L., S. K. Komatsu, and R. E. Feeney (1970). "Chemical and physical properties of freezing point-depressing glycoproteins from antarctic fishes". *Journal of Biological Chemistry* 245, pp. 2901–2908.

Decho, A. W. and G. J. Herndl (1995). "Microbial activities and the transformation of organic matter within mucilaginous material". *Science of The Total Environment* 165.1-3, pp. 33–42. DOI: 10.1016/0048-9697(95)04541-8.

Dieckmann, G., G. Rohardt, H. Hellmer, and J. Kipfstuhl (1986). "The occurrence of ice platelets at 250 m depth near the Filchner Ice Shelf and its significance for sea ice biology". *Deep Sea Research Part A. Oceanographic Research Papers* 33.2, pp. 141–148. DOI: 10.1016/0198-0149(86)90114-7.

Dieckmann, G. S., K. Arrigo, and C. W. Sullivan (1992). "A high-resolution sampler for nutrient and chlorophyll a profiles of the sea ice platelet layer and underlying water column below fast ice in polar oceans preliminary results." *Marine Ecology Progress Series* 80, pp. 291–300.

Doucet, C. J., L. Byass, L. Elias, D. Worrall, M. Smallwood, and D. J. Bowles (2000). "Distribution and characterization of recrystallization inhibitor activity in plant and lichen species from the UK and maritime Antarctic". *Cryobiology* 40.3, pp. 218–227. DOI: 10.1006/cryo.2000.2241.

Doucet, D., V. Walker, and W. Qin (2009). "The bugs that came in from the cold: Molecular adaptations to low temperatures in insects". *Cellular and Molecular Life Sciences* 66 (8), pp. 1404–1418. DOI: 10.1007/s00018-009-8320-6.

Duman, J. G. (2001). "Antifreeze and ice nucleation proteins in terrestrial arthropods". *Annual Review of Physiology* 63.1, pp. 327–357. DOI: 10.1146/annurev.physiol.63.1.327.

Duman, J. G. and A. L. DeVries (1976). "Isolation, characterization, and physical properties of protein antifreezes from the winter flounder, *Pseudopleuronectes americanus*". *Comparative Biochemistry and Physiology Part B: Comparative Biochemistry* 54.3, pp. 375–380. DOI: 10.1016/0305-0491(76)90260-1.

Duman, J. G. and T. M. Olsen (1993). "Thermal hysteresis protein activity in bacteria, fungi, and phylogenetically diverse plants". *Cryobiology* 30.3, pp. 322–328. DOI: 10.1006/cryo.1993.1031.

Duman, J. G., D. W. Wu, T. M. Olsen, M. Urrutia, and D. Tursman (1993). "Advances in low-temperature biology". JAi Press Ltd. Chap. Thermal hysteresis proteins, pp. 131–182.

Durbin, R., S. Eddy, A. Krogh, and G. Mitchison (1998). *Biological sequence analysis: probabilistic models of proteins and nucleic acids*. Cambridge University Press.

Edgcomb, V. P., D. T. Kysela, A. Teske, A. de Vera Gomez, and M. L. Sogin (2002). "Benthic eukaryotic diversity in the Guaymas Basin hydrothermal vent environment". *Proceedings of the National Academy of Sciences of the United States of America* 99.11, pp. 7658–7662. DOI: 10.1073/pnas.062186399.

Eicken, H. (1992). "The role of sea ice in structuring Antarctic ecosystems". *Polar Biology* V12.1, pp. 3–13.

Eicken, H. and M. A. Lange (1989). "Development and Properties of Sea Ice in the Coastal Regime of the Southeastern Weddell Sea". *J. Geophys. Res.* 94, pp. 8193–8206.

Elwood, H., G. Olsen, and M. Sogin (1985). "The small-subunit ribosomal RNA gene sequences from the hypotrichous ciliates *Oxytricha nova* and *Stylonychia pustulata*". *Molecular Biology and Evolution* 2.5, pp. 399–410.

Ewart, K. V., Q. Lin, and C. L. Hew (1999). "Structure, function and evolution of antifreeze proteins". *Cellular and Molecular Life Sciences* 55.2, pp. 271–283.

Feeney, R. E., T. S. Burcham, and Y Yeh (1986). "Antifreeze glycoproteins from polar fish blood". *Annual Review of Biophysics and Biophysical Chemistry* 15.1, pp. 59–78. DOI: 10.1146/annurev.bb.15.060186.000423.

Frias-Lopez, J., Y. Shi, G. W. Tyson, M. L. Coleman, S. C. Schuster, S. W. Chisholm, and E. F. DeLong (2008). "Microbial community gene expression in ocean surface waters". *Proceedings of the National Academy of Sciences of the United States of America* 105.10, 3805–3810. DOI: 10.1073/pnas.0708897105.

Garrison, D., A. Close, and E. Reimnitz (1989). "Algae concentrated by frazil ice: evidence from laboratory experiments and field measurements". *Antarctic Science* 1.4, pp. 313–316.

Garrison, D. L. and K. R. Buck (1986). "Organism losses during ice melting: A serious bias in sea ice community studies". *Polar Biology* 6.4, pp. 237–239.

Gauthier, S. Y., C. M. Kay, B. D. Sykes, V. K. Walker, and P. L. Davies (1998). "Disulfide bond mapping and structural characterization of spruce budworm antifreeze protein". *European Journal of Biochemistry* 258.2, pp. 445–453.

Gilbert, J. A., P. L. Davies, and J. Laybourn-Parry (2005). "A hyperactive, Ca^{2+}-dependent antifreeze protein in an Antarctic bacterium". *FEMS Microbiology Letters* 245.1, pp. 67–72.

Gleitz, M. and D. N. Thomas (1992). "Physiological responses of a small Antarctic diatom (*Chaetoceros sp.*) to simulated environmental constraints associated with sea-ice formation". *Marine Ecology Progress Series* 88, pp. 271–278.

Gong, Z., K. V. Ewart, Z. Hu, G. L. Fletcher, and C. L. Hew (1996). "Skin antifreeze protein genes of the winter flounder, *Pleuronectes americanus*, encode distinct and active polypeptides without the secretory signal and prosequences". *Journal of Biological Chemistry* 271.8, pp. 4106–4112. DOI: 10.1074/jbc.271.8.4106.

Graether, S. P., M. J. Kuiper, S. M. Gagne, V. K. Walker, Z. Jia, B. D. Sykes, and P. L. Davies (2000). "ß-Helix structure and ice-binding properties of a hyperactive antifreeze protein from an insect". *Nature* 406.6793, pp. 325–328.

Graham, L. A., Y.-C. Liou, V. K. Walker, and P. L. Davies (1997). "Hyperactive antifreeze protein from beetles". *Nature* 388.6644, pp. 727–728.

Graham, L. A., C. B. Marshall, F.-H. Lin, R. L. Campbell, and P. L. Davies (2008). "Hyperactive antifreeze protein from fish contains multiple ice-binding sites". *Biochemistry* 47.7, pp. 2051–2063. DOI: 10.1021/bi7020316.

Grant, S., W. D. Grant, D. A. Cowan, B. E. Jones, Y. Ma, A. Ventosa, and S. Heaphy (2006). "Identification of eukaryotic open reading frames in metagenomic cDNA libraries made from environmental samples". *Appl. Environ. Microbiol.* 72.1, pp. 135–143. DOI: 10.1128/AEM.72.1.135-143.2006.

Griffith, M. and M. W. Yaish (2004). "Antifreeze proteins in overwintering plants: a tale of two activities". *Trends in Plant Science* 9.8, pp. 399–405. DOI: 10.1016/j.tplants.2004.06.007.

Griffith, M., P. Ala, D. S. C. Yang, W.-C. Hon, and B. A. Moffatt (1992). "Antifreeze protein produced endogenously in winter rye leaves". *Plant Physiology* 100.2, 593–596.

Guillard, R. R. L. and J. H. Ryther (1962). "Studies of marine planktonic diatoms: I. *Cyclotella nana* Hustedt, and *Detonula confervacea* (Cleve) gran." *Canadian Journal of Microbiology* 8.2, 229–239. DOI: 10.1139/m62-029.

Guindon, S. and O. Gascuel (2003). "A simple, fast, and accurate algorithm to estimate large phylogenies by maximum likelihood". *Systematic Biology* 52.5, pp. 696–704. DOI: 10.1080/10635150390235520.

Gwak, I. G., W. sic Jung, H. J. K. Kim, S.-H. Kang, and E. Jin (2010). "Antifreeze protein in Antarctic marine diatom, *Chaetoceros neogracile*". *Mar. Biotechnol.* 12.6, pp. 630–639. DOI: 10.1007/s10126-009-9250-x.

Haas, C., A. Friedrich, Z. Li, M. Nicolaus, A. Pfaffling, and T. Toyota (2009). "Regional variability of sea ice properties and thickness in the northwestern Weddell Sea obtained by in-situ and satellite measurements." *The expedition of the research vessel "Po-*

larstern" to the Antarctic in 2006 (ANT-XXIII/7). Ed. by P. Lemke. Vol. 586. Berichte zur Polar- und Meeresforschung. Alfred-Wegener-Institut für Polar- und Meeresforschung, Bremerhaven, 36–74.

Haase, S. (2007). "Eukaryotic biodiversity of Arctic and Antarctic sea ice – a molecular approach". MA thesis. Technische Universität Braunschweig.

Hager, J. (2008). "Winterliche Meereislebensgemeinschaft im nordwestlichen Weddellmeer". MA thesis. Universität Bremen.

Hamner, W. M. and P. P. Hamner (2000). "Behavior of Antarctic krill (*Euphausia superba*): schooling, foraging, and antipredatory behavior". *Canadian Journal of Fisheries and Aquatic Sciences* 57.S3, pp. 192–202. DOI: 10.1139/f00-195.

Han, M. and C. Zmasek (2009). "phyloXML: XML for evolutionary biology and comparative genomics". *BMC Bioinformatics* 10.1, p. 356. DOI: 10.1186/1471-2105-10-356.

Hanekamp, K., U. Bohnebeck, B. Beszteri, and K. Valentin (2007). "PhyloGena - a user-friendly system for automated phylogenetic annotation of unknown sequences". *Bioinformatics* 23.7, pp. 793–801. DOI: 10.1093/bioinformatics/btm016.

Hasle, G. R. and B. R. Heimdal (1998). "The net phytoplankton in Kongsfjorden, Svalbard, July 1988, with general remarks on species composition of arctic phytoplankton". *Polar Research* 17.1, pp. 31–52. DOI: 10.1111/j.1751-8369.1998.tb00257.x.

Heidelberg, K. B., J. A. Gilbert, and I. Joint (2010). "Marine genomics: at the interface of marine microbial ecology and biodiscovery". *Microbial Biotechnology* 3.5, pp. 531–543. DOI: 10.1111/j.1751-7915.2010.00193.x.

Hitchcock, G. L. (1982). "A comparative study of the size-dependent organic composition of marine diatoms and dinoflagellates". *Journal of Plankton Research* 4.2, pp. 363–377. DOI: 10.1093/plankt/4.2.363.

Hop, H., T. Pearson, E. N. Hegseth, K. M. Kovacs, C. Wiencke, et al. (2002). "The marine ecosystem of Kongsfjorden, Svalbard". *Polar Research* 21.1, pp. 167–208.

Horner, R, S. F. Ackley, G. S. Dieckmann, B Gulliksen, T Hoshiai, et al. (1992). "Ecology of sea ice biota. 1. Habitat, terminology, and methodology." *Polar Biology* 12.3-4, pp. 417–427.

Hoshino, T., M. Kiriaki, S. Ohgiya, M. Fujiwara, H. Kondo, et al. (2003). "Antifreeze proteins from snow mold fungi". *Canadian Journal of Botany* 81.7, pp. 1175–1181.

Janech, M. G., A. Krell, T. Mock, J.-S. Kang, and J. A. Raymond (2006). "Ice-binding proteins from sea ice diatoms (Bacillariophyceae)". *Journal of Phycology* 42.2, pp. 410–416.

Jia, Z. and P. L. Davies (2002). "Antifreeze proteins: an unusual receptor-ligand interaction". *Trends in Biochemical Sciences* 27.2, pp. 101–106. DOI: 10.1016/S0968-0004(01)02028-X.

John, D. E., B. L. Zielinski, and J. H. Paul (2009). "Creation of a pilot metatranscriptome library from eukaryotic plankton of a eutrophic bay (Tampa Bay, Florida)". *Limnology and Oceanography: Methods* 7, pp. 249–259. DOI: 10.4319/lom.2009.7.249.

Kiko, R. (2010). "Acquisition of freeze protection in a sea-ice crustacean through horizontal gene transfer?" *Polar Biology* 33.4, pp. 543–556.

Kirst, G. O. (1990). "Salinity tolerance of eukaryotic marine algae". *Annual Review of Plant Physiology and Plant Molecular Biology* 41.1, pp. 21–53. DOI: 10.1146/annurev.pp.41.060190.000321.

Kirst, G. O. and C. Wiencke (1995). "Ecophysiology of polar algae". *Journal of Phycology* 31.2, pp. 181–199.

Knight, C. A., C. C. Cheng, and A. L. DeVries (1991). "Adsorption of alpha-helical antifreeze peptides on specific ice crystal surface planes". *Biophysical Journal* 59.2, pp. 409–418.

Knight, C. A. and J. G. Duman (1986). "Inhibition of recrystallization of ice by insect thermal hysteresis proteins: A possible cryoprotective role". *Cryobiology* 23.3, pp. 256–262. DOI: 10.1016/0011-2240(86)90051-9.

Knight, C. A., A. L. De Vries, and L. D. Oolman (1984). "Fish antifreeze protein and the freezing and recrystallization of ice". *Nature* 308.5956, pp. 295–296.

Knight, C. A., J. Hallett, and A. L. Devries (1988). "Solute effects on ice recrystallization: An assessment technique". *Cryobiology* 25, pp. 55–60.

Koski, L. B. and G. B. Golding (2001). "The closest BLAST hit is often not the nearest neighbor". 52.6, pp. 540–542.

Kraft, M., U. Knüpfer, R. Wenderoth, A. Kacholdt, P. Pietschmann, B. Hock, and U. Horn (2007). "A dual expression platform to optimize the soluble production of heterologous proteins in the periplasm of *Escherichia coli*". *Applied Microbiology and Biotechnology* 76 (6), pp. 1413–1422. DOI: 10.1007/s00253-007-1121-7.

Kramer, M. and R. Kiko (2011). "Brackish meltponds on Arctic sea ice–a new habitat for marine metazoans". *Polar Biology* 34.4, pp. 603–603–608.

Krell, A. (2006). "Salt stress tolerance in the psychrophiloc diatom *Fragilariopsis cylindrus*". PhD thesis. University Bremen.

Krell, A., D. Funck, I. Plettner, U. John, and G. Dieckmann (2007). "Regulation of proline metabolism under salt stress in the psychrophilic diatom *Fragilariopsis cylindrus* (*Bacillariophyceae*)". *Journal of Phycology* 43.4, pp. 753–762.

Krell, A., B. Beszteri, G. Dieckmann, G. Glöckner, K. Valentin, and T. Mock (2008). "A new class of ice-binding proteins discovered in a salt-stress-induced cDNA library of the psychrophilic diatom *Fragilariopsis cylindrus* (Bacillariophyceae)". *Journal of Phycology* 43.4, pp. 423 –433. DOI: 10.1080/09670260802348615.

Krembs, C., R. Gradinger, and M. Spindler (2000). "Implications of brine channel geometry and surface area for the interaction of sympagic organisms in Arctic sea ice". *Journal of Experimental Marine Biology and Ecology* 243.1, pp. 55 –80. DOI: 10.1016/S0022-0981(99)00111-2.

Krembs, C., H. Eicken, K. Junge, and J. W. Deming (2002). "High concentrations of exopolymeric substances in Arctic winter sea ice: implications for the polar ocean carbon cycle and cryoprotection of diatoms". *Deep Sea Research Part I: Oceanographic Research Papers* 49.12, pp. 2163–2181.

Krembs, C., H. Eicken, and J. W. Deming (2011). "Exopolymer alteration of physical properties of sea ice and implications for ice habitability and biogeochemistry in a warmer Arctic". *Proceedings of the National Academy of Sciences*. DOI: 10.1073/pnas.1100701108.

Kristiansen, E. and K. E. Zachariassen (2005). "The mechanism by which fish antifreeze proteins cause thermal hysteresis". *Cryobiology* 51.3, pp. 262–280. DOI: 10.1016/j.cryobiol.2005.07.007.

Kuiper, M. J., C. Lankin, S. Y. Gauthier, V. K. Walker, and P. L. Davies (2003). "Purification of antifreeze proteins by adsorption to ice". *Biochemical and Biophysical Research Communications* 300.3, pp. 645–648. DOI: 10.1016/S0006-291X(02)02900-5.

Laemmli, U. K. . (1970). "Cleavage of structural proteins during the assembly of the head of bacteriophage T4". *Nature* 227.5259, pp. 680–685.

Lange, M. A., S. F. Ackley, P. Wadhams, G. S. Dieckmann, and H. Eiken (1989). "Development of sea ice in the Weddell Sea". *Annals of Glaciology, Cambridge, Eng., 1989.* Vol. 12, pp. 92–96.

Legendre, L, S. F. Ackley, G. S. Dieckmann, B Gulliksen, R Horner, et al. (1992). "Ecology of sea ice biota. 2. Global significance." *Polar Biology* 12.3-4, pp. 429–444.

Li, N, C. A. Andorfer, and J. G. Duman (1998). "Enhancement of insect antifreeze protein activity by solutes of low molecular mass." *Journal of Experimental Biology* 201.15, pp. 2243–51.

Liu, Y., Z. Li, Q. Lin, J. Kosinski, J. Seetharaman, et al. (2007). "Structure and evolutionary origin of Ca^{2+}-dependent herring type II antifreeze protein". *PLoS ONE* 2.6, e548. DOI: 10.1371/journal.pone.0000548.

Lizotte, M. P. (2001). "The contributions of sea ice algae to Antarctic marine primary production". *American Zoologist* 41, pp. 57–73.

Lizotte, M. P., D. H. Robinson, and C. W. Sullivan (1998). "Algal pigment signatures in Antarcic sea ice". *Antarctic sea ice biological processes, interactions and variability.* Vol. 73. Antarctic Research Series, pp. 93–105.

Loeb, V., V. Siegel, O. Holm-Hansen, R. Hewitt, W. Fraser, W. Trivelpiece, and S. Trivelpiece (1997). "Effects of sea-ice extent and krill or salp dominance on the Antarctic food web". *Nature* 387.6636, pp. 897–900.

Ludwig, W., O. Strunk, R. Westram, L. Richter, H. Meier, et al. (2004). "ARB: a software environment for sequence data". *Nucleic Acids Research* 32.4, pp. 1363–1371. DOI: 10.1093/nar/gkh293.

Lundholm, N and G. Hasle (2008). "Are *Fragilariopsis cylindrus* and *Fragilariopsis nana* bipolar diatoms?—morphological and molecular analyses of two sympatric species". *Nova Hedwig Beih* 133, 231–250.

Margulies, M., M. Egholm, W. E. Altman, S. Attiya, J. S. Bader, et al. (2005). "Genome sequencing in microfabricated high-density picolitre reactors". *Nature* 437.7057, pp. 376–380.

Marshall, C. B., G. L. Fletcher, and P. L. Davies (2004). "Hyperactive antifreeze protein in a fish". *Nature* 429.6988, pp. 153–153.

Matsen, F., R. Kodner, and E. V. Armbrust (2010). "pplacer: linear time maximum-likelihood and Bayesian phylogenetic placement of sequences onto a fixed reference tree". *BMC Bioinformatics* 11.1, p. 538. DOI: 10.1186/1471-2105-11-538.

Maxwell, K. and G. N. Johnson (2000). "Chlorophyll fluorescence–a practical guide". *Journal of Experimental Botany* 51.345, pp. 659–668. DOI: 10.1093/jexbot/51.345.659.

Medlin, L. K., H. J. Elwood, S. Stickel, and M. L. Sogin (1988). "The characterization of enzymatically amplified eukaryotic 16S-like rRNA coding regions". *Gene* 71, pp. 491–499.

Meiners, K. M., L. Norman, M. A. Granskog, A. Krell, P. Heil, and D. N. Thomas (2011). "Physico-ecobiogeochemistry of East Antarctic pack ice during the winter-spring transition". *Deep Sea Research Part II: Topical Studies in Oceanography* 58.9-10. Antarctic Sea Ice Research during the International Polar Year 2007-2009, pp. 1172 –1181. DOI: 10.1016/j.dsr2.2010.10.033.

Mock, T. and A. Kirkham (2011). "What can we learn from genomics approaches in marine ecology? From sequences to eco-systems biology!" *Marine Ecology*, no–no. DOI: 10.1111/j.1439-0485.2011.00479.x.

Mock, T. and D. N. Thomas (2005). "Recent advances in sea-ice microbiology". *Environmental Microbiology* 7.5, pp. 605–619.

Mock, T. and K. Valentin (2004). "Photosynthesis and cold acclimation: molecular evidence from a polar diatom". *Journal of Phycology* 40.4, pp. 732–741.

Monroe, E. A., J. G. Johnson, Z. Wang, R. K. Pierce, and F. M. Van Dolah (2010). "Characterization and expression of nuclear-encoded polyketide synthases in the brevetoxin-producing dinoflagellate *Karenia brevis*". *Journal of Phycology* 46.3, pp. 541–552. DOI: 10.1111/j.1529-8817.2010.00837.x.

Nichols, D. S., P. D. Nichols, and T. A. McMeekin (1995). "Ecology and physiology of psychrophilic bacteria from Antarctic saline lakes and sea-ice". *Science Progress* 78, p. 311.

Nielsen, H, J Engelbrecht, S Brunak, and G von Heijne (1997). "Identification of prokaryotic and eukaryotic signal peptides and prediction of their cleavage sites". *Protein Engineering* 10.1, pp. 1–6. DOI: 10.1093/protein/10.1.1.

Nishimiya, Y., H. Kondo, M. Takamichi, H. Sugimoto, M Suzuki, A Miura, and S Tsuda (2008). "Crystal structure and mutational analysis of Ca^{2+}-indipendent type II antifreeze protein from longsnout poacher, *Brachyopsis rostratus*". *Journal of Molecular Biology* 382, pp. 734–746.

O'Grady, S. M., J. C. Ellory, and A. L. DeVries (1982). "Protein and glycoprotein antifreezes in the intestinal fluid of polar fishes". *Journal of Experimental Biology* 98.1, pp. 429–438.

O'Grady, S. M., J. C. Ellory, and A. L. Devries (1983). "The role of low molecular weight antifreeze glycopeptides in the bile and intestinal fluid of Antarctic fish". *Journal of Experimental Biology* 104.1, pp. 149–162.

Patterson, J. L. and J. G. Duman (1979). "Composition of a protein antifreeze from larvae of the beetle, *Tenebrio molitor*". *Jounal of Experimental Zoology* 210.2, pp. 361–367.

Pruesse, E., C. Quast, K. Knittel, B. M. Fuchs, W. Ludwig, J. Peplies, and F. O. Glöckner (2007). "SILVA: a comprehensive online resource for quality checked and aligned ri-

bosomal RNA sequence data compatible with ARB". *Nucleic Acids Research* 35.21, pp. 7188–7196. DOI: 10.1093/nar/gkm864.

R Development Core Team (2008). "R: A Language and Environment for Statistical Computing". ISBN 3-900051-07-0.

Raymond, J. A. and A. L. DeVries (1977). "Adsorption inhibition as a mechanism of freezing resistance in polar fishes". *Proceedings of the National Academy of Sciences of the United States of America* 74.6, 2589–2593.

Raymond, J. A., P Wilson, and A. L. DeVries (1989). "Inhibition of growth of nonbasal planes in ice by fish antifreezes". *Proceedings of the National Academy of Sciences of the United States of America* 86.3, pp. 881–885.

Raymond, J. A. (2000). "Distribution and partial characterization of ice-active molecules associated with sea-ice diatoms". *Polar Biology* 23.10, pp. 721–729.

Raymond, J. A. (2011). "Algal ice-binding proteins change the structure of sea ice". *Proceedings of the National Academy of Sciences* 108.24, E198. DOI: 10.1073/pnas.1106288108.

Raymond, J. A. and C. H. Fritsen (2000). "Ice-active substances associated with Antarctic freshwater and terrestrial photosynthetic organisms". *Antarctic Science* 12.04, pp. 418–424. DOI: 10.1017/S0954102000000493.

Raymond, J. A. and M. G. Janech (2009). "Ice-binding proteins from enoki and shiitake mushrooms". *Cryobiology* 58.2, pp. 151 –156. DOI: 10.1016/j.cryobiol.2008.11.009.

Raymond, J. A. and C. A. Knight (2003). "Ice binding, recrystallization inhibition, and cryoprotective properties of ice-active substances associated with Antarctic sea ice diatoms". *Cryobiology* 46.2, pp. 174 –181. DOI: 10.1016/S0011-2240(03)00023-3.

Raymond, J. A., C. W. Sullivan, and A. L. DeVries (1994). "Release of an ice-active substance by Antarctic sea ice diatoms". *Polar Biology* 14.1, pp. 71–75.

Raymond, J. A., C. Fritsen, and K. Shen (2007). "An ice-binding protein from an Antarctic sea ice bacterium". *FEMS Microbiology Ecology* 61.2, pp. 214–221.

Rousch, J. M., S. E. Bingham, and M. R. Sommerfeld (2004). "Protein expression during heat stress in thermo-intolerant and thermo-tolerant diatoms". *Journal of Experimental Marine Biology and Ecology* 306.2, pp. 231–243. DOI: 10.1016/j.jembe.2004.01.009.

Rudolph, R., G. Böhm, H. Lilie, and R. Jaenicke (1997). "Protein function, a practical approach". Ed. by T. Creighton. Oxford press. Chap. Folding proteins, pp. 57–99.

Rusch, D. B., A. L. Halpern, G. Sutton, K. B. Heidelberg, S. Williamson, et al. (2007). "The *Sorcerer II* Global Ocean Sampling Expedition: Northwest Atlantic through Eastern Tropical Pacific". *PLoS Biol* 5.3, e77. DOI: 10.1371/journal.pbio.0050077.

Russell, N. J. (1997). "Psychrophilic bacteria–Molecular adaptations of membrane lipids". *Comparative Biochemistry and Physiology Part A: Physiology* 118.3, pp. 489 –493. DOI: 10.1016/S0300-9629(97)87354-9.

Ryan, K. G., P. Ralph, and A. McMinn (2004). "Acclimation of Antarctic bottom-ice algal communities to lowered salinities during melting". *Polar Biology* 27.11, pp. 679–686.

Sandve, S., H. Rudi, T. Asp, and O. Rognli (2008). "Tracking the evolution of a cold stress associated gene family in cold tolerant grasses". *BMC Evolutionary Biology* 8.1, p. 245. DOI: 10.1186/1471-2148-8-245.

Schloss, P. D., S. L. Westcott, T. Ryabin, J. R. Hall, M. Hartmann, et al. (2009). "Introducing mothur: open-source, platform-independent, community-supported software for describing and comparing microbial communities". *Appl. Environ. Microbiol.* 75.23, pp. 7537–7541. DOI: 10.1128/AEM.01541-09.

Scotter, A. J., C. B. Marshall, L. A. Graham, and J. A. Gi (2006). "The basis for hyperactivity of antifreeze proteins". *Cryobiology* 53, pp. 229–239.

Sebastian, M. and J. W. Ammerman (2009). "The alkaline phosphatase PhoX is more widely distributed in marine bacteria than the classical PhoA". *The ISME Journal* 3.5, pp. 563–572.

Shen, H. T. and N. L. Ackermann (1990). "Wave-induced sediment enrichment in coastal ice cover". *Sea ice properties and processes*. Ed. by S. F. Ackley and W. F. Weeks. Vol. 90-1. CRREL Monogr. U.S. Army Corps of Engineers, Hanover, NH, pp. 100–102.

Simonsen, R. (1974). "The diatom plankton of the Indian Odean expedition of RV "Metero" 1964- 1965". *Forschungsergebnisse*. Reihe D 19. Deutsche Forschungsgesellschaft.

Siurkus, J., J. Panula-Perala, U. Horn, M. Kraft, R. Rimseliene, and P. Neubauer (2010). "Novel approach of high cell density recombinant bioprocess development: Optimisation and scale-up from microlitre to pilot scales while maintaining the fed-batch cultivation mode of *E. coli* cultures". *Microbial Cell Factories* 9.1, p. 35. DOI: 10.1186/1475-2859-9-35.

Sönnichsen, F. D., C. I. DeLuca, P. L. Davies, and B. D. Sykes (1996). "Refined solution structure of type III antifreeze protein: hydrophobic groups may be involved in the energetics of the protein-ice interaction". *Structure* 4.11, pp. 1325–1337.

Spreen, G., L. Kaleschke, and G. Heygster (2008). "Sea ice remote sensing using AMSR-E 89-GHz channels". *J. Geophys. Res.* 113.C2, C02S03–.

Staden, R. (1996). "The staden sequence analysis package". *Molecular Biotechnology* 5.3, pp. 233–241.

Stretch, J., P. Hamner, W. Hamner, W. Michel, J Cook, and C. Sullivan (1988). "Foraging behavior of Antarctic krill *Euphausia superba* on sea ice microalgae". *Marine Ecology Progress Series* 44.2, pp. 131–139.

Tamura, K., J. Dudley, M. Nei, and S. Kumar (2007). "MEGA4: Molecular Evolutionary Genetics Analysis (MEGA) Software Version 4.0". *Molecular Biology and Evolution* 24.8, pp. 1596–1599. DOI: 10.1093/molbev/msm092.

Thomas, D. N. and G. S. Dieckmann (2002). "Antarctic sea ice–a habitat for extremophiles". *Science* 295.5555, pp. 641–644. DOI: 10.1126/science.1063391.

Thomashow, M. F. (1998). "Role of cold-responsive genes in plant freezing tolerance". *Plant Physiology* 118, pp. 1–7.

Throndsen, J. (1978). "Phytoplankton manual". Ed. by A. Sournia. UNESCO, Paris. Chap. Preservation and storage, pp. 69–74.

Uhlig, C. (2006). "Anti-Freeze-Proteine in Meereis-Diatomeen - Ihre Diversität und Expression am Beispiel von *Fragilariopsis curta*". MA thesis. Fachhochschule Aachen, Abteilung Jülich.

Uhlig, C., J. Kabisch, G. J. Palm, K. Valentin, T. Schweder, and A. Krell (2011). "Heterologous expression, refolding and functional characterization of two antifreeze proteins from *Fragilariopsis cylindrus* (Bacillariophyceae)". *Cryobiology*, pp. –. DOI: 10.1016/j.cryobiol.2011.08.005.

Urrutia, M. E., J. G. Duman, and C. A. Knight (1992). "Plant thermal hysteresis proteins". *Biochimica et Biophysica Acta (BBA) - Protein Structure and Molecular Enzymology* 1121.1-2, pp. 199–206. DOI: 10.1016/0167-4838(92)90355-H.

Vargo, G. A., K. Fanning, C. Heil, and L. Bell (1986). "Growth rates and the salinity response of an Antarctic ice microflora community". *Polar Biology* 5.4, pp. 241–247.

Venter, J. C., K. Remington, J. F. Heidelberg, A. L. Halpern, D. Rusch, et al. (2004). "Environmental genome shotgun sequencing of the Sargasso Sea". *Science* 304.5667, pp. 66–74. DOI: 10.1126/science.1093857.

Walters, K. R., A. S. Serianni, T. Sformo, B. M. Barnes, and J. G. Duman (2009). "A nonprotein thermal hysteresis-producing xylomannan antifreeze in the freeze-tolerant Alaskan beetle *Upis ceramboides*". *Proceedings of the National Academy of Sciences* 106.48, pp. 20210–20215. DOI: 10.1073/pnas.0909872106.

Weeks, W. F. and S. F. Ackley (1982). "The growth, structure and properties of sea ice". Vol. 82-1. CRREL Monogr. Cold Regions Research Engineering Laboratory, Hanover, NH, 117 pp.

Weissenberger, J., G. Dieckmann, R. Gradinger, and M. Spindler (1992). "Sea ice: a cast technique to examine and analyze brine pockets and channel structure". *Limnology and Oceanography* 37, pp. 179–183.

Wen, D. and R. A. Laursen (1992). "A model for binding of an antifreeze polypeptide to ice". *Biophysical Journal* 63.6, pp. 1659–1662.

Wharton, D. A., P. W. Wilson, J. S. Mutch, C. J. Marshall, and M. Lim (2007). "Recrystallization inhibition assessed by splat cooling and optical recrystallometry". *CryoLetters* 28.1, pp. 61–68.

Wolfe, J., G. Bryant, and K. L. Koster (2002). "What is 'unfreezable water', how unfreezable is it and how much is there?" *CryoLetters* 23, pp. 157–166.

Worrall, D., L. Elias, D. Ashford, M. Smallwood, C. Sidebottom, et al. (1998). "A carrot leucine-rich-repeat protein that inhibits ice recrystallization". *Science* 282.5386, pp. 115–117. DOI: 10.1126/science.282.5386.115.

Wu, H., A. M. Cockshutt, A. McCarthy, and D. A. Campbell (2011). "Distinctive PSII photoinactivation and protein dynamics in marine diatoms". *Plant Physiology*. DOI: 10.1104/pp.111.178772.

Xiao, N., K. Suzuki, Y. Nishimiya, H. Kondo, A. Miura, S. Tsuda, and T. Hoshino (2010). "Comparison of functional properties of two fungal antifreeze proteins from *Antarctomyces psychrotrophicus* and *Typhula ishikariensis*". *FEBS Journal* 277.2, pp. 394–403.

Yooseph, S., G. Sutton, D. B. Rusch, A. L. Halpern, S. J. Williamson, et al. (2007). "The *Sorcerer II* Global Ocean Sampling Expedition: Expanding the universe of protein families". *PLoS Biol* 5.3, e16. DOI: 10.1371/journal.pbio.0050016.

Zachariassen, K. E. and J. A. Husby (1982). "Antifreeze effect of thermal hysteresis agents protects highly supercooled insects". *Nature* 298.5877, pp. 865–867.

Zor, T. and Z. Selinger (1996). "Linearization of the Bradford protein assay increases its sensitivity: theoretical and experimental studies". *Analytical Biochemistry* 236.2, pp. 302 –308. DOI: 10.1006/abio.1996.0171.

A Tables species

Table A.1: List of Antarctic polar diatom species tested to date for antifreeze activity. Species with molecular support shown in bold. For further taxonomical information on species investigated in this study refer to chapter 2. All Antarctic species exhibited antifreeze activity.

Polar species	Order, family	Isolated from ice type	Reference
McMurdo Sound - Antarctic			
Amphiprora kufferathii	Naviculales, Amphipleuraceae	platelet ice	Raymond 2000
Amphiprora sp.	Naviculales, Amphipleuraceae	platelet ice	Raymond 2000
Berkeleya sp.	Naviculales, Berkeleyaceae	platelet ice	Raymond 2000
Eucampia antarctica	Hemiauales, Hemiaulaceae	ice edge 25 m	this study
Nitzschia curta	Bacillariales, Bacillariaceae	platelet ice	Raymond 20000
Nitzschia stellata	Bacillariales, Bacillariaceae	platelet ice	Raymond et al. 1994
Porosira pseudodenticulata	Thalassiosirales, Thalassiosiraceae	platelet ice	Raymond et al. 1994
Pleurosigma sp.	Naviculales, Peurosigmataceae	platelet ice	Raymond 2000
Cape Evens – Antarctica			
Navicula glacei	Naviculales, Naviculaceae	sea ice	Janech et al. 2006

continued on next page

Table A.1: List of Antarctic polar diatom species tested to date for antifreeze activity. Species with molecular support shown in bold. For further taxonomical information on species investigated in this study refer to chapter 2. All Antarctic species exhibited antifreeze activity.

Polar species	Order, family	Isolated from ice type	Reference
Near King George Island – Antarctica			
Chaetoceros neogracile	Chaetocerotales, Chaetocerotaceae	no information	Janech et al. 2006, Gwak et al. 2010
Fragilariopsis pseudonana	Bacillariales, Bacillariaceae	no information	Janech et al. 2006
Stellarima microtrias	Coscinodiscales, Coscinodiscaceae	no information	Janech et al. 2006
Weddell Sea – Antarctica			
Fragilariopsis curta	Bacillariales, Bacillariaceae	sea ice	Bayer-Giraldi et al. 2010, this study
Fragilariopsis cylindrus	Bacillariales, Bacillariaceae	sea ice	Janech et al. 2006, Krell et al. 2008, Bayer-Giraldi et al. 2010, this study
Antarctic undefined			
Porosira glacialis	Thalassiosirales, Thalassiosiraceae	no information	this study
Proboscia inermis	Rhizosoleniales, Rhizosoleniaceae	no information	this study

Table A.2: List of Arctic diatom species tested to date for antifreeze activity. For further taxonomical information on species investigated in this study refer to chapter 2. All Arctic species exhibited antifreeze activity.

Polar species	Order, family	Isolated from ice type	Reference
North Atlantic, Tromsø- Arctic			
Thalassiosira nordenskioeldii	Thalassiosirales, Thalassiosiraceae	n.d.	this study
Kongsfjord – Arctic			
Entomoneis sp.	Suriellales, Entomoneidaceae	congelation ice	this study
Fragilariopsis nana	Bacillariales, Bacillariaceae	congelation ice	this study
Navicula sp. I	Naviculales, Naviculaceae	congelation ice	this study
Navicula sp. II	Naviculales, Naviculaceae	congelation ice	this study
Navicula sp. III	Naviculales, Naviculaceae	congelation ice	this study
Nitzschia sp.	Bacillariales, Bacillariaceae	congelation ice	this study
Arctic undefined			
Amphora sp.	Thalassiophysales, Catenulaceae	no information	Janech et al. 2006
Attheya sp.	Chaetocerotales, Attheyaceae	no information	Janech et al. 2006
Synendra sp.	Fragilariales, Fragilariaceae	no information	Janech et al. 2006

Table A.3: List of temperate diatom species tested to date for antifreeze activity. Species with molecular information shown in bold. Temperate species did not exhibit antifreeze activity.

Temperate species	Order, family	Habitat	Reference
Achnanthes brevipes	Achnanthales, Achnanthaceae	marine	Raymond et al. 1994
Phaeodactylum tricornutum	Naviculales, Phaeodactylaceae	marine	Raymond et al. 1994, Janech et al. 2006, this study
Thalassiosira pseudonana	Thalassiosirales, Thalassiosiraceae	marine	Janech et al. 2006
Thalassiosira sp.	Thalassiosirales, Thalassiosiraceae	marine	Raymond et al. 1994
Cyclotella meneghiniana	Thalassiosirales, Stephanodiscaceae	freshwater	Raymond et al. 1994
Nitzschia palea	Bacillariales, Bacillariaceae	freshwater	Raymond et al. 1994

B Lists of figures and tables

List of figures

1.1 Sea ice extent . . . 1
1.2 Diatoms attached to ice platelets . . . 3
1.3 The sea ice habitat . . . 5
1.4 Diatoms in brine pockets . . . 6
1.5 Thermal hysteresis . . . 7
1.6 Effects of AFPs on ice . . . 8
1.7 Adsorption inhibition model . . . 9

2.1 Calibration optical recrystallometer . . . 29
2.2 *Navicula sp.* sensu lato I - KFI B2 . . . 34
2.3 *Fragilariopsis nana* Arc - KFII A4 . . . 35
2.4 *Navicula sp.* sensu lato II - KFIII A2 . . . 36
2.5 *Entomoneis sp.* - KFV B4 . . . 37
2.6 *Navicula sp.* sensu lato III - KFV C1 . . . 38
2.7 *Nitzschia sp.* - KFV C2 . . . 39
2.8 *Thalassiosira nordenskioeldii* - CCMP 997 . . . 40
2.9 *Fragilariopsis nana* - TM99 . . . 41
2.10 *Eucampia antarctica* - CCMP 1452 . . . 42
2.11 *Proboscia inermis* - UTS08 . . . 43
2.12 *Porosira glacialis* - UEA09 . . . 44
2.13 AFP equivalents . . . 46
2.14 AFP stability . . . 47
2.15 18S phylogeny part 1 . . . 56
2.16 18S phylogeny part 2 . . . 57

2.17 Taxonomy plate KFI B2 58
2.18 Taxonomy plate KFII A4 59
2.19 Taxonomy plate KFIII A2 60
2.20 Taxonomy plate KFV B4 61
2.21 Taxonomy plate KFV C1 62
2.22 Taxonomy plate KFV C2 63
2.23 Immunoblott 64

3.1 Recombinant AFP expression and purification 76
3.2 Crystal morphology 77
3.3 Thermal hysteresis vs. buffer salinity 78
3.4 Thermal hysteresis vs. recombinant protein concentration 79
3.5 Schematic drawing of ice crystal shapes 83
3.6 Protein sequences of constructs for heterologous expression 90
3.7 Phylogeny of *Fragilariopsis* AFPs 91

4.1 Reference tree 102
4.2 Phylogenetic placement A4 and J4 103
4.3 Number of AFP sequences 104
4.4 Phylogenetic placement KF1 112
4.5 Phylogenetic placement G5 and S5 113
4.6 Phylogenetic placement G3/S3 114

List of Tables

2.1 Arctic diatom species 22
2.2 Antarctic diatom species 23
2.3 Exponential growth rates 55

3.1 Recombinant AFPs and corresponding isoforms 69
3.2 Destination vectors 70
3.3 AFP primers 88
3.4 Destination vectors 89

4.1 Sampling sites and conditions 97
4.2 Samples and processing 99
4.3 Number of AFP sequences in clades according to pplacer 105
4.4 *F. cylindrus* AFP names 115
4.5 Number of AFP sequences in clades according to BLAST 115
4.6 Contig names and read numbers 116

5.1 Diatom families investigated 118
5.2 Diatom assemblages investigated 120

A.1 Antarctic species 149
A.1 Antarctic species 150
A.2 Arctic species 151
A.3 Temperate species 152

Christiane Uhlig
Friedrichstr. 13
27570 Bremerhaven
Christiane.Uhlig@awi.de

Bremerhaven, den 21.10.2011

Erklärung gemäß §6 (5) PromO (vom 14. März 2007)

Hiermit erkläre ich, dass ich die vorliegende Doktorarbeit mit dem Titel:

Living inside Sea Ice – Distribution and Functional Characterisation of Antifreeze Proteins in Polar Diatoms

1. ohne unerlaubte fremde Hilfe angefertigt habe,
2. keine anderen als die von mir angegebenen Quellen und Hilfsmittel benutzt habe,
3. die den benutzten Werken wörtlich oder inhaltlich entnommenen Stellen als solche kenntlich gemacht habe.

Ebenfalls erkläre ich hiermit eidesstattlich, dass es sich bei den von mir abgegebenen Arbeiten um 3 identische Exemplare handelt.

.....
(Christiane Uhlig)